Pollution of the Urban Midlands (PUMA)

Development of an 'urban airshed' model for the West Midlands

Hadley Centre technical note 31

This work was prepared for Professor Roy Harrison at Birmingham University as part of the NERC PUMA Project.

It was supported under the Government Meteorological Research Programme at the Met Office.

Alison Redington, Dick Derwent, Derrick Ryall, Steven Matthew & Alistair Manning

28 September 2001

Met Office

Contents

Pollution of the Urban Midlands Atmosphere (PUMA)

Development of an 'urban airshed' model for the West Midlands

1.0 Introduction

There is growing interest and concern over air quality levels within the UK, particularly in large urban areas such as London and Birmingham. One of the key aims of the PUMA project has been to develop an 'urban airshed' model capable of producing urban background concentrations of key atmospheric pollutants at hourly timescales and at a resolutions of 2km or better. Recent papers on modelling air quality levels in urban areas (Malcolm & Manning 2001, Russell & Dennis 2000, Manning 1999) have highlighted the importance of a number of factors including:

1. The need for detailed and accurate emissions of all primary species, including their time dependence, such as diurnal and seasonal cycles. Power station emissions are of particular concern, as their emissions are highly variable in time.

2. The importance of representing the detailed evolution of the boundary layer structure, particularly the stable to unstable transition following sunrise.

3. The need to properly represent urban effects, due to increased roughness and changes in surface energy balances.

4. The need to include contributions from both local and distant sources, including European emissions. The contribution to pollutant levels from distant sources is particularly important for particulate and ozone forecasting.

5. The need to represent the detailed chemical transformations occurring at both local and regional scales, both in and above the boundary layer.

6. The difficulties in interpreting and utilising pollution observations to compare with model predictions. Observations are point values highly influenced by local scale emissions and concentration fluctuations, whilst models typically generate volume and time averaged concentrations.

To address limitations in the representation of the urban boundary layer the mesoscale RAMS model has been used to generate high resolution meteorological fields to drive the Met Office's Lagrangian dispersion model NAME. In addition chemistry schemes in the NAME model have been developed to include sulphur, nitrogen and hydrocarbon chemistry in an attempt to improve the representation of secondary pollutants such as particulates and ozone.

In the first section of this report we discuss the application of RAMS data to drive NAME, assessing the impact of increased resolution. We compare Unified Model and RAMS data with observations and compare NAME model NO_x predictions using RAMS and mesoscale Unified Model data. The second half of the report describes the chemical scheme and presents detailed model validation against measurement data from the two PUMA campaigns.

2.0 Analysis of Meteorological Data

2.1 The NAME model

The Met Office's dispersion model NAME is a Lagrangian particle model developed to simulate the transport of atmospheric pollutants on scales of 1-1000's km. Originally developed after the Chernobyl incident, one of its key operational applications is emergency response and planning for nuclear, volcanic and other major atmospheric releases. In recent years the model has been applied to a range of air quality related problems including: national air quality forecasting (Manning 1999), secondary PM_{10} modelling (Malcolm & Manning 2001), estimating European greenhouse and ozone depleting gas emissions (Ryall et al 2001).

Pollutants are represented by large numbers of imaginary particles, which are released into the model atmosphere and advected in three dimensions by the local mean wind field. Various random walk techniques are used to represent turbulent diffusion and mixing processes and parametrisations are available to represent entrainment processes between the boundary layer and the free troposphere, for mixing by deep convection, and for wet and dry deposition. Boundary layer depths are directly determined from wind and temperature profiles using a Richardson number or parcel technique. The model uses wind fields and other meteorological data from both the global and mesoscale versions of the Met Office's Unified Model (UM) (Cullen 1993), using a nested structure. The global model has a horizontal resolution of 0.833° x 0.555° and 30 levels in the vertical. The mesoscale model, which covers the United Kingdom and north-western Europe, has a 0.11° resolution with 38 levels in the vertical. Global fields are available at six hour intervals and mesoscale at three hourly intervals.

As NAME was originally developed to utilise UM data, it has a similar horizontal and vertical grid structure. The horizontal grid is based on an Arakara B grid, with u and v components of wind offset by half a grid length from temperature grid points in both the x and y directions. A hybrid h coordinate is used in the vertical, giving terrain following levels near the surface and constant pressure in the upper atmosphere, with a smooth transition between ie.

$$h = \frac{A}{p_0} + B$$

Where A and B values are defined at each model level and P_0 is a reference pressure (10^5Pa). Vertical velocities are defined by $\dot{h}$, the rate of change of h with time. Pressure at a given model level can be determined from

$$p = A + Bp_*$$

where p_* is the surface pressure. This means that the height above ground of a given model varies spatially and in time, depending on surface pressure and vertical temperature profiles. The global model grid is on an equidistant cylindrical projection, whilst the mesoscale model is based on a rotated equatorial projection.

2.2 The RAMS model

The RAMS model is a non-hydrostatic mesoscale model developed at the University of Colorado, and has been successfully applied to a number of urban scale problems in North America. The potential advantage of the RAMS model over the UM is that it is non-hydrostatic, enabling it to be applied at resolutions below 10 km. For PUMA the model has been applied at approximately 8km resolution over a domain covering most of southern and mid parts of the UK, and at 2km resolution

over the Birmingham area, with both grids both on a polar stereographic projection. The two grids and associated topography are illustrated in Figure 2.1. In both versions 29 vertical levels were used, with a greater density of levels in the lower atmosphere. Full three dimensional fields are generated at hourly intervals.

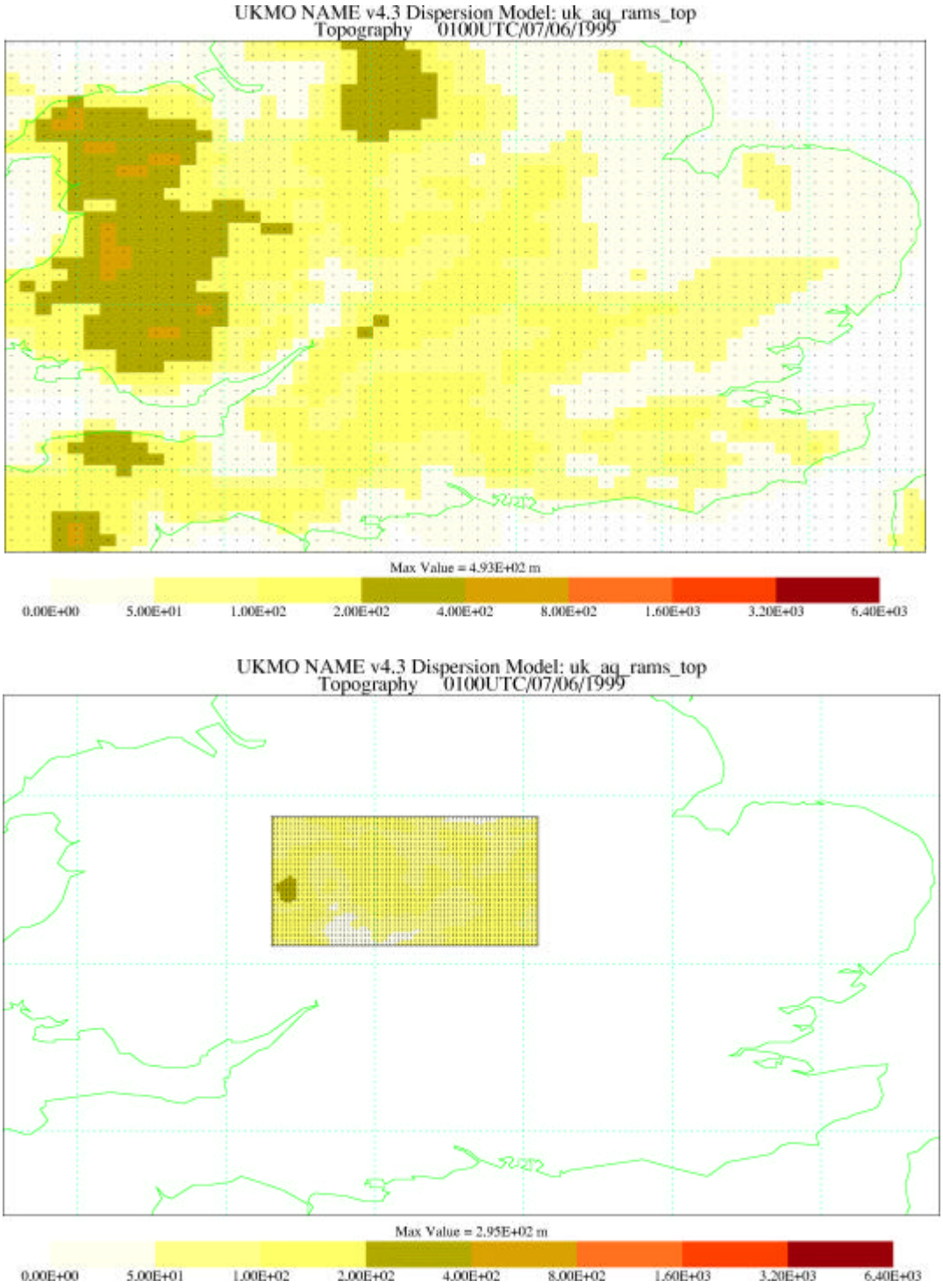

Figure 2.1 RAMS grids and topography

The RAMS model uses an Arakara C grid, in which the u component is offset in the x direction, and the v component is offset in the y direction. The vertical coordinate is based on height above ground, but is 'compressed' over elevated topography, to maintain the same model top. Given the

different grid structures of RAMS and Unified model data, RAMS data has been interpolated both horizontally and vertically to a Unified Model type grid, with a similar resolution to the RAMS grid. In the horizontal RAMS data has been interpolated from a polar stereographic projection to cylindrical projection, and in the vertical data have been interpolated to 38 h levels.
A number of meteorological fields were not generated by RAMS, including precipitation, cloud water, cloud ice, and convective cloud information. All of these were defaulted to zero, resulting in a 'dry' atmosphere.

The RAMS model was applied to both the summer 1999 and winter 2000 campaign periods. In order to initialise the RAMS model, analyses fields from the mesoscale version of the UM were provided at six hourly intervals, with data interpolated onto the RAMS grid structure. Analyses fields were extracted from operational mesoscale model output, which is run four times daily.

2.3 Comparison of Unified Model and RAMS meteorological data

The key assumption behind using RAMS data in preference to operational UM data to drive NAME is that the higher resolution of RAMS is likely to generate more detailed and accurate meteorology over the Birmingham area, leading to more accurate dispersion predictions. Of particular relevance to dispersion modelling is the detailed boundary layer structure and its evolution, which itself is strongly dependent on surface energy balances. Whilst a detailed validation of RAMS data against surface and profile data is beyond the scope of this study, it is useful to compare RAMS and Unified Model predictions of wind and temperature with available surface observations. Here we compare observations with predictions from the 60km resolution global model, 12km resolution mesoscale model and 2km resolution RAMS model, to assess the level of added skill and accuracy obtained from increased resolution.

The two main sources of meteorological data for the two campaigns are Coleshill and Pritchatts Road. Coleshill is a synoptic station just to the east of Birmingham, in an exposed and largely rural site. Standard synoptic observations are available hourly, including pressure, screen height temperature, and wind speed and direction at 10m. At Pritchatts Road, an urban site within the University Campus, observations of pressure, temperature, and wind data were obtained at 15 minute intervals during both the summer 1999 and winter 2000 campaigns. Data for Coleshill has been retrieved from Met Office archives, while Pritchatts Road data has been retrieved from the BADC web site[1].

2.4 Coleshill data

In Figure 2.2 observations of surface temperature, 10m wind speed and wind direction at Coleshill are plotted for the summer 1999 campaign period, together with global, mesoscale and RAMS model predictions. Also shown are model predicted sensible heat flux, friction velocity and boundary layer depth. Figure 2.3 shows the same data, but as mean diurnal cycles. Similar plots are shown for the winter 2000 campaign in Figures 2.4 and 2.5. A range of statistical comparisons have been made between model and observed data, including correlation (r), bias, normalised mean square error (nmse) and percentage of points within a factor of 2 (FAC2%), these are listed in Table 2.1 for both the summer and winter campaigns. Note that the time periods studied represent the period of overlap between RAMS, UM, Coleshill and Pritchatts Road data.

Whilst there are clearly differences between the three models, it is difficult to visually identify which model provides the closest match with observations. The statistics indicate that the highest skill overall is from the mesoscale version of the Unified Model. However a detailed inspection of the data reveals that no one model appears to provide the best fit with observations at all times.

[1] http://www.badc.rl.ac.uk click on Data from NERC Programmes, Urban Regeneration and the Environment (URGENT), PUMA Consortium Project.

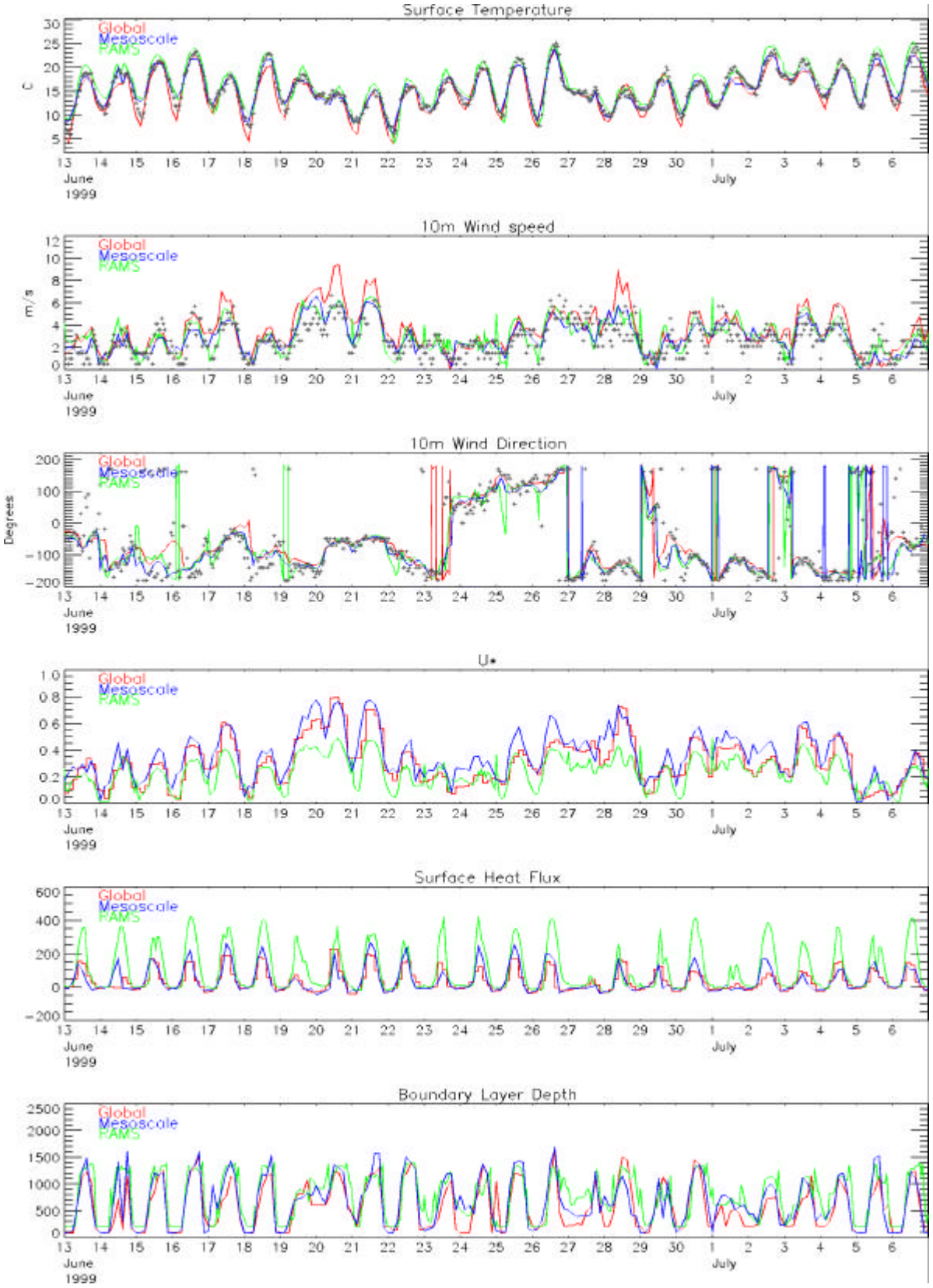

Figure 2.2 Comparison of Global, Mesoscale and RAMS model data and observations at Coleshill, summer 1999.

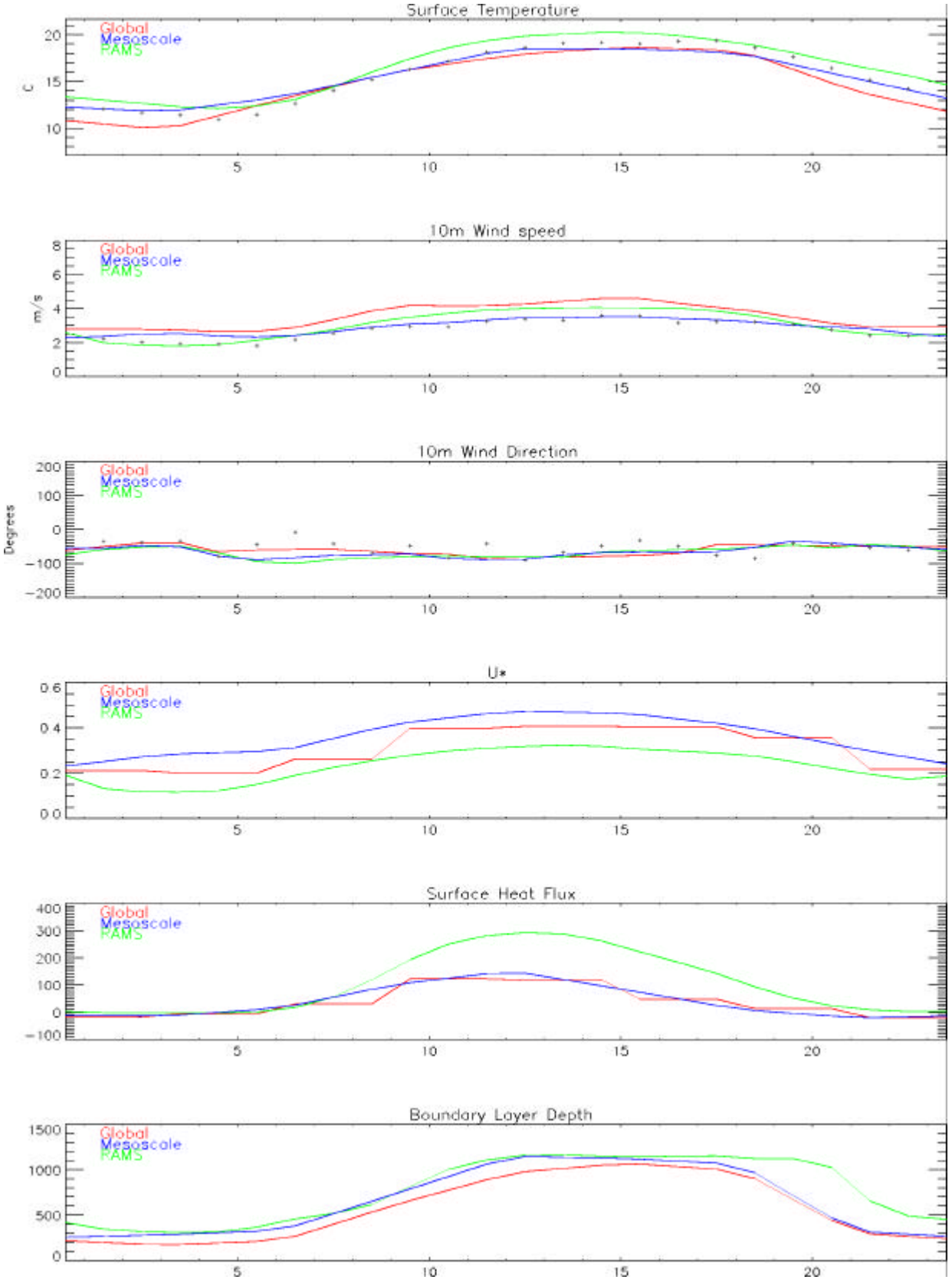

Figure 2.3 Diurnal cycles modelled and observed at Coleshill, summer 1999.

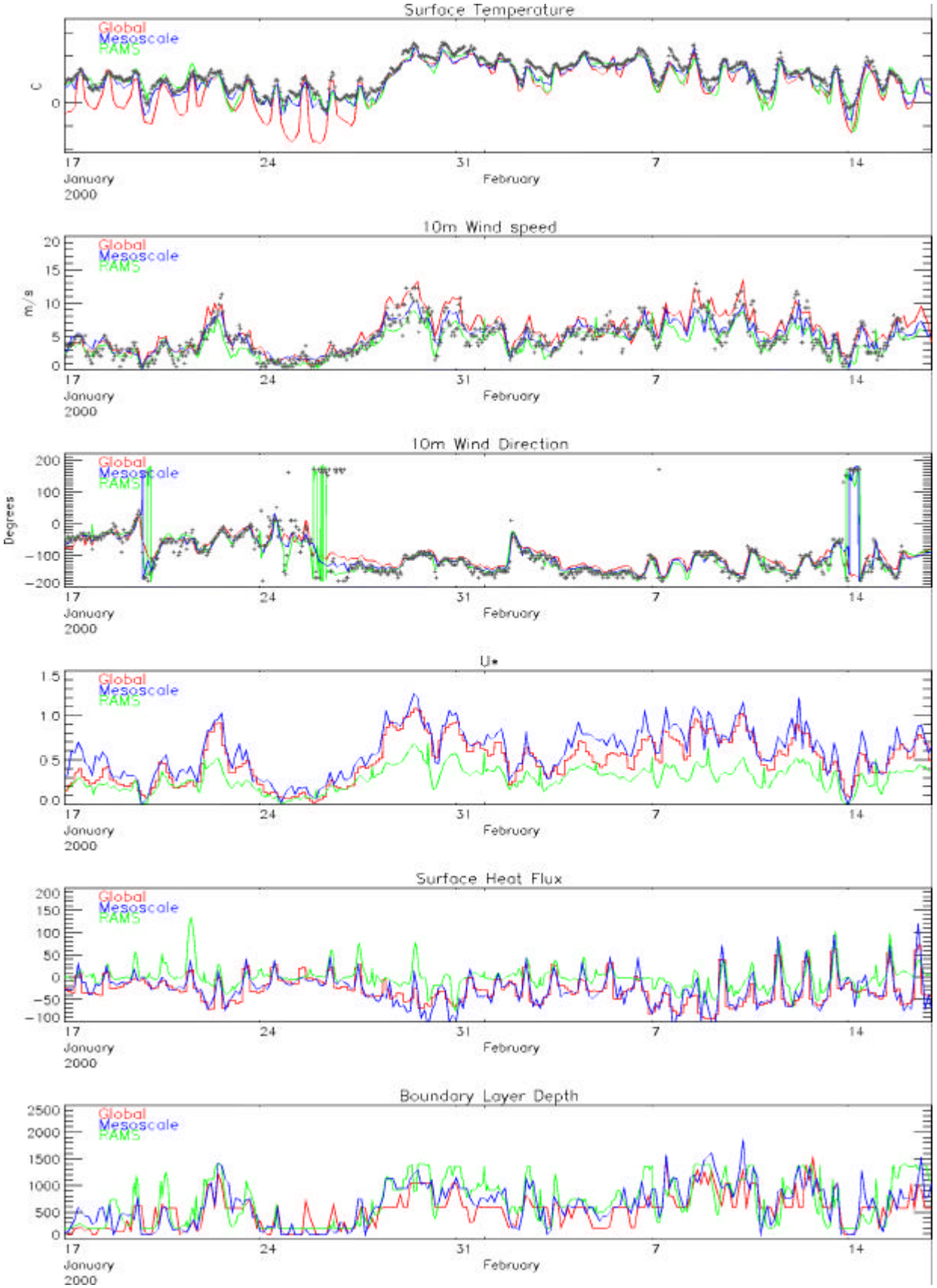

Figure 2.4 Comparison of Global, Mesoscale and RAMS model data and observations at Coleshill, winter 2000.

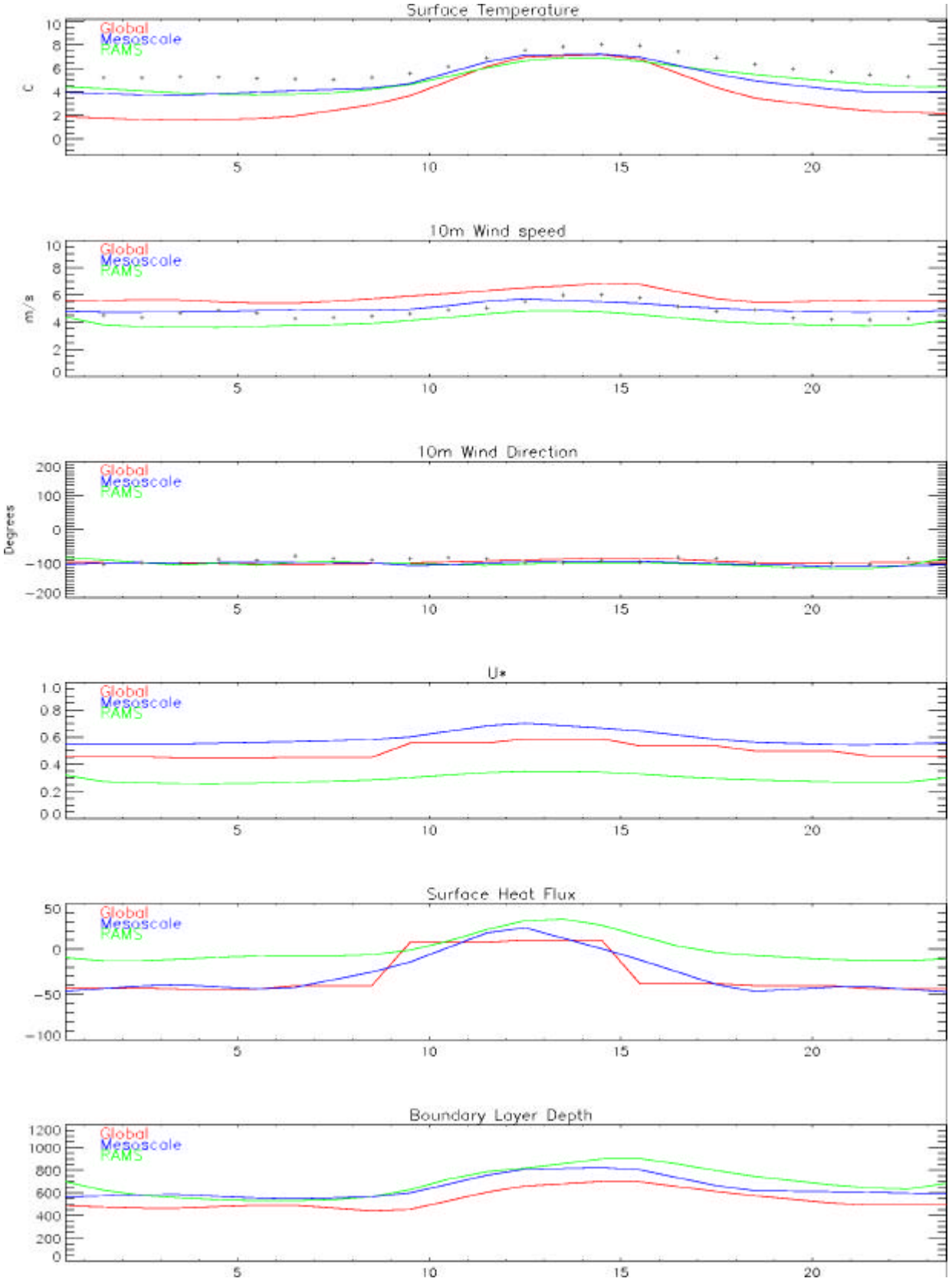

Figure 2.5 Diurnal cycles modelled and observed at Coleshill, winter 2000.

	Summer 1999				Winter 2000			
Temperature	r	bias	nmse	FAC2	r	bias	nmse	FAC2
Global UM/Coleshill	0.96	-0.68	0.01	100.00	0.91	-2.37	0.48	64.40
MesoscaleUM/Coleshill	0.97	-0.04	0.00	100.00	0.97	-0.99	0.06	86.90
RAMS/Coleshill	0.95	0.93	0.01	100.00	0.91	-0.96	0.10	81.80
Wind speed								
Global UM/Coleshill	0.74	0.82	0.23	80.60	0.86	0.97	0.11	91.10
MesoscaleUM/Coleshill	0.76	0.19	0.12	85.20	0.88	0.16	0.07	93.00
RAMS/Coleshill	0.74	0.34	0.15	86.50	0.86	0.75	0.12	92.90
Wind direction								
Global UM/Coleshill	0.92	14.75	1.33		0.94	15.01	0.13	
Mesoscale UM/Coleshill	0.94	0.42	0.72		0.95	6.15	0.08	
RAMS/Coleshill	0.92	1.72	0.89		0.96	-0.26	0.05	

Table 2.1 Statistics of model versus observations at Coleshill

Perhaps unsurprisingly the global model achieved the lowest overall skill, slightly overpredicting wind speeds and underpredicting temperatures, particularly at night and during winter. The global model was particularly poor at predicting night time temperatures between the 17 and 28 January 2000, underpredicted by up to 5C or more. This is probably a result of the global model not representing low cloud layers or fog.

Similar biases are evident in the mesoscale model, but at reduced levels. In general the mesoscale model appears to overpredict temperatures and wind speeds in the early morning. No biases can be seen in the wind direction plots, mainly due to high variability and the relatively short time periods studied.

The RAMS model appears to overpredict summer temperatures, but like the global and mesoscale models significantly underpredicts winter temperatures, again mostly due to night time errors. Day time wind speeds are overpredicted, but night time wind speeds are more accurately reproduced. Major differences between RAMS and the other models include:

1) consistently lower friction velocities, both at night and day;

2) much higher day time sensible heat fluxes, with fluxes often double mesoscale values;

3) less negative night time fluxes during the winter;

4) generally higher boundary layer depths, especially in the late afternoon when deep boundary layer depths are sustained for longer;

5) higher night time boundary layer depths during stable summer nights.

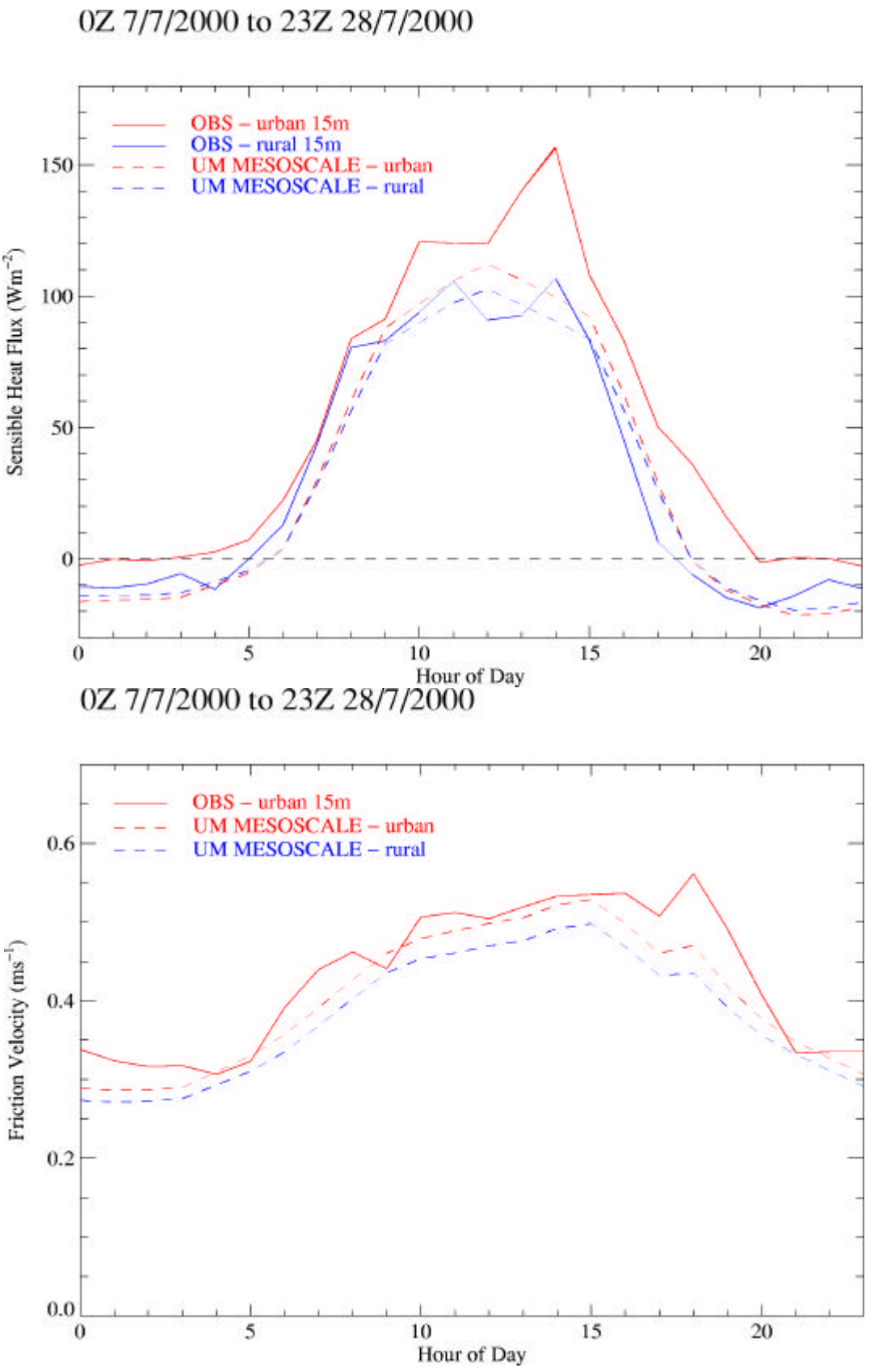

Figure 2.6 Diurnal trends of sensible heat flux and friction velocity at Coleshill and Dunlop site.

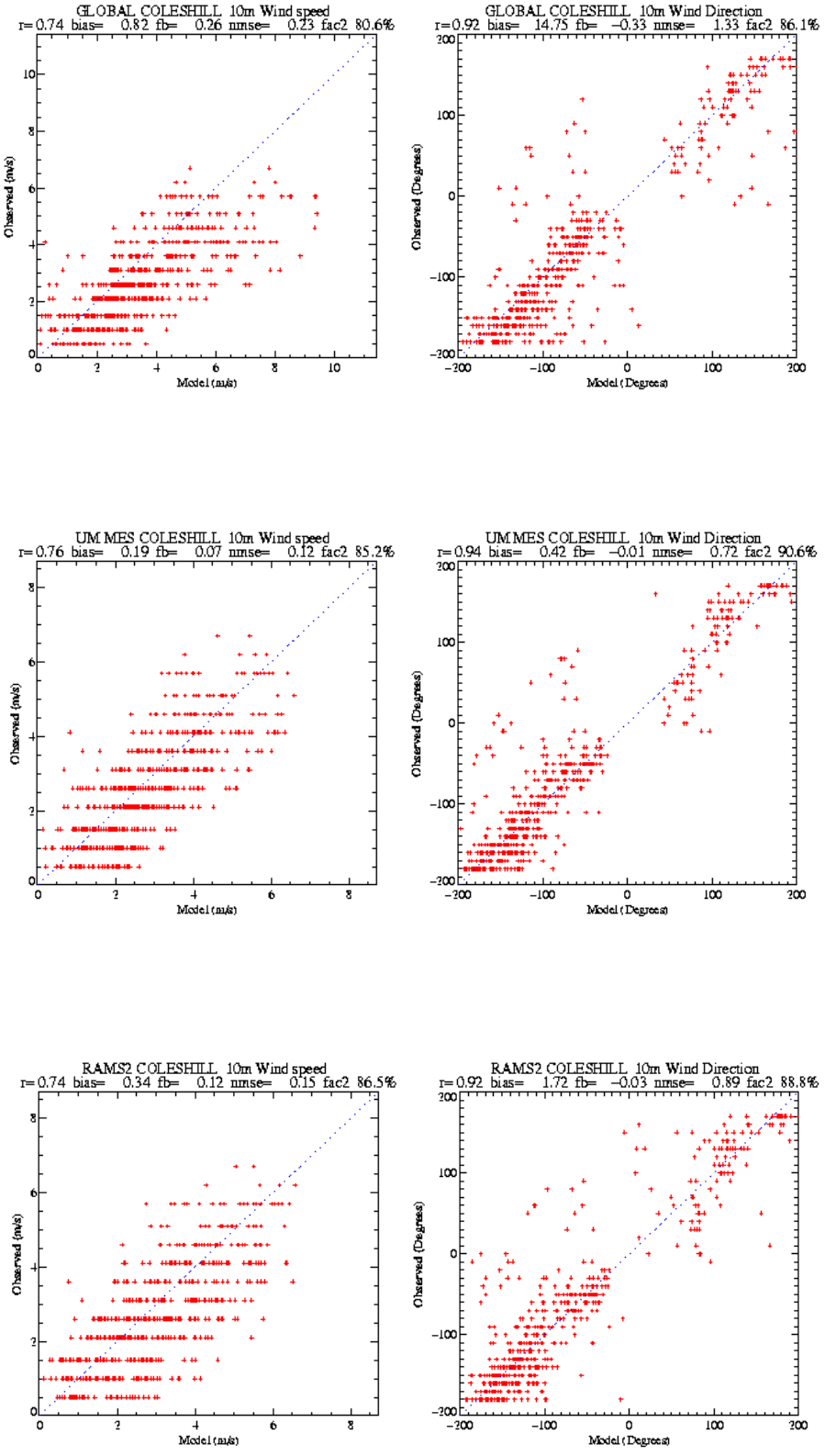

Figure 2.7 Cross plots of observed winds versus observations at Coleshill, summer 1999

Without detailed surface flux and boundary layer wind and turbulence observations it is difficult to comment on these differences, however, the Met Office has carried out a number of measurement

campaigns in Birmingham over between 1998 and 2000, with the aim of better understanding the urban boundary layer and its effect on urban dispersion (Ellis & Middleton 2000). As yet unpublished results from 1999 and 2000 show no significant bias in mesoscale model predictions of heat flux and friction velocity (figure 2.6), suggesting that the differences revealed here are mainly due to biases in the RAMS data. One possibility is that the RAMS model is not properly representing latent heat fluxes due to evaporation of moisture, leading to erroneously high sensible heat fluxes. High heat fluxes are likely to result in excessive boundary layer turbulence and evolution. The reasons for low friction velocity are less clear.

Overall the improvement in skill offered by the mesoscale model over the global model and RAMS is small, cross plots of model versus observed winds in Figure 2.7 show a similar level of scatter for each of the models model data, suggesting that any increase in skill for the mesoscale model is modest, and that all the models have difficulty predicting the detailed patterns observed in the in wind speed and direction data.

2.5 Pritchatts Road data

As Pritchatts Road wind data is measured at 10m, well within the urban canopy layer, caution is required when using and interpreting the data. Measurements are likely to be strongly influenced by local features such as buildings and trees, making detailed comparisons with model data inappropriate. However, as Pritchatts Road provides the only significant set of continuous urban measurements, it is interesting to compare with both model and Coleshill data.

Figures 2.8 and 2.9 show model and observed data for Pritchatts Road for the two campaigns. The statistical data for Pritchatts Road are shown in table 2.2. There appears to be a large number of wind direction observations between -100° and -120°, sometimes for extended periods of up to a day. It is not clear if this points to a measurement error, or if it is a result of some local feature dominating in particular conditions.

Key differences between Pritchatts Road data and Coleshill include greater scatter in wind speed and direction, and significantly lower wind speeds. Some of the scatter can be explained by different measurement techniques: synoptic wind measurements at Coleshill are 10 minute averages, while Pritchatts Road measurements are 5 minute averages of 10 second scans, thus showing greater variation due to short timescale turbulence. Increased scatter, combined with lower wind speeds may also represent an urban effect, with higher turbulence levels and lower winds due to increased surface roughness. Observed night time temperatures are generally higher at Pritchatts Road.

These differences are consistent with urban met measurements in Birmingham, which indicate reduced wind speeds, higher temperatures (particularly at night), and a slight backing in wind direction when compared with Coleshill.

Overall, none of the models show any significant differences between Coleshill and Pritchatts Road, the exception being the mesoscale model which shows a slight reduction in wind speed, presumably due to increased roughness With a resolution of 60km it is not surprising that no differences are evident in the global data.

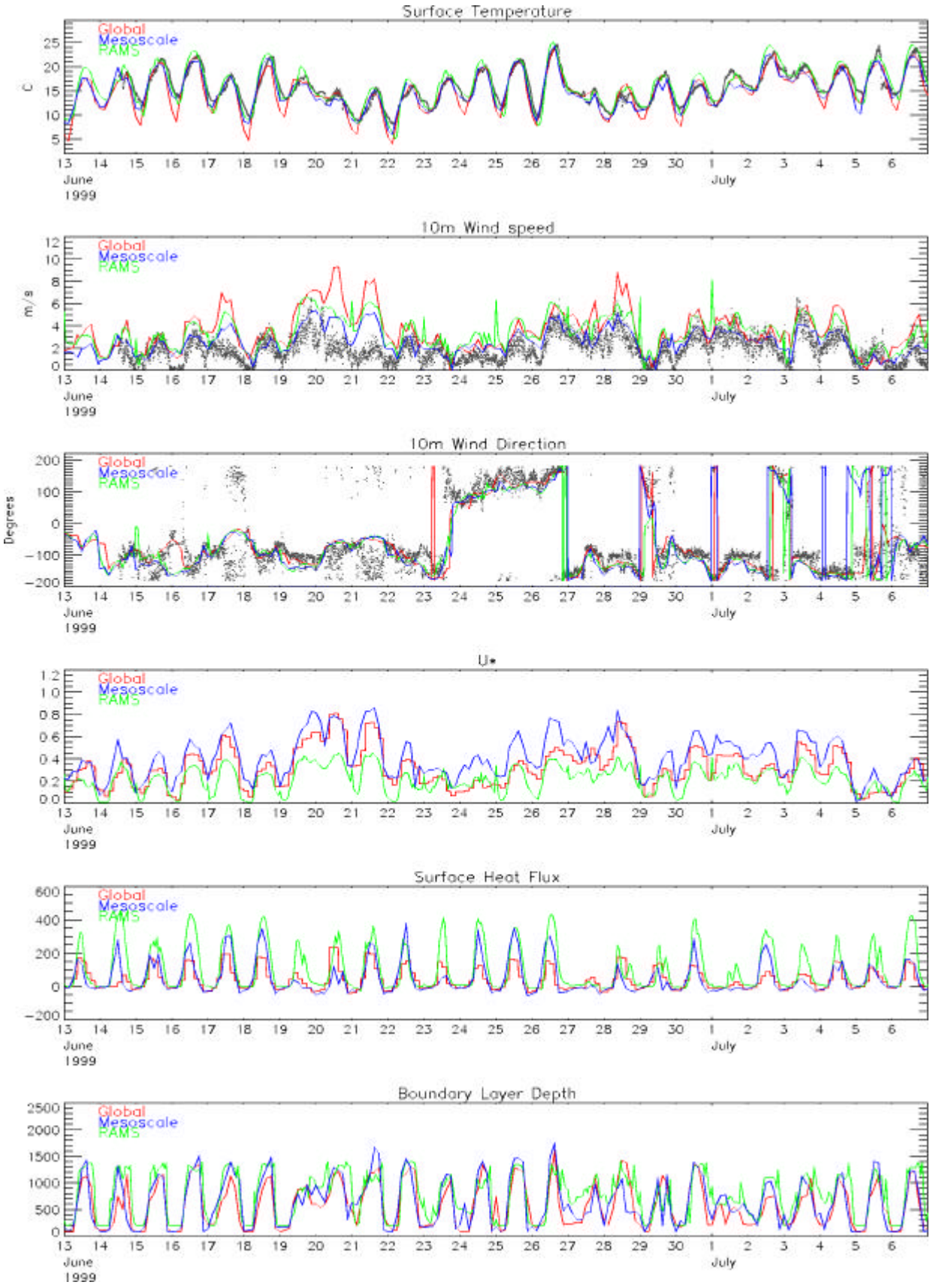

Figure 2.8 Comparison of Global, Mesoscale and RAMS model data and observations at Pritchatts Road, summer 1999.

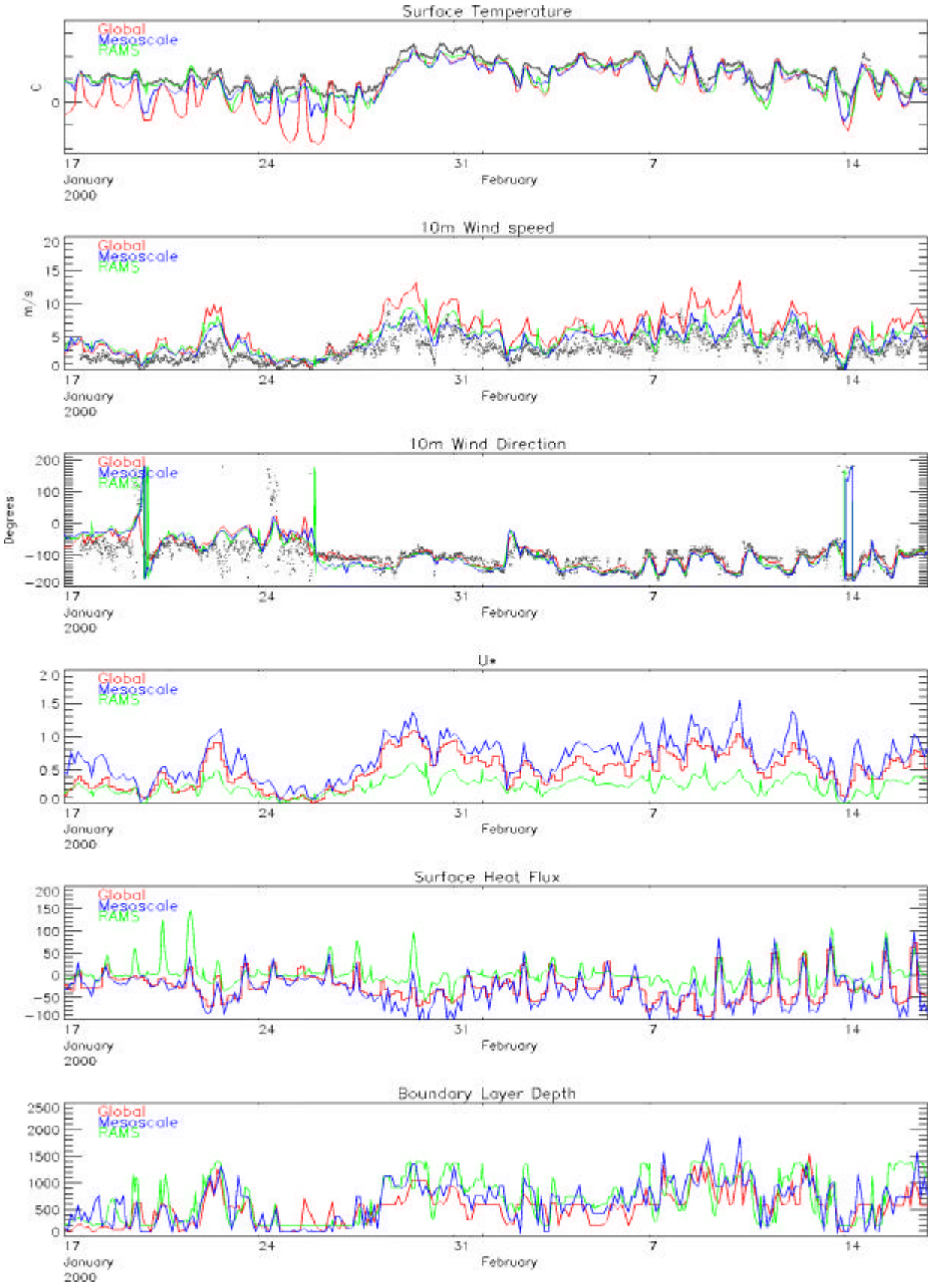

Figure 2.9 Comparison of Global, Mesoscale and RAMS model data and observations at Pritchatts Road, winter 2000.

	Summer 1999				Winter 2000			
Temperature	r	bias	nmse	FAC2	r	bias	nmse	FAC2
Global UM/Pritchatts	0.90	-0.89	0.01	99.90	0.88	-2.60	0.59	64.90
Mesoscale UM/Pritchatts	0.94	-0.66	0.01	100.00	0.94	-1.57	0.13	78.80
RAMS/Pritchatts	0.94	0.29	0.01	100.00	0.92	-1.13	0.09	84.00
Wind speed								
Global UM/Pritchatts	0.57	1.70	0.71	54.90	0.82	2.62	0.52	58.50
Mesoscale UM/Pritchatts	0.63	0.67	0.27	71.70	0.81	1.15	0.18	83.30
RAMS/Pritchatts	0.65	1.49	0.50	57.60	0.77	1.36	0.23	76.10
Wind direction								
Global UM /Pritchatts	0.90	2.82	0.66		0.76	6.72	0.11	
Mesoscale UM/Pritchatts	0.89	-10.88	0.71		0.76	-0.77	0.13	
RAMS/Pritchatts	0.88	-5.83	0.72		0.76	-0.79	0.12	

Table 2.2 Statistics of model versus observations at Pritchatts Road

2.6 NAME model simulations

Comparison of a limited number of parameters with surface data can only tell part of the story. As another test of the model data we have used both RAMS and mesoscale model data to simulate NO_x levels over Birmingham during the two campaign periods. In this study we assume NO_x has a relatively long lifetime relative to transport times and do not include any nitrogen chemistry. In order to maintain a high resolution over Birmingham, the model domain was limited to the RAMS 2 model domain, as shown in Figure 2.1. Emissions of NO_x at 1km resolution were taken from the National Emissions Inventory generated by NETCEN[2]. Traffic emissions have been weighted in time to represent diurnal and weekly patterns of traffic flow (Manning 1999). When released from specified point sources, emissions are released between the stack height and 1.5 times the stack height to represent plume rise effects. Traffic emissions are released between the surface and 20m with all other emissions between 10 and 50m. All non-traffic emissions are released continuously with no time dependence. Time series of NO_x concentrations between 0 and 80m were generated at 2km resolution and at 5 minute intervals.

The model was run with global, mesoscale and 2km RAMS data. Comparison of NAME predictions with observations at the two sites Birmingham and Birmingham East are shown in Figures 2.10 – 2.13. Both time series and mean diurnal cycles are shown. Table 2.3 lists a range of comparative statistics.

Again visual inspection does not reveal any major differences between the runs, with no one model producing consistently better NAME predictions. Looking at the statistics the global data appears to produce the best results in the summer, with mesoscale and RAMS data producing slightly better results in the winter.

[2] http://www.aeat.co.uk/netcen/airqual/index.html

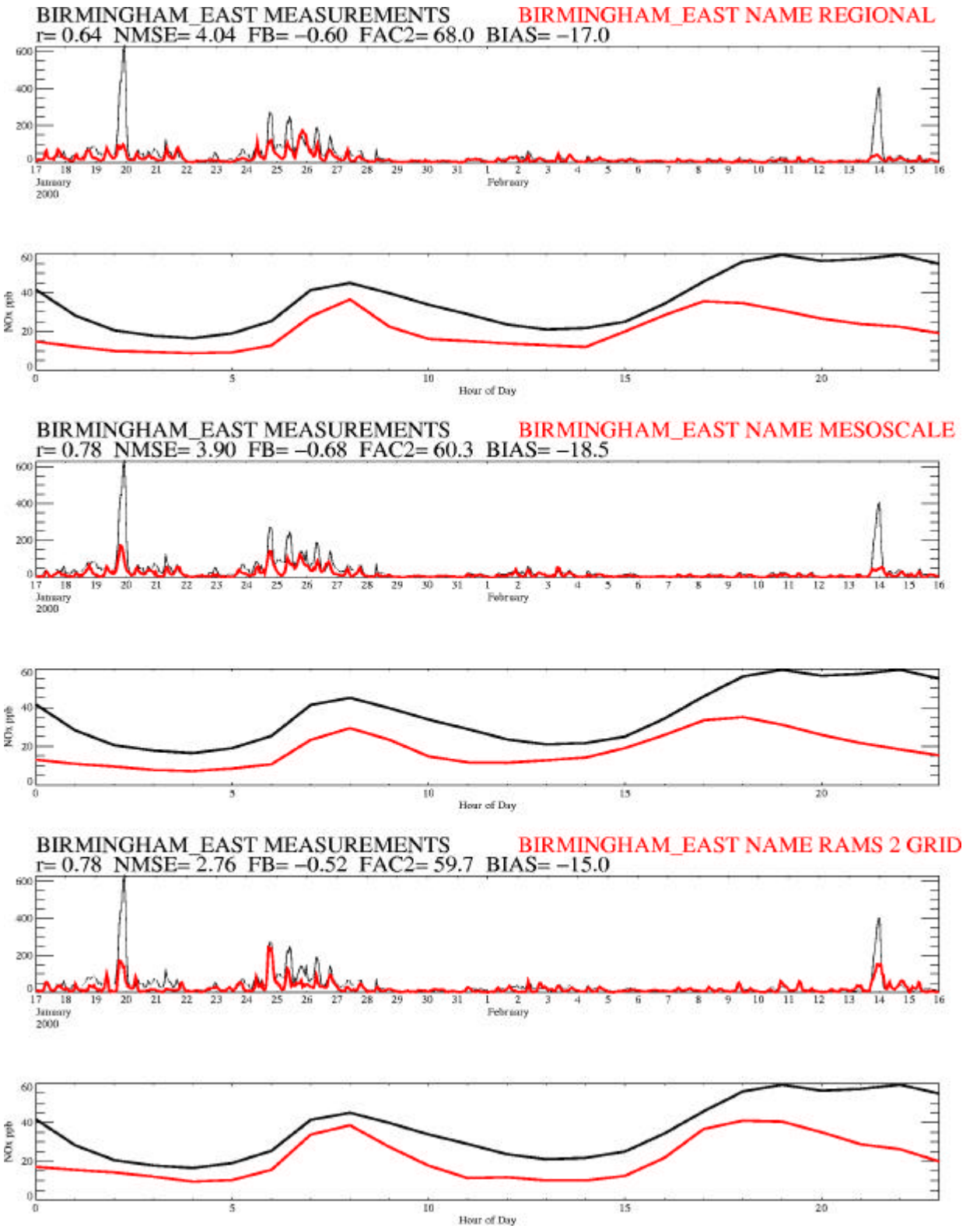

Figure 2.10 NAME model predictions of NO_x at Birmingham East during winter 2000.

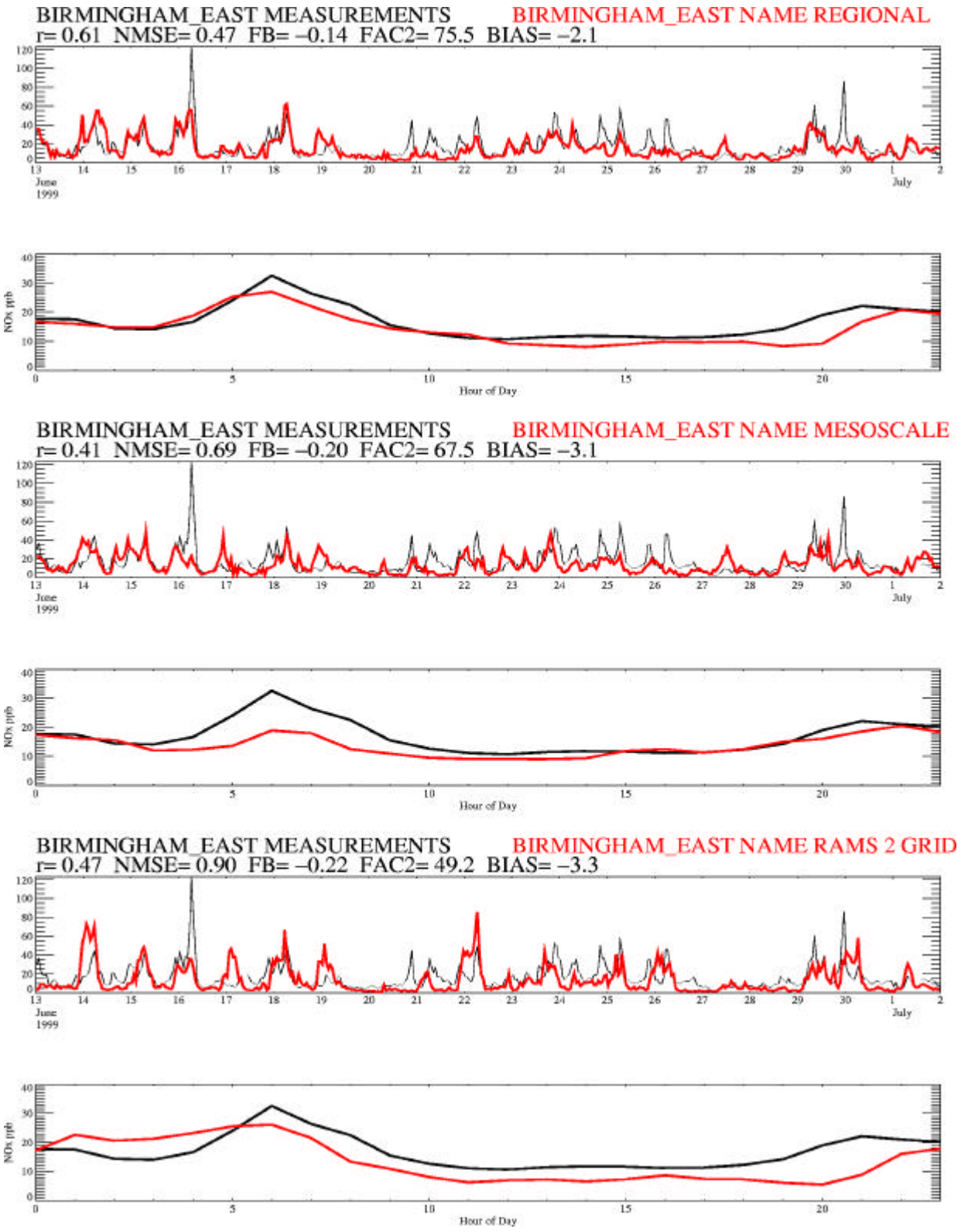

Figure 2.11 NAME model predictions of NO_x at Birmingham East during summer 2000.

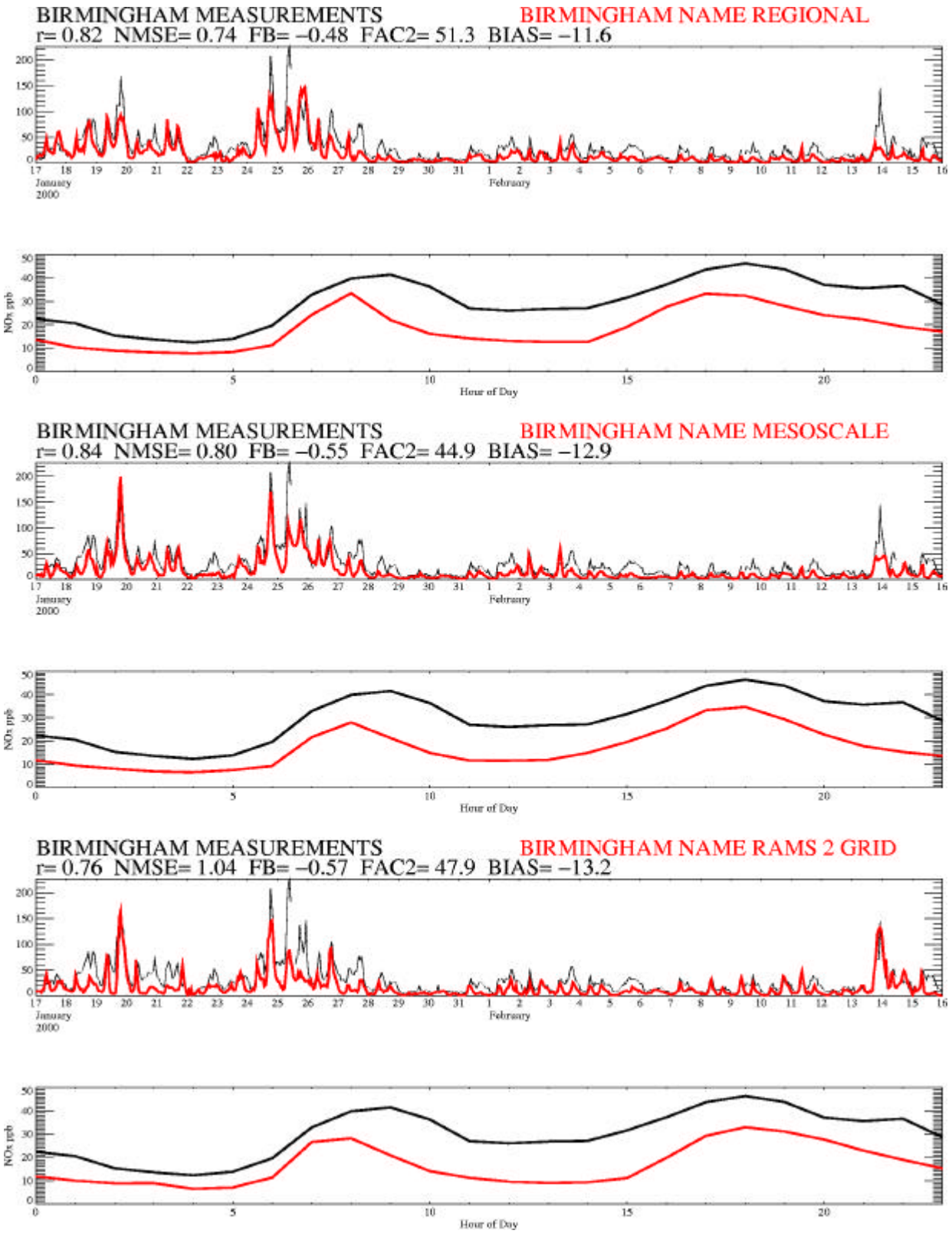

Figure 2.12 NAME model predictions of NO_x at Birmingham during winter 2000.

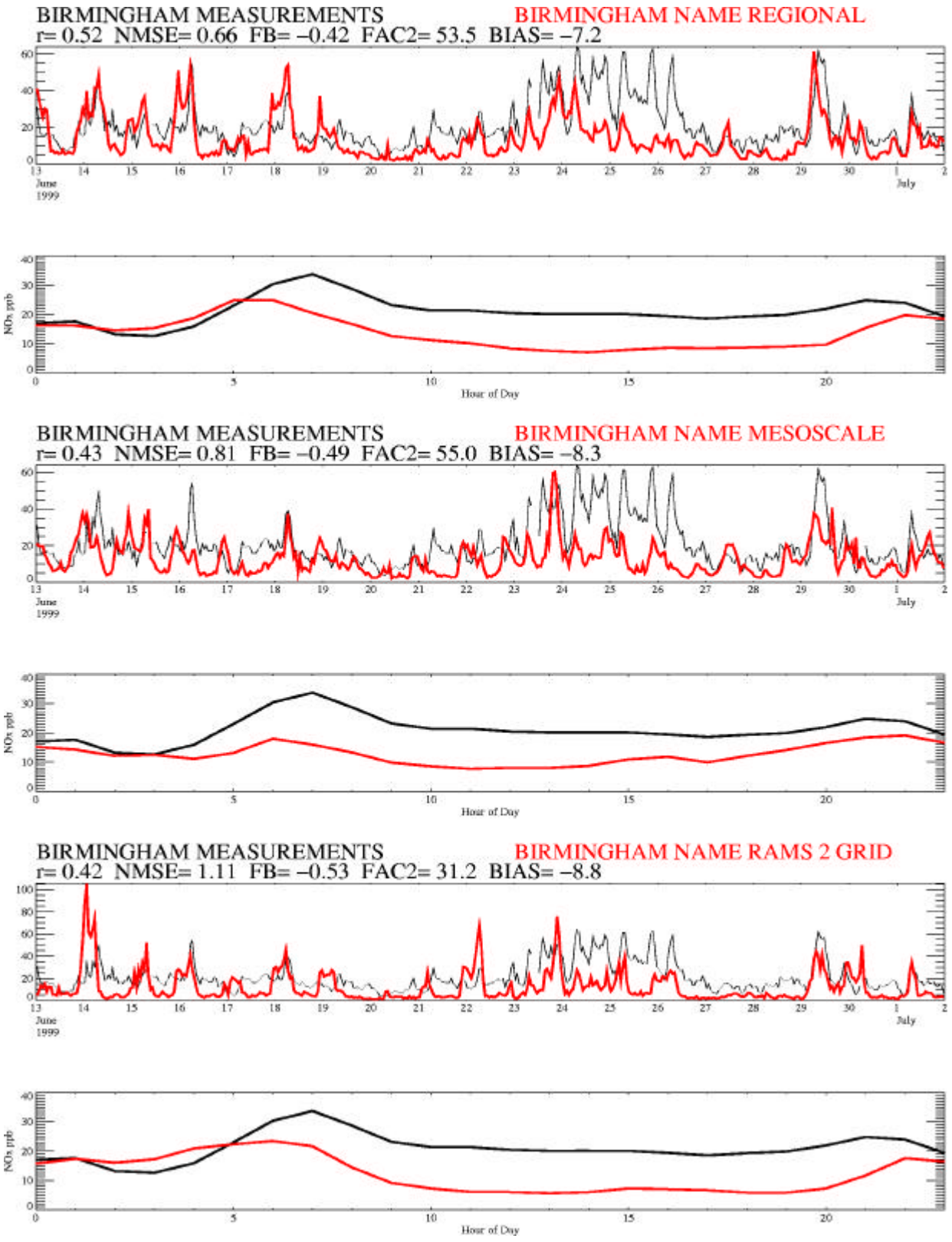

Figure 2.13 NAME model predictions of NO_x at Birmingham during summer 2000.

	Summer 1999				Winter 2000			
Birmingham	**r**	**bias**	**nmse**	**FAC2**	**r**	**bias**	**nmse**	**FAC2**
Global	0.52	-7.2	0.66	53.5	0.82	-11.6	0.74	51.3
Mesoscale	0.43	-8.3	0.81	55.0	0.84	-12.9	0.80	44.9
RAMS	0.42	-8.8	1.11	31.2	0.76	-13.2	1.04	47.9
Birmingham East								
Global	0.61	-2.1	0.47	75.5	0.64	-17.0	4.04	68.0
Mesoscale	0.41	-3.1	0.69	67.5	0.78	-18.5	3.9	60.3
RAMS	0.47	-3.3	0.90	49.2	0.78	-15.0	2.76	59.7

Table 2.3 NAME model results for Birmingham and Birmingham East using Global, Mesoscale and RAMS data

Whichever meteorology is used, NAME appears to underpredict concentrations, the exception being at night during the summer when concentrations are sometimes overpredicted. Comparisons with met data suggest that winds are generally too high over urban areas, which may in part explain this underprediction. Other possible explanations include:

1) inaccurate emission estimates;
2) biases in meteorological fields, such as excessively deep boundary layers;
3) NAME model biases, for example excessive horizontal and/or vertical mixing;
4) not properly representing the import of pollution from distant sources;
5) loss of NO_x due to photochemistry;
6) biases in NO_x measurements;
7) Local variations not represented in the emissions or captured by meteorology.

In practice there are likely to be a number of biases present, and an apparent increase in skill may simply be due to two biases partially cancelling each other out. Without detailed meteorological observations or NO_x measurements this makes it difficult to establish which factors dominate.

2.7 Long Range component

To establish the role of imported pollution NAME has also been run over a much larger area, with a domain stretching from 44 to 63 N, 15W to 14E. For this run global analysis meteorology was used and output resolution was reduced to 15km. Major sources (top 10%) were represented on a 1 km grid with all other UK sources mapped onto a 10km grid. For Europe 50km resolution emissions were taken from the EMEP[3] inventory. Figure 2.14 compares model predictions of NO_x against AUN observations at Birmingham, and table 2.4 shows the statistics calculated.

These results show a significant improvement in performance, suggesting that it is important to represent the import of pollution from sources outside Birmingham. It is interesting to note that reducing output and emission resolution have not caused any apparent loss of skill, and may indeed have contributed to an increase in performance.

[3] Co-operative Programme for Monitoring and Evaluation of the Long Range Transmission of Air Pollutants in Europe http://www.emep.int

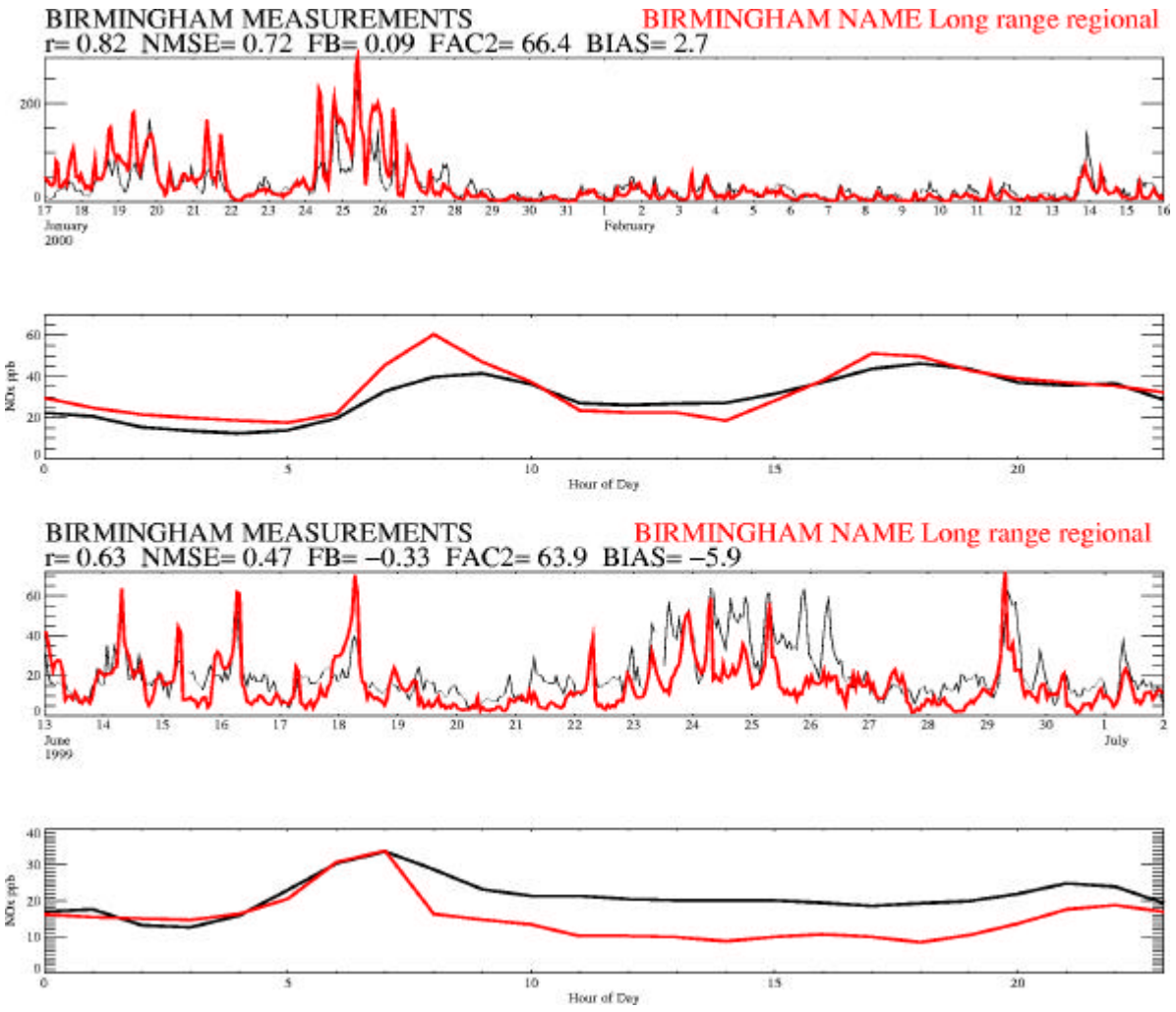

Figure 2.14 NAME model predictions of NOx at Birmingham during winter 2000 using global resolution meteorology, 15km output resolution, and domain including the UK and North West Europe.

Birmingham	r	bias	nmse	FAC2	r	bias	nmse	FAC2
Global	0.63	-5.9	0.47	63.9	0.82	2.7	0.72	66.4

Table 2.4 NAME model results for Birmingham using global data, 15km resolution and domain covering UK and North West Europe.

Overall these results show minimal sensitivity to the meteorology used, with no clear model generating the best all round results. Again this suggests that local forcing is relatively small compared to broad synoptic scale forcing, and that local forcing is not being properly represented in the higher resolution models.

2.8 Discussion

Due to the comparatively short periods studied, and limited range of observational data available, some caution is required when interpreting these results. The main findings are:

1) There are minimal differences in skill between the three met models in predicting temperature, wind speed and direction at Coleshill and Pritchatts Road. Overall the mesoscale model showed slightly higher skill.

2) Minimal differences were also found between NAME NO_x predictions and observations in Birmingham using global, mesoscale and RAMS met data. However, the best overall results were obtained using global model data.

3) Neither the UM or RAMS properly represent urban effects such as increased heat flux.

4) The differences in performance between the three models are small, suggesting that increasing resolution from 60 to 2 km is providing limited extra information over the West Midlands during the periods studied.

So why is it that higher resolution RAMS data does not appear to add any skill relative to the mesoscale model? There are likely to be a number of factors involved.

It is possible that the RAMS data has been degraded due to interpolation between native and UM type grids, both when interpolating mesoscale data to the RAMS grid for initialisation and boundary conditions, and when interpolating back to a UM type grid for use in NAME. However, interpolation errors are likely to be small, and are unlikely to explain the significant biases observed.

Both versions of the UM benefit from a continuous assimilation cycle, utilising a wide range of atmospheric and surface observations. In contrast RAMS utilises a limited range of mesoscale model fields to provide boundary conditions at six hourly intervals.

The Unified Model is an operational forecast model, and its performance is assessed daily against a range of observations including wind speed and direction, cloud base and cover, temperature and visibility to generate an overall skill index. Model development is focused on improving this score, resulting in major biases being readily identified and removed.

In contrast RAMS is a research model used mainly to explore meteorological features generated by strong local forcing, which often dominate over the broader synoptic scale forcing. In regions where local forcing dominates the higher resolution of RAMS is likely to be of direct benefit, for example by representing the effects of topography or coastal effects. Over the West Midlands area, which is relatively flat, local forcing is likely to be small compared to synoptic scale forcing, making it difficult to represent local effects.

Local forcing in the West Midlands area is likely to be dominated by urban effects, with influences including: higher roughness, increased heat capacity, modified albedo, redistribution of surface moisture, and anthropogenic heat fluxes. Detailed parametrisations of these effects are not yet available, and are very much the subject of ongoing research. The UM at the time of the campaigns did not attempt to parametrise these effects, and the biases evident in the RAMS data suggest that RAMS has not properly represented these effects.

This study has only looked at the long term skill of the models covering a range of meteorological conditions. In specific situations where local forcing is stronger, the higher resolution RAMS model may well represent features not resolved by the mesoscale or global models. However this does raise the question of how to use such information in dispersion modelling. Due to the stochastic nature of local meteorology, high resolution models like RAMS are likely to produce

‘representative’ fields rather than actual detail. For example a model may predict enhanced convection, but would not be able to predict the evolution of a specific convective cell. The handling such information may require some thought and development. Possible approaches include ensemble based predictions, or probabilistic approaches.

The scatter between model and observed wind data, even outside of Birmingham, is a reminder of the difficulties in predicting ‘real life’ dispersion at ranges of a few kilometres or less. An error of just 10° in wind direction will result in a plume being incorrectly modelled, and in excess of half of all predicted winds from all three models in this study are in error by over 10°. Plumes from multiple sources will therefore be incorrectly mixed, resulting in subsequent errors in chemistry and deposition patterns. Better results may often be obtained by modelling at a coarser scale, thus ‘smoothing’ out local variability. This may well explain why the best results are obtained when using global meteorology and coarse analysis grids.

As a consequence of the results presented here, it was decided that there was unlikely to be any significant benefit in running the detailed chemistry model on the RAMS data. By using the Met Office mesoscale meteorological data we can also benefit from the moisture variables required for the aqueous phase chemistry and deposition processes.

3.0 Development of the chemistry model

3.1 Model description

The chemistry scheme was initially developed to model sulphate aerosol (SA) and was used to assess the contribution to secondary particulate matter arriving in the UK from sources in Europe (Malcolm *et al* 2000). The aqueous phase of the chemistry scheme was subsequently revised to improve the parametrization of wintertime sulphate aerosol concentrations the results of which are presented in Derwent & Malcolm 2000. The original scheme used monthly average fields of photo-oxidants extracted from the Met Office global chemistry model, STOCHEM (Collins *et al* 1997). The gas phase chemistry scheme has been developed through this project to include the release and formation of many more species, in particular nitrate aerosol, the hydroxyl and hydroperoxy radicals, ozone and nitrogen dioxide.

The NAME model simulates the release of primary pollutants by emitting particles that represent air parcels. Each parcel can represent the released mass of many different species. There are twenty three species carried on particles, and of these the emitted species are sulphur dioxide (SO_2), nitric oxide (NO), ammonia (NH_3), carbon monoxide (CO), formaldehyde (HCHO), ethylene (C_2H_4), propylene (C_3H_6), isoprene (C_5H_8), o-xylene ($C_6H_4(CH_3)_2$), toluene ($C_6H_5CH_3$), 1,3-butadiene (C_4H_6), nitrous acid (HONO) and primary particulate matter (PM_{10}).

In order to calculate the production and loss terms for chemical reactions it is necessary to calculate species concentrations. This is done by effectively constructing a three-dimensional grid over the model domain, and adding up the total mass of each species carried on the parcels, within the grid box, and hence calculating a concentration. At the end of the chemistry timestep the new concentrations are converted back to masses and by using the information about the particle plume before the chemistry, it is possible to allocate production and loss terms in proportion with the original amount of primary species that particle previously carried. This avoids artificially spreading the primary species within the grid box.

Secondary pollutants, that is to say those pollutants formed by chemical reactions involving precursor species, are difficult to represent in a Lagrangian dispersion model because they are not directly emitted into the atmosphere. Nevertheless, their precursor species are primary pollutants, and so they are carried on the particles. The main secondary pollutants of interest in this study are ozone, PAN, sulphate aerosol, nitrate aerosol, nitric acid and hydrogen peroxide. The grid box concentrations of the secondary species are converted back to masses and then assigned to air parcels in proportion to the original mass of the precursor species carried by that parcel.

The model ozone is treated slightly differently than the other secondary species, due to the difficulty is modelling its long atmospheric lifetime. The time development of ozone concentration in an air parcel is described in the same manner as other species using the following differential equation:

$$\frac{d[O_3]}{dt} = P - L[O_3]$$

where P describes the instantaneous ozone production rate and L the instantaneous ozone loss coefficient. In the atmospheric boundary layer, dry deposition largely controls the ozone loss, with a time constant of approximately 50 hours. The ozone in an air parcel is therefore the result of the integrated ozone production over the timescales of several multiples of the 50 hour timescale.

In practice, the description of ozone production over such long timescales represents a huge computational task and some simplification is necessary. Often it suffices to set up the model domain at the edges of continental Europe and to define input ozone concentration at these boundaries using observations at remote sites. In this study, a model domain has been established

to cover southern England and the ozone production has been described using the Lagrangian approach.

The secondary pollutant production terms, P, are calculated on the 3D grid using the concentrations of the precursor species (calculated from the parcels as described above) and then assigned as masses, back to particles. Ozone however is an exception to this as we have instead used an estimated regional ozone concentration to give the ozone concentration over the 3D grid. (This value is set by taking a monthly average background value (generated on a 3D grid by the STOCHEM model) for the appropriate month, and subtracting from it the amount of modelled NO_2.) This approximation is necessary as we have had to neglect the ozone production from precursors transported into the region, and therefore cannot represent the full ozone concentration with the model. This value is used for the calculations within the chemistry scheme and, on comparison with observed values, gives a suitable concentration.

In order to estimate the production of ozone due to the precursor emissions within the model domain, the local ozone term is calculated and is assigned back to particles carrying NO or NO_2, so that it can be advected within the model and provide a spatial distribution of the local ozone production.

In future work, the intention is to use the sum of the regional ozone concentration and the local ozone production. However the regional ozone concentration must include the ozone production from precursors transported into the region, and this will require careful consideration. It is non-trivial to develop a method of importing concentrations of measured ozone into a Lagrangian framework.

A further problem arises in the representation of the highly reactive free radicals such as hydroxyl (OH) and hydroperoxy (HO_2) which are generated within the atmosphere and are more indirectly linked to primary emissions and hence cannot be simulated by the standard release of particles within the model. The ideal solution would be to continue with the Lagrangian approach and simulate the generation of such species by allowing particles to be borne throughout the 3-D grid, at the appropriate times, which could then be transported in exactly the same manner as the surface emissions. The computational cost of this approach is however prohibitive, as it would result in many hundreds of thousands more particles and it would not be possible to model a sufficiently large area to be useful. An alternative method to allow advection of the photooxidant fields would be to calculate the grid box values in the chemistry scheme, and then use a small number of temporary particles (which would not need to be remembered from one timestep to the next and thus reduce the overhead) to work out the advection of the grid box. On further examination however this scheme was considered to introduce too much diffusion. Going over to an entirely Eulerian approach was considered to be too complex at this stage and thus the current status is that a number of species are currently modelled on a 3-D grid which is static spatially. This is obviously an approximation to reality which is reasonable for species with very short atmospheric lifetimes, for example OH, but is much less appropriate for other species.

$HO_2 + HO_2$ (+M,H_2O) ? $H_2O_2 + O_2$
$OH + SO_2 + M$? $HOSO_2 + M$
$HOSO_2 + O_2 = HO_2 + SA$
$NO + O_3$? $NO_2 + O_2$
$NO_2 + O_3$? $NO_3 + O_2$
$NO_2 + NO_3 + M$? $N_2O_5 + M$
$NO_2 + OH + M$? $HNO_3 + M$
NO_3^- ? nitrate aerosol *
$OH + HNO_3$? $NO_3 + H_2O$
$NO_3 + NO_3$? $NO_2 + NO_2 + O_2$
$NO_3 + HO_2$? $HNO_3 + O_2$
$NO_3 + HO_2$? $OH + NO_2 + O_2$
$NO + NO_3$? $NO_2 + NO_2$
$NO_2 + NO_3$? $NO + NO_2 + O_2$
$N_2O_5 + M$? $NO_2 + NO_3 + M$
$O + O_2 + M$? $O_3 + M$
$O + NO + M$? $NO_2 + M$
$O^1D + M$? $O + M$
$O^1D + H_2O$? $OH + OH$

$NH_3 + HNO_3$? NH_4NO_3
$OH + O_3$? $HO_2 + O_2$
$HO_2 + O_3$? $OH + O_2 + O_2$
$NO_2 + O$? $NO + O_2$
$NO + HO_2$? $OH + NO_2$
$NO_2 + HO_2 + M$? $HO_2NO_2 + M$
$HO_2NO_2 + M$? $HO_2 + NO_2 + M$
$OH + HO_2NO_2$? $H_2O + NO_2 + O_2$
$HO_2 + OH$? $H_2O + O_2$
$OH + H_2O_2$? $H_2O + HO_2$
$OH + H_2$? $HO_2 + H_2O$
$OH + CH_3OOH$? $CH_3O_2 + H_2O$
$OH + CH_3OOH$? $OH + HCHO$
$OH + CH_4$? $CH_3O_2 + H_2O$
$NO + CH_3O_2 = CH_3O + NO_2 = HCHO + HO_2 + NO_2$
$NO_3 + C_2H_4 = C_2H_4NO_3 = CH_2(NO_3)CHO + HO_2$
$NO_3 + C_3H_6 = C_3H_6NO_3 = CH_3CH(NO_3)CHO + HO_2$
$NO_3 + CH_3CHO = CH_3CO + HNO_3$
$= CH_3COO_2 + HNO_3$
$NO_3 + C_5H_8 = (NO_3)C_4H_6CHO + HO_2$
$NO + CH_3C_6H_5(OH)(O_2) = CH_3COCHCHCHO$
$+ (CHO)_2 + HO_2 + NO_2$
$OH + (C_6H_4)(CH_3)_2 = HO(C_6H_4)(CH_3)_2$
$= HO(C_6H_4)(CH_3)_2O_2$
$HO(C_6H_4)(CH_3)_2(O_2) + NO$
$= HO(C_6H_4)(CH_3)_2(O) + NO_2$
$= CH_3COCHO + HO_2 + CH_3COCHCHCHO + NO_2$
$OH + CH_3COCHCHCHO = CH_3COCH(OH)CHCHO$
$= CH_3COCH(OH)CH(O_2)CHO$
$OH + HONO = H_2O + NO_2$
$OH + NO$ (+M) = HONO (+M)
$OH + C_7H_8 = CH_3C_6H_5(OH)(O_2)$
$OH + C_4H_6 = HOCH_2CH_2O_2$
$HOCH_2CH_2O_2 + NO = NO_2 + (CHO)_2 + HO_2$
$OH + C_2H_4$ (+O_2) = $HOC_2H_4O_2$
$HOC_2H_4O_2 + NO = HOC_2H_4O + NO_2$
$= HCHO + HO_2 + HCHO + NO_2$
$CH_3COCH(OH)CH(O_2)CHO + CH_3O_2 = 2HO_2$
$+ HCHO + CH_3COCHO + (CHO)_2$
$CH_3C_3H_3(OH)CH_2(O_2) + CH_3O_2 = 2HO_2 + HCHO$
$+ CH_3COCHCH_2$

$CH_3O_2 + CH_3O_2 = CH_3O + CH_3O + O_2$
$= HCHO + HCHO + HO_2 + HO_2$
$CH_3O_2 + CH_3O_2 = CH_3OH + HCHO + O_2$
$CH_3O_2 + HO_2 = CH_3OOH + O_2$
$OH + HCHO = HCO + H_2O = HO_2 + CO + H_2O$
$NO_3 + HCHO = HO_2 + CO + HNO_3$
$OH + CO = H + CO_2 = HO_2 + CO_2$
$OH + CH_3CHO = CH_3CO + H_2O = CH_3COO_2 + H_2O$
$CH_3COO_2 + NO_2 + M = CH_3COO_2NO_2 + M$
$CH_3COO_2NO_2 + M = CH_3COO_2 + NO_2 + M$
$CH_3COO_2 + NO = CH_3COO + NO_2$
$= CH_3 + CO_2 + NO_2$
$= CH_3O_2 + CO_2 + NO_2$
$CH_3O_2 + CH_3COO_2 = CH_3O + CH_3COO + O_2$
$= HCHO + HO_2 + CH_3 + CO_2 + O_2$
$= HCHO + HO_2 + CH_3O_2 + CO_2 + O_2$
$CH_3O_2 + CH_3COO_2 = HCHO + CH_3COOH + O_2$
$CH_3COO_2 + CH_3COO_2 = CH_3COO + CH_3COO + O_2$
$= CH_3 + CH_3 + CO_2 + CO_2 + O_2$
$= CH_3O_2 + CH_3O_2 + CO_2 + CO_2 + O_2$
$OH + CH_3COO_2NO_2 = CH_3COO_2 + HNO_3$
$CH_3O_2 + HOC_2H_4O_2 = CH_3O + HOC_2H_4O + O_2$
$= HCHO + HO_2 + HCHO + HCHO + HO_2 + O_2$
$O_3 + C_2H_4 = HCHO + 0.47CH_2O_2 + 0.31CO +$
$0.22CO_2 + 0.31H_2O + 0.13H_2 + 0.20HO_2$
$O_3 + C_3H_6 = HCHO + 0.30CH_4 + 0.40CO + 0.60CO_2$
$+ 0.28OH + 0.12CH_3OH + 0.30HO_2 + 0.58CH_3O_2$
$O_3 + C_3H_6 = CH_3CHO + 0.24H_2 + 0.58CO + 0.42CO_2$
$+ 0.58H_2O + 0.18HO_2$
$OH + C_3H_6$ (+O_2) = $HOC_3H_6O_2$
$HOC_3H_6O_2 + NO = HOC_3H_6O + NO_2$
$= CH_2OH + CH_3CHO + NO_2$
$= HCHO + HO_2 + CH_3CHO + NO_2$
$CH_3O_2 + HOC_3H_6O_2 = CH_3O + HOC_3H_6O + O_2$
$= HCHO + HO_2 + CH_2OH + CH_3CHO + O_2$
$= HCHO + HO_2 + HCHO + HO_2 + CH_3CHO + O_2$
$O_3 + C_5H_8 = CH_3COCHCH_2 + 0.78CO + 0.22CH_2OO$
$+ 0.27HO_2 + 0.27OH$
$O_3 + CH_3COCHCH_2 = CH_3COCHO + 0.76CO$
$+ 0.24CH_2OO + 0.36HO_2 + 0.36OH$
$CH_2OO + NO = NO_2 + HCHO$
$CH_2OO + NO_2 = NO_3 + HCHO$
$CH_2OO + H_2O = HCOOH + H_2O$
$CH_2OO + SO_2 = SA + HCHO$
$CH_3COCH(OH)CH(O_2)CHO + NO$
$= CH_3COCH(OH)CH(O)CHO + NO_2$
$= HO_2 + CH_3COCHO + (CHO)_2 + NO_2$
$OH + C_5H_8 = CH_3C_3H_3(OH)CH_2(O_2) + H_2O$
$CH_3C_3H_3(OH)CH_2(O_2) + NO = CH_3COCHCH_2 + HO_2$
$+ HCHO + NO_2$
$OH + CH_3COCHCH_2 = CH_3COC(OH)CHO_2 + H_2O$
$CH_3COC(OH)CHO_2 + NO = CH_3COCHO + CH_2O$
$+ HO_2 + NO_2$

$CH_3COC(OH)CHO_2 + CH_3O_2 = 2HO_2 + HCHO + CH_3COCHO$ $CH_3C_3H_3(OH)CH_2(O_2) + HO_2 = CH_3C_3H_3(OH)CH_2OOH + O_2$ $CH_3C_3H_3(OH)CH_2OOH + OH = CH_3COCHCH_2 + HCHO + OH$ $CH_3COC(OH)CHO_2 + HO_2 = CH_3COC(OH)CH_2OOH + O_2$ $CH_3COC(OH)CH_2OOH + OH = CH_3COCHO + HCHO + OH$ $CH_3COCHO + OH = CH_3COO_2 + CO$ $(CHO)_2 + OH = HO_2 + CO + CO$	*Photolysis Reactions* $NO_2 + hv \rightarrow NO + O$ $NO_3 + hv \rightarrow NO$ $NO_3 + hv \rightarrow NO_2 + O$ $N_2O_5 + hv \rightarrow NO_2 + NO_3$ $O_3 + hv \rightarrow O + O_2$ $O_3 + hv \rightarrow O^1D + O_2$ $H_2O_2 + hv \rightarrow OH + OH$ $HNO_3 + hv \rightarrow NO_2 + OH$ $HCHO + hv \rightarrow HO_2 + HO_2 + CO$ $HCHO + hv \rightarrow H_2 + CO$ $CH_3OOH + hv \rightarrow HCHO + HO_2 + OH$ $HO_2NO_2 + hv \rightarrow HO_2 + NO_2$ $CH_3CHO + hv \rightarrow CH_3O_2 + HO_2 + CO$ $CH_3COO_2NO_2 + hv \rightarrow CH_3COO_2 + NO_2$ $HONO + hv \rightarrow OH + NO$ $(CHO)_2 + hv \rightarrow HCHO + CO$ $CH_3COCHO + hv \rightarrow CH_3CHO + HO_2 + CO$

Table 3.1 Gas phase reactions included in the NAME chemistry scheme. (* This term allows for uptake of NO_3^- to particulate nitrate not in the form of ammonium nitrate. M denotes air molecules, N_2 and O_2.)

The gas phase reactions included in the NAME chemistry scheme are shown in table 3.1. The chemistry is calculated with a 100 second timestep over an advection timestep of 15 minutes. The photolysis rates are calculated using dissociation rate coefficients for clear sky, which are then adjusted by the cloud column above the grid cell (Hough 1988). Reaction rates and coefficients used in NAME can be found in Collins et al 1997 except for the HONO chemistry, and the ammonia, nitric acid equilibria with ammonium nitrate. The ammonia nitric acid equilibria is based on the scheme used by the EMEP Lagrangian model (EMEP 1989). Ammonia is rapidly combined with available sulphate to form ammonium sulphate after which any ammonia that remains will form an equilibria with nitric acid and ammonium nitrate. The equilibrium coefficient is dependent on temperature and relative humidity and its calculation is described in detail in EMEP 1989. An additional kinetic constraint has also been applied to this equilibria according to Harrison & MacKenzie 1990.

Direct emissions of HONO are emitted at 1% of the NO emissions in line with work by Kurtenbach et al 2001. The gas phase reactions of HONO production and loss are shown in table 3.1 (with rates from DeMore et al 1997), along with the photodissociation by UV radiation (rate calculated using measured values in PORG 1997). It is well established that an important mechanism for the production of HONO is the heterogeneous conversion of NO_2 on different surfaces, and the exact processes are the subject of ongoing research. Harrison et al 1996 derived an effective rate coefficient of 5.6×10^{-6} x (100/mixing height in m) s^{-1}, for the reaction $2NO_2 + H_2O \rightarrow HNO_3 + HONO$. This was put into the NAME chemistry scheme, however it was found that the inclusion of the heterogeneous reaction resulted in a very large over prediction of HONO particularly in the summer period, where it also caused over-production of OH. It was decided that this mechanism needed further consideration before its implementation in NAME and hence it is not included in the scheme presented here.

Aqueous phase chemistry is carried out in a grid box if there is a non-zero cloud fraction and cloud water present. At the end of the time step it is assumed that the cloud has evaporated leaving particulate aerosol. This would be automatically dissolved again at the start of the next timestep if the cloud were still present.

The aqueous phase oxidation of sulphur dioxide by hydrogen peroxide and ozone makes an important contribution to the formation of sulphate aerosol. The reactions and equilibria included in the NAME scheme are shown in table 3.2. The mechanism used in the NAME model is based on that used in the Met Office global chemistry model, STOCHEM (Collins *et al* 1997). The gas to liquid phase equilibria for the incorporation of soluble species into cloud droplets is described by Henry's law. The gaseous species dissolved into the cloud are nitric acid (HNO_3), ozone (O_3), carbon dioxide (CO_2), hydrogen peroxide (H_2O_2), ammonia (NH_3) and sulphur dioxide (SO_2).

Gas to liquid phase equilibria:	Aqueous production of sulphate:
H_2O ? $H^+ + OH^-$ HNO_3 ? $H^+ + NO_3^-$ SO_2 ? $H^+ + HSO_3^-$ HSO_3- ? $H^+ + SO_3^{2-}$ NH_3 ? $OH^- + NH_4^+$ CO_2 ? $H^+ + HCO_3^-$	$[HSO_3^-] + [H_2O_2]$? $[SO_4^{2-}] + [H^+] + [H_2O]$ $[HSO_3^-] + [O_3]$? $[SO_4^{2-}] + [H^+] + [O_2]$ $[SO_3^{2-}] + [O_3]$? $[SO_4^{2-}] + [O_2]$
	Formation of ammonium sulphate: $2NH_4^+ + SO_4^{2-} = (NH_4)_2SO_4$
Equation of acid balance: $[H^+] = [HSO_3^-] + [SO_3^{2-}] + [HCO_3^-] + 2[SO_4^{2-}] + [NO_3^-] - [NH_4^+]$	

Table 3.2 Aqueous phase reactions included in the NAME chemistry scheme.

The dissociation of dissolved species such as SO_2 means that these species are actually more soluble than Henry's law suggests, which is also taken into account. The hydrogen ion concentration $[H^+]$ and the pH are calculated from the equation of acid-base balance. This equation cannot be solved directly as some of the species concentrations depend on $[H^+]$. The solution is found using a minimisation approach after an initial search to establish the approximate value. The aqueous phase production of sulphate is then calculated from the reactions shown in table 3.2. If there is any ammonium present the sulphate is assumed to react instantaneously to form ammonium sulphate.

All the SO_4 in the cloud is assumed to be completely dissolved. The initial concentration is calculated from the amount of sulphate aerosol (H_2SO_4) present, with the production and loss terms as described above. The loss of the aqueous phase concentrations of SO_2, H_2O_2 and NH_3 are mixed into the gas phase calculations.

3.2 Emissions

Emission information for primary PM_{10}, sulphur dioxide, ammonia, nitric oxide, carbon monoxide, formaldehyde, ethylene, propylene, isoprene, o-xylene, toluene and 1,3-butatdiene were required over the UK. These, with the exception of ammonia, were extracted from the National Atmospheric Emissions Inventory for 1998 (the latest available) compiled by the National Environmental Technology Centre[4] (NETCEN) on behalf of the Department for Environment Food and Rural Affairs (DEFRA). The 1 km X 1 km inventory, together with point source information for the largest emitters, was used to compile source files for PM_{10}, SO_2, NO, CO and the VOCs. The largest sources were kept as either point sources or 1 km sources. In the emission regions with lowest emission densities the 1 km x 1 km information was combined into 10 km x 10 km area releases in order to reduce the total number of model particles that need be released to represent the lower emission densities. Where release height information was available for large point sources, this was used, with the particles being released between this height and approximately 100m above it in order to allow in a simplistic way for the effects of plume buoyancy and momentum. For SO_2 the remaining 1 km x 1 km and 10 km x 10 km sources for which no release height information was

[4] http://www.aeat.co.uk/netcen/airqual/index.html

given were emitted over 0-50m. The PM_{10}, NO, CO and VOC emissions were all treated in the same manner with a mixture of 1 km x 1 km and 10 km x 10 km area sources being split into traffic emissions and other emissions. The 'other' sources were emitted from 10–50m and the traffic sources were emitted from 0-20m and had a traffic cycle applied to the emission to weight the release by time of day and day of week.

The VOC emission data are provided as a sum of all VOC emissions for each 1 km x 1 km grid that is broken down by source ie. road, domestic or industrial, but is not speciated. The VOC speciation is only provided in the form of a UK annual total for each compound, again divided into the different source sectors, thus the spatial distribution of the different species is not known. This creates a problem for the emission of isoprene as it is of largely biogenic origin. Test model runs emitting isoprene as per the annual total, but spatially distributed as the other anthropogenic VOCs resulted in a large model over-prediction of the isoprene measured at the Birmingham East site. This indicated that it was not appropriate to emit isoprene in this way and given no spatial information for the biogenic release it was decided to only emit the proportion of the emission that results from anthropogenic sources. This emission was estimated from the benzene emission using a scaling factor based on urban background observations derived from Derwent et al 2000.

The VOCs emitted, whilst being some of the more reactive, only represent 20% of the total VOC emission, which is comprised some 570 species (see National Environmental Technology Centre web site[5]). In order to represent the full potential for ozone creation, the model was run with the VOC emissions scaled up to 100% of the inventory. The model was also run without scaling so that the VOCs could be compared with measurement data where available.

The UK emissions for ammonia were extracted from the EMEP[6] 50 km x 50 km area database. The release of ammonia particles was made over the height range 0-20m.

4.0 The Summer Campaign

In the following sections the NAME model output is compared with measurement data from a variety of sources for the summer campaign 12th June - 12th July 1999. The majority of the data were collected especially for the PUMA campaigns at the Pritchatts Road site in Birmingham and can be found at the British Atmospheric Data Centre web site[7]. The individual data files contain information regarding the measurement equipment used, the set up and errors, and will not be repeated here. Measurement data from the national network was obtained from the NETCEN web site for the Birmingham Centre, Birmingham East, Ladybower and Bottesford sites. The model domain was that of the RAMS1 grid with the chemistry scheme run at 8 km x 8 km resolution. The study carried out in Section 2 assessed the meteorological data available to be used as input to NAME for the campaign periods and concluded that the Met Office mesoscale data should be used.

In the following figures the model data are plotted as hourly averages (shown in red). The observed data were either given as an hourly average and plotted as such, or if more frequent, made into an hourly average (shown in blue). Nitrate and sulphate aerosol observations are provided as daily averages, therefore the model data have also been presented as a daily average. Where observed data have been shown in green, actual data points are plotted, marked by crosses or asterisks, which are joined by straight lines. These data were for variable time intervals and therefore to average the data may have been misleading. As the model data points and those measured do not directly correspond it is not possible to provide a correlation. Correlation values

[5] http://www.aeat.co.uk/netcen/airqual/index.html
[6] Co-operative Programme for Monitoring and Evaluation of the Long Range Transmission of Air Pollutants in Europe http://www.emep.int
[7] http://www.badc.rl.ac.uk click on Data from NERC Programmes, Urban Regeneration and the Environment (URGENT), PUMA Consortium Project.

are provided for the majority of the plots, however caution should be exercised in interpreting and comparing these numbers, as the data sets are generally quite small.

Whilst studying the model results the reader may find it useful to refer to the plots in Appendix A, which indicate where the air arriving in Birmingham over the last 24 hour period has originated from. Generally speaking the summer campaign was dominated by westerly winds, with the exception of the periods from 25th – 27th June and 9th – 11th July where there was an easterly component.

4.1 NO, NO_2, NO_X

Figures 4.1-4.3 show plots of modelled and observed NO, NO_2 and NO_X concentrations for Birmingham Centre, Birmingham East and Ladybower sites. Ladybower is a rural site in the Peak District situated in an area of open moorland and is close to the edge of the model domain. Birmingham Centre is located within a pedestrianised area of the city centre, with the nearest busy urban road being 60m away. Birmingham East is located within an urban residential area, with a residential road 10m away and the nearest busy road 250m away. A large industrial complex is located 400m to the northeast of the site.

The model performs reasonably well at Birmingham Centre, with correlations of around 0.5, but generally underpredicts NO, NO_2 and NO_X. The same picture is evident at Birmingham East, though with a more pronounced underprediction of NO. At Ladybower the levels both modelled and measured are much lower as would be expected at a rural site, however the correlations of NO_2 and NO_X in particular are greatly reduced. The model also fails to capture a peak of 40ppb (NO and NO_2) on 26/6/99.

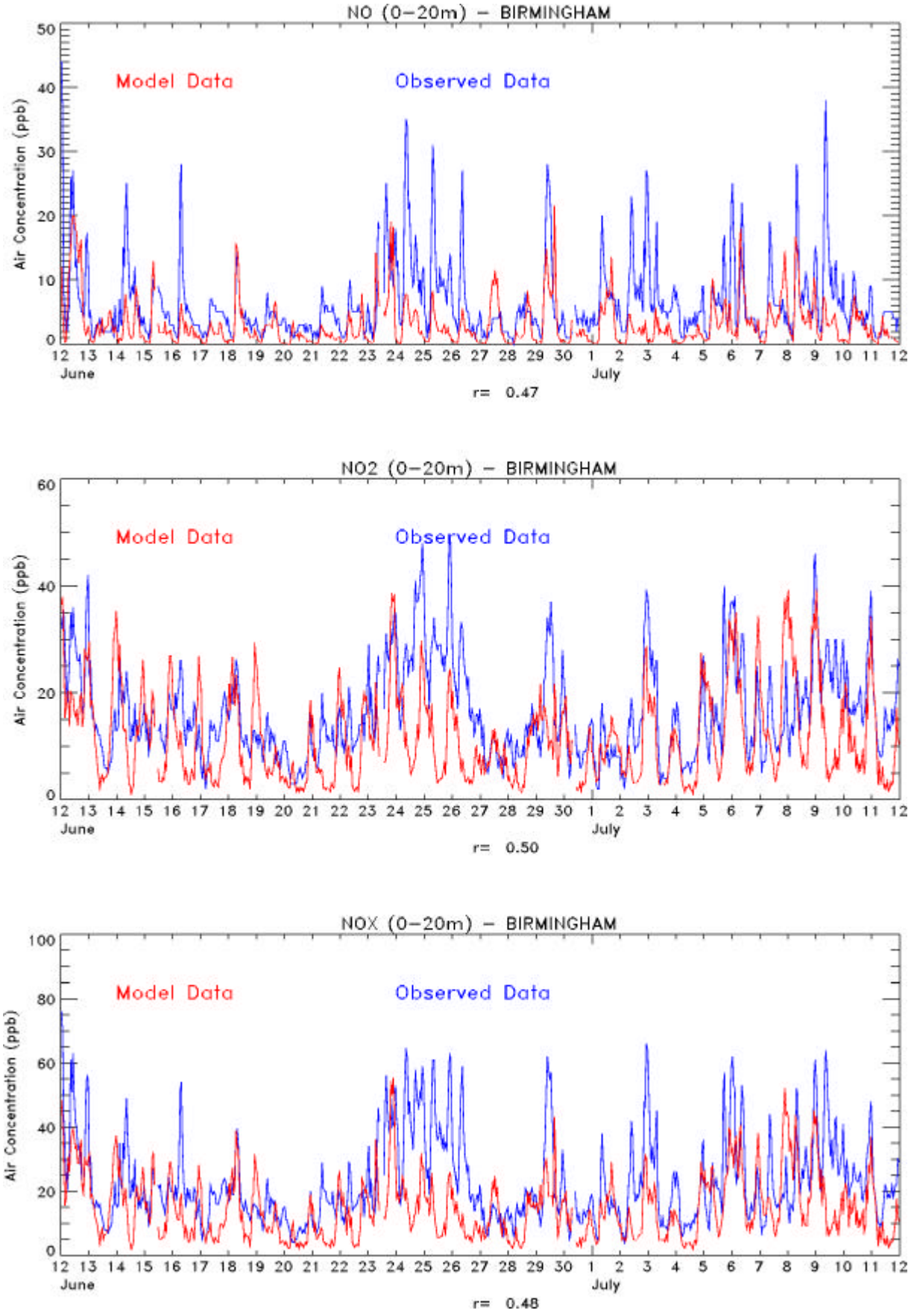

Figure 4.1 Modelled versus observed concentrations of NO, NO_2 and NO_X at Birmingham Centre.

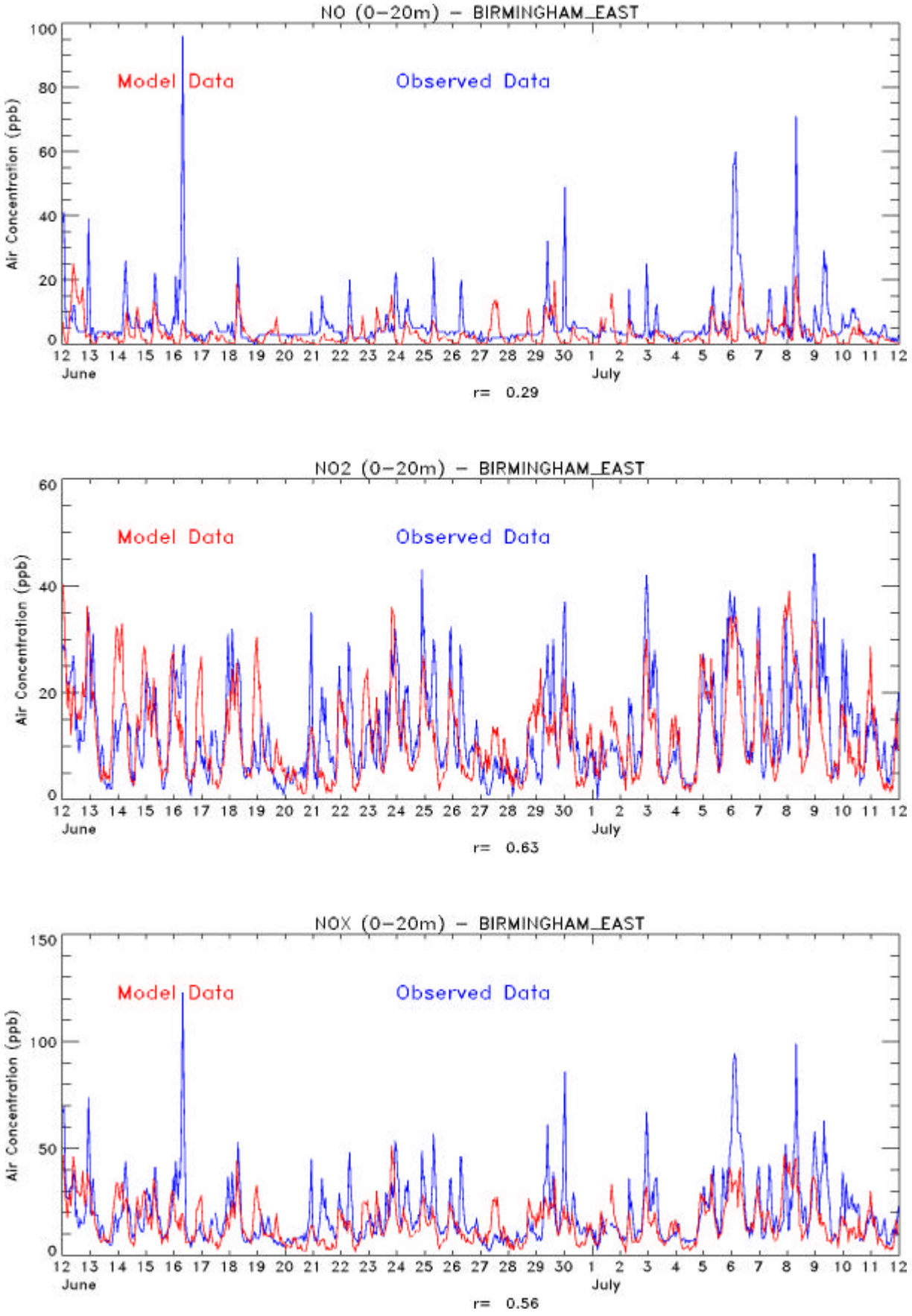

Figure 4.2 Modelled versus observed concentrations of NO, NO_2 and NO_X at Birmingham East.

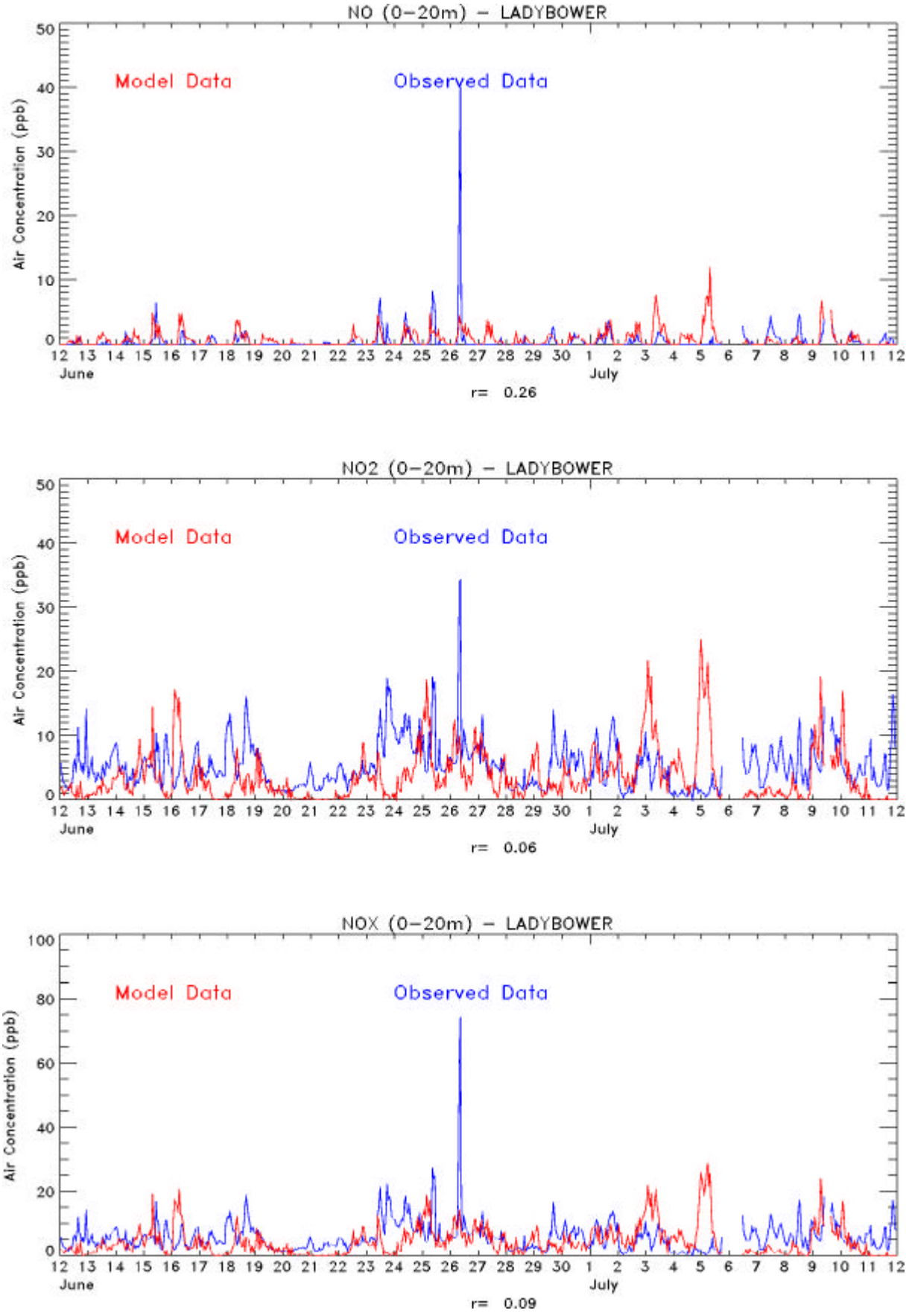

Figure 4.3 Modelled versus observed concentrations of NO, NO_2 and NO_X at Ladybower.

4.2 O_3

Figures 4.4-4.7 show plots of the model background ozone concentration plotted against observed ozone at Birmingham, Birmingham East, Ladybower and Bottesford. Bottesford is a rural site to the east of Birmingham and is situated on open heathland with the nearest road being an access road 60m away.

It can be seen that the method used to estimate background ozone in the model is somewhat limited but does represent some of the diurnal variation seen in the measurements. The approximation performs better at the urban locations than the rural. The model ozone, particularly at Bottesford, is not depleted sufficiently at nighttime. The model is not able to represent the peak in ozone occurring on 26/27th June which is around 80ppb as an hourly average at all the sites shown. The origin of this peak is likely to be ozone advected from outside the model domain as air arriving at Birmingham over this period is originating from Europe (see Appendix A).

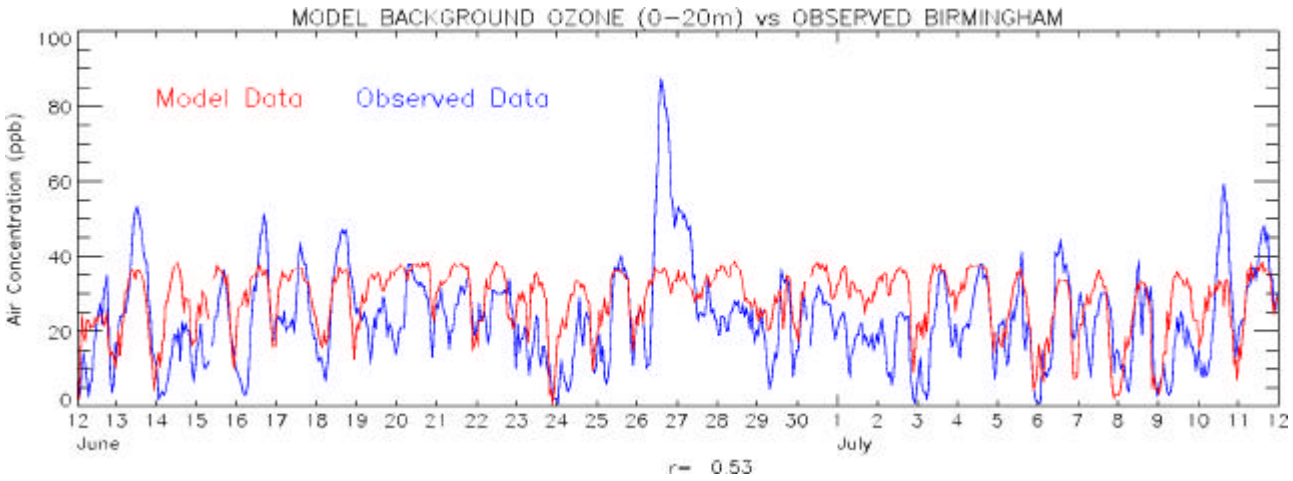

Figure 4.4 Model background ozone plotted against observed ozone at Birmingham Centre.

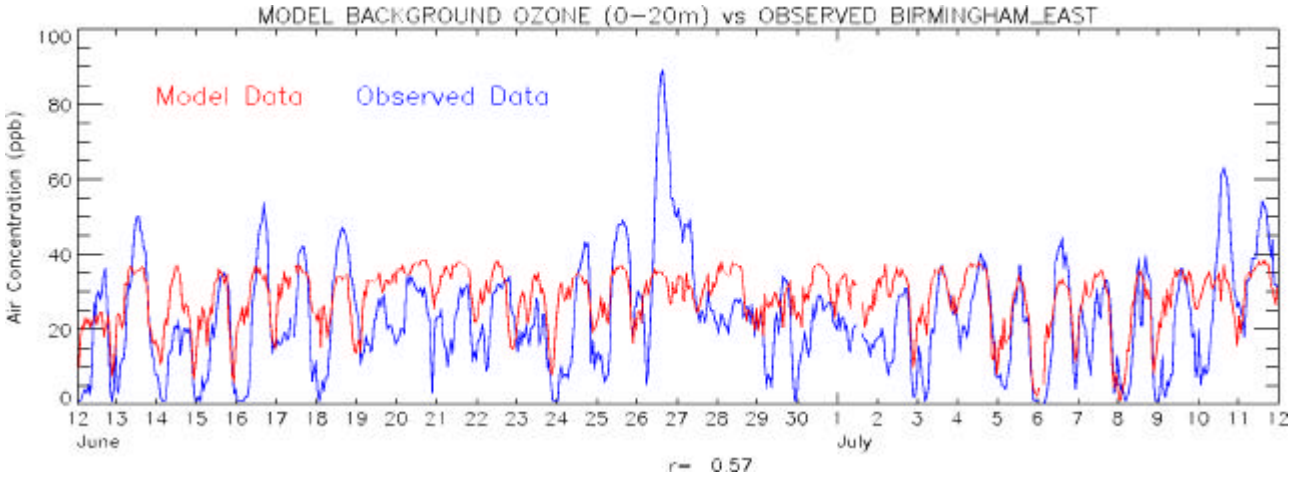

Figure 4.5 Model background ozone plotted against observed ozone at Birmingham East.

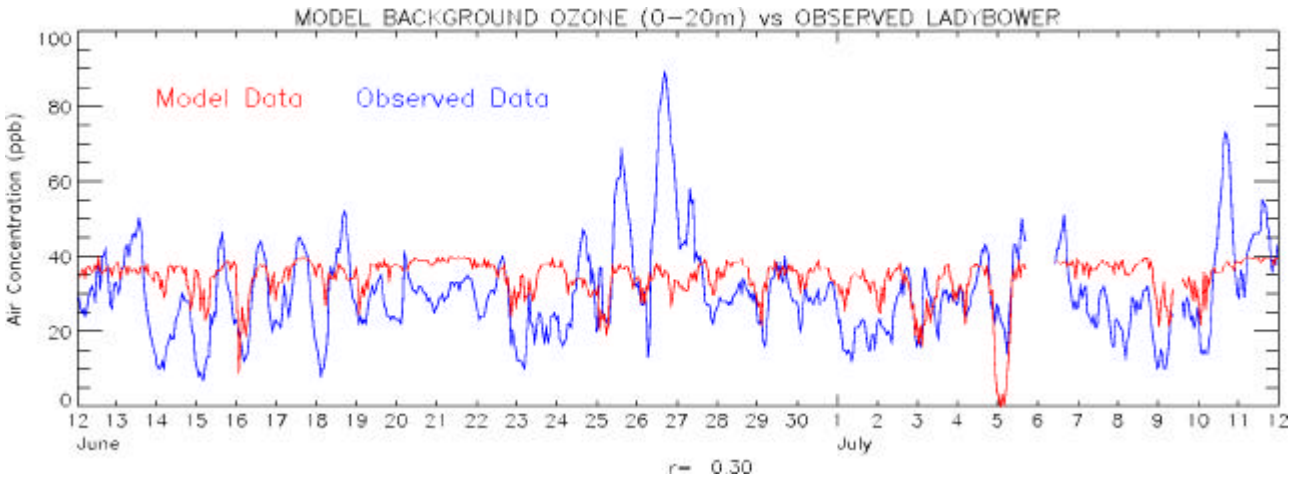

Figure 4.6 Model background ozone plotted against observed ozone at Ladybower.

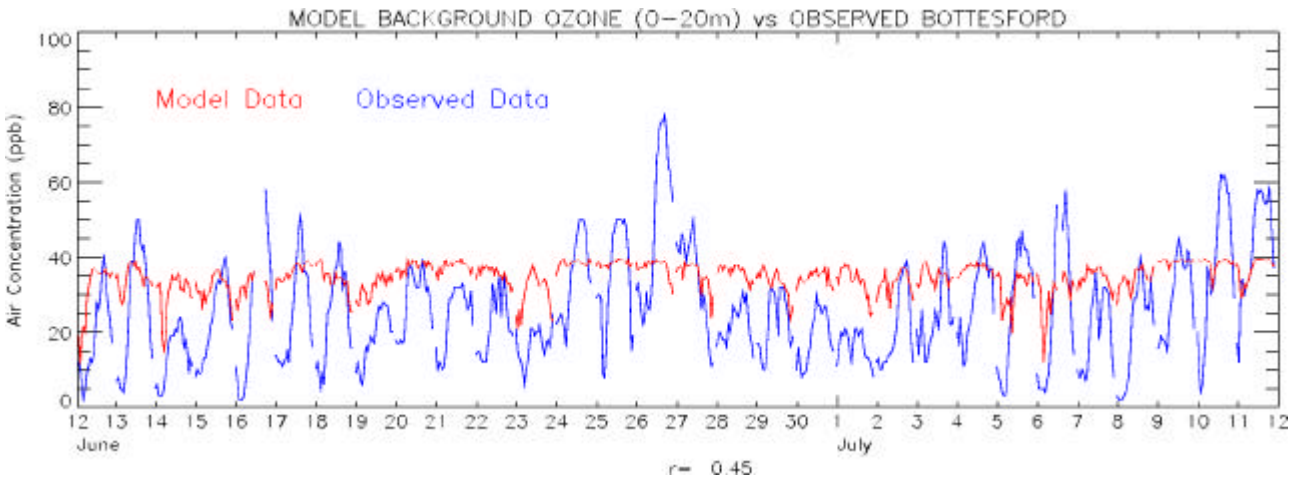

Figure 4.7 Model background ozone plotted against observed ozone at Bottesford.

As explained in section 3.1, the model also calculates an ozone production term on the plume particles, which represents the local production of ozone. In order to try to validate this, data from a rural ozone site at Aston Hill have been obtained. Aston Hill is situated directly to the west of Birmingham, some 75km away. This site was chosen rather than Bottesford (north-east of Birmingham) or Ladybower (north of Birmingham) as the dominant wind direction throughout both campaigns was westerly. The modelled ozone production term should represent the ozone formed during its transport over the Birmingham region; figure 4.8 shows 3 plots designed to help validate this. The top plot shows measured O_3 and NO_2 at Birmingham Centre. The sum of these two measurements gives an estimate of the total oxidant at Birmingham. This value is then compared with the measured O_3 at Aston Hill on the second plot. Ideally the comparison would be between the sum of O_3 and NO_2 at Aston Hill, however NO_2 is not measured at Aston Hill. The contribution from NO_2 at Aston Hill will however be lower than that seen in central Birmingham due to its rural location. The difference between these two traces represents the ozone production between Aston Hill and Birmingham and is calculated and plotted against the modelled ozone production term in the third graph. The method used is only correct for days when the air is travelling directly from Aston Hill to Birmingham, ie. when the wind is westerly, so for example the period 25th-27th June will not be represented at all well. The model is clearly underpredicting the amount of ozone produced, though does show some agreement with the measured data. Some part of the difference between the measured estimate of ozone production and that modelled will be due to the local NO_2 at Aston Hill.

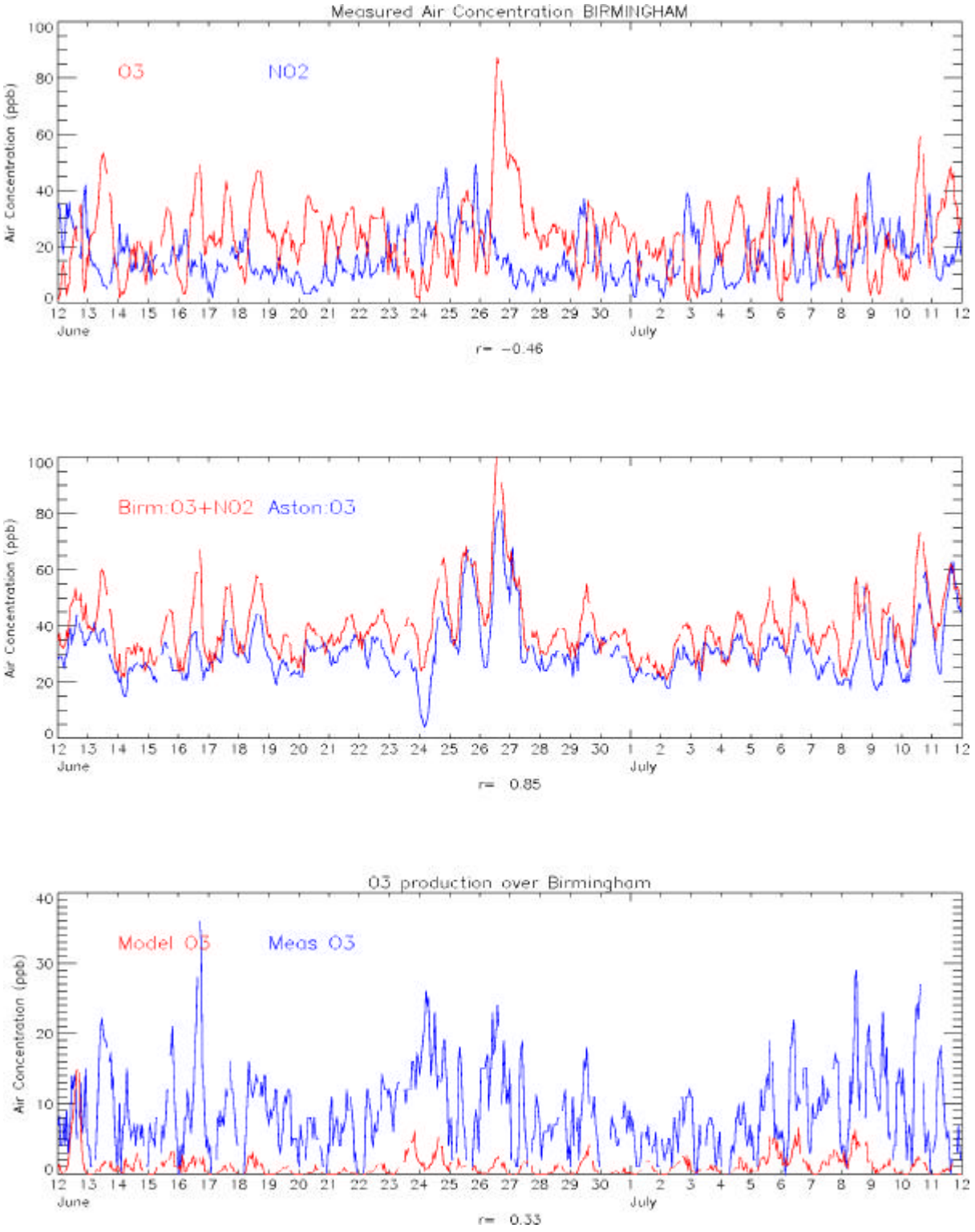

Figure 4.8 *Top*: observed O_3 and NO_2 air concentrations at Birmingham Centre. *Middle*: The sum of Birmingham Centre observed O_3 and NO_2 plotted against observed O_3 at Aston Hill. *Bottom*: Modelled ozone production at Birmingham plotted against the difference between the Birmingham oxidants (O_3 + NO_2) and the Aston Hill O_3 (which is labelled 'Meas O3').

4.3 OH, HO_2

Figures 4.9 and 4.10 show modelled OH and HO_2 concentrations plotted against measured data. The model data are available throughout the period, but for clarity has only been plotted where measured data are available. The modelled OH appears to be performing reasonably well against the observations, with a positive if low correlation, though this is calculated over a fairly limited number of data points. Assessing by eye, there is no clear bias in the modelled OH and it is estimated that most model data are within a factor of two of that measured, either over or under estimating. The exceptions are levels on the 18th and 25th June which are more of the order of a factor of three lower than that measured.

The agreement between the modelled HO_2 and the observations is not however as good. Figure 4.10 shows that the model is greatly underestimating the measured values and does not rise above $0.5x10^8$ molecule/cm^3, whereas the measured data rises over 6 $x10^8$ molecule/cm^3 on the 15th and 16th June, that is an order of magnitude higher.

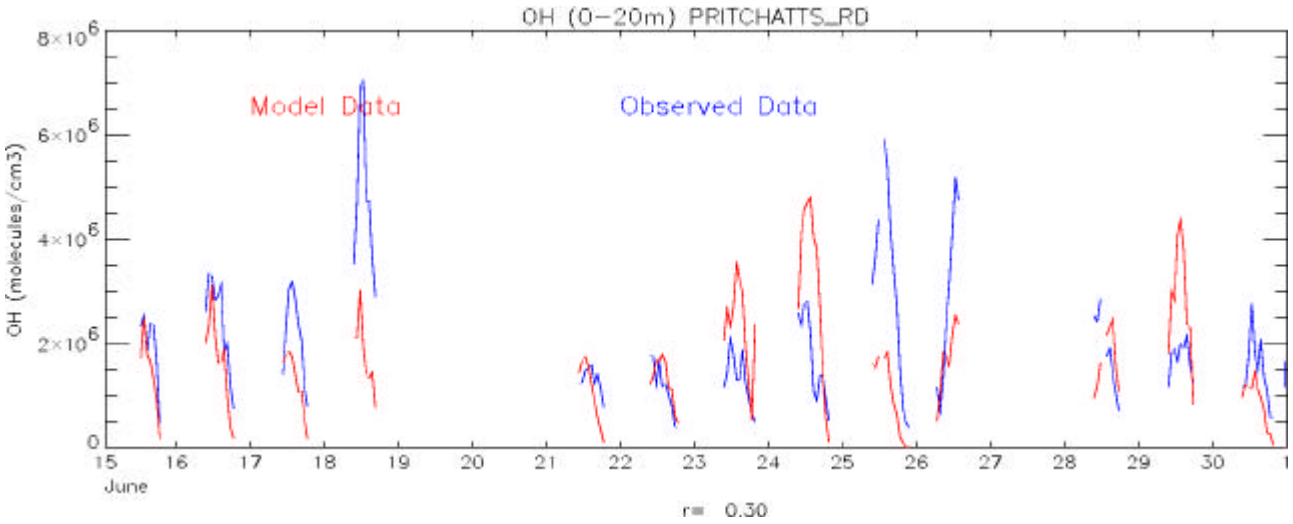

Figure 4.9 Modelled versus observed OH in molecule/cm^3 at Pritchatts Road.

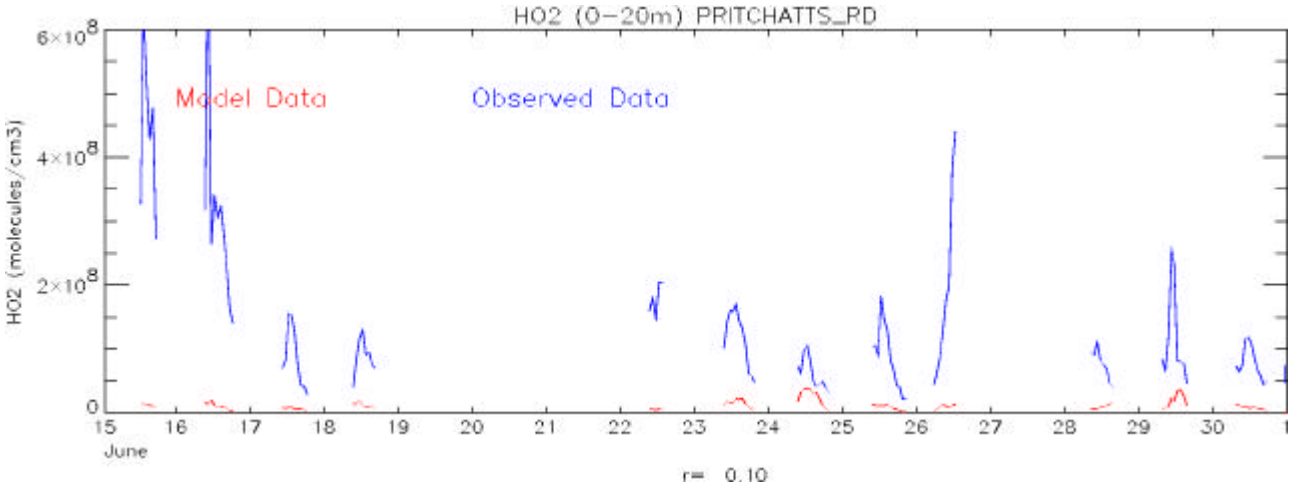

Figure 4.10 Modelled versus observed HO_2 in molecule/cm^3 at Pritchatts Road.

4.4 VOC

Figures 4.11-4.15 show plots of 1,3 butadiene, ethylene, isoprene, formaldehyde and toluene concentrations respectively. Where available the model output has been plotted against both data from the Birmingham East and Pritchatts Road sites. The modelled 1,3 butadiene has quite a reasonable correlation with the Birmingham East data, in general underpredicting slightly and underpredicting in particular night-time peaks on 13th June and 3rd, 6th & 9th July. The Pritchatts Road data also compare well, looking on average slightly higher than that modelled.

The ethylene concentrations also compare well at Birmingham East with a correlation of 0.59, the main difference being the failure to capture the full extent of some of the modelled peaks. The modelled isoprene is considerably lower than that measured at both sites. This is expected as we are only modelling the anthropengic emission of isoprene and are neglecting the biogenic emissions that are likely to dominate in the summer months.

The modelled formaldehyde is much lower than that measured at Pritchatts Road. The toluene compares quite well with that measured in terms of magnitude, but again misses some sharp peaks in concentration, some of which are at the same time (eg. 13th June) as those missed in the 1,3 butadiene data. Figures 4.11-4.15 allow us to conclude that the UK inventory and NAME are able to give a credible description of the VOC inventory across the the West Midlands.

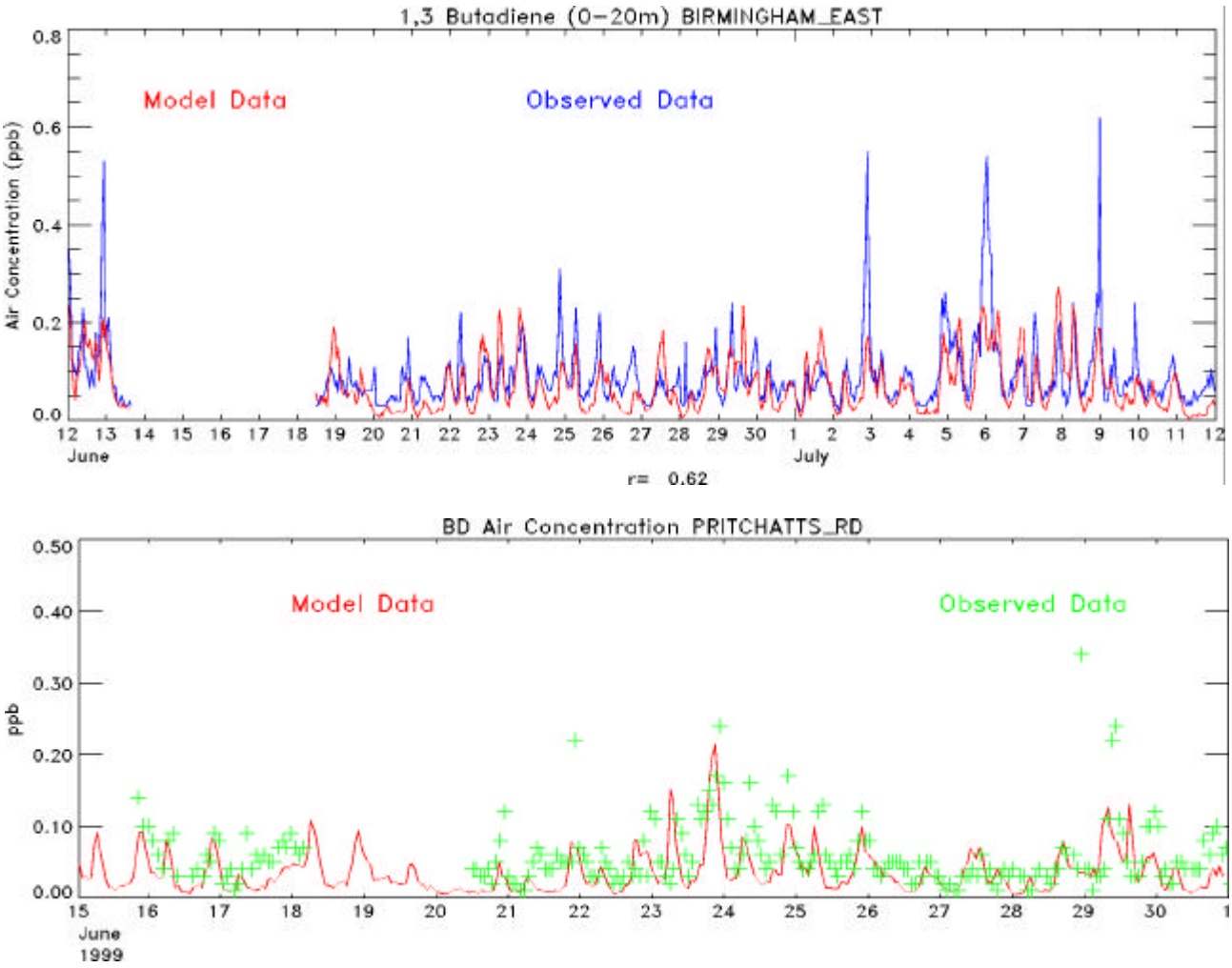

Figure 4.11 *Top*: Modelled versus observed 1,3 butadiene at Birmingham East. *Bottom*: Modelled and observed 1,3 butadiene at Pritchatts Road.

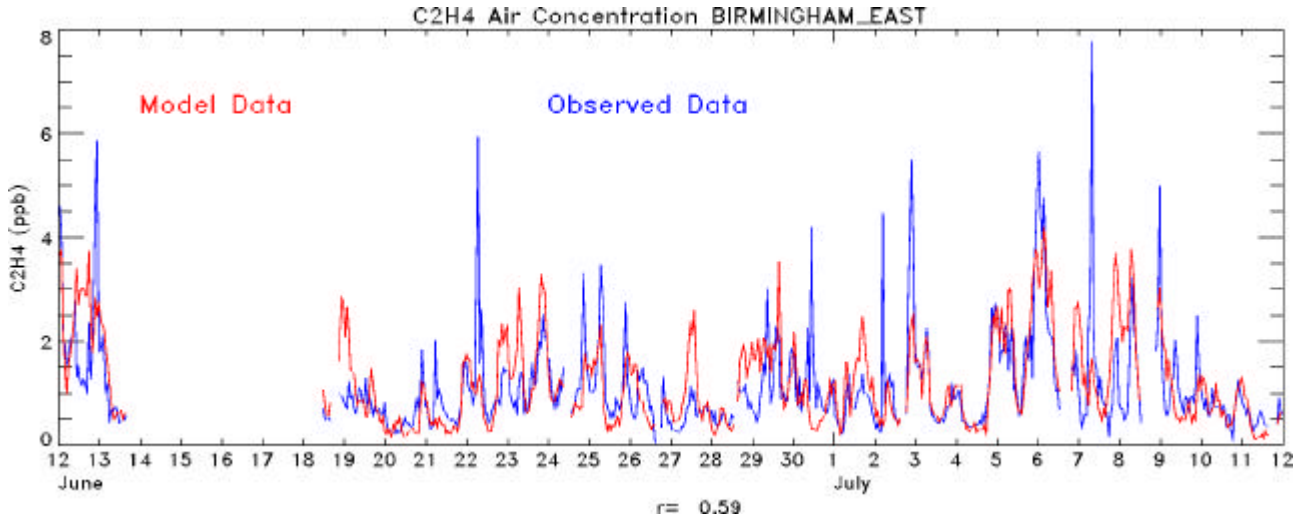

Figure 4.12 Model versus observed ethylene at Birmingham East.

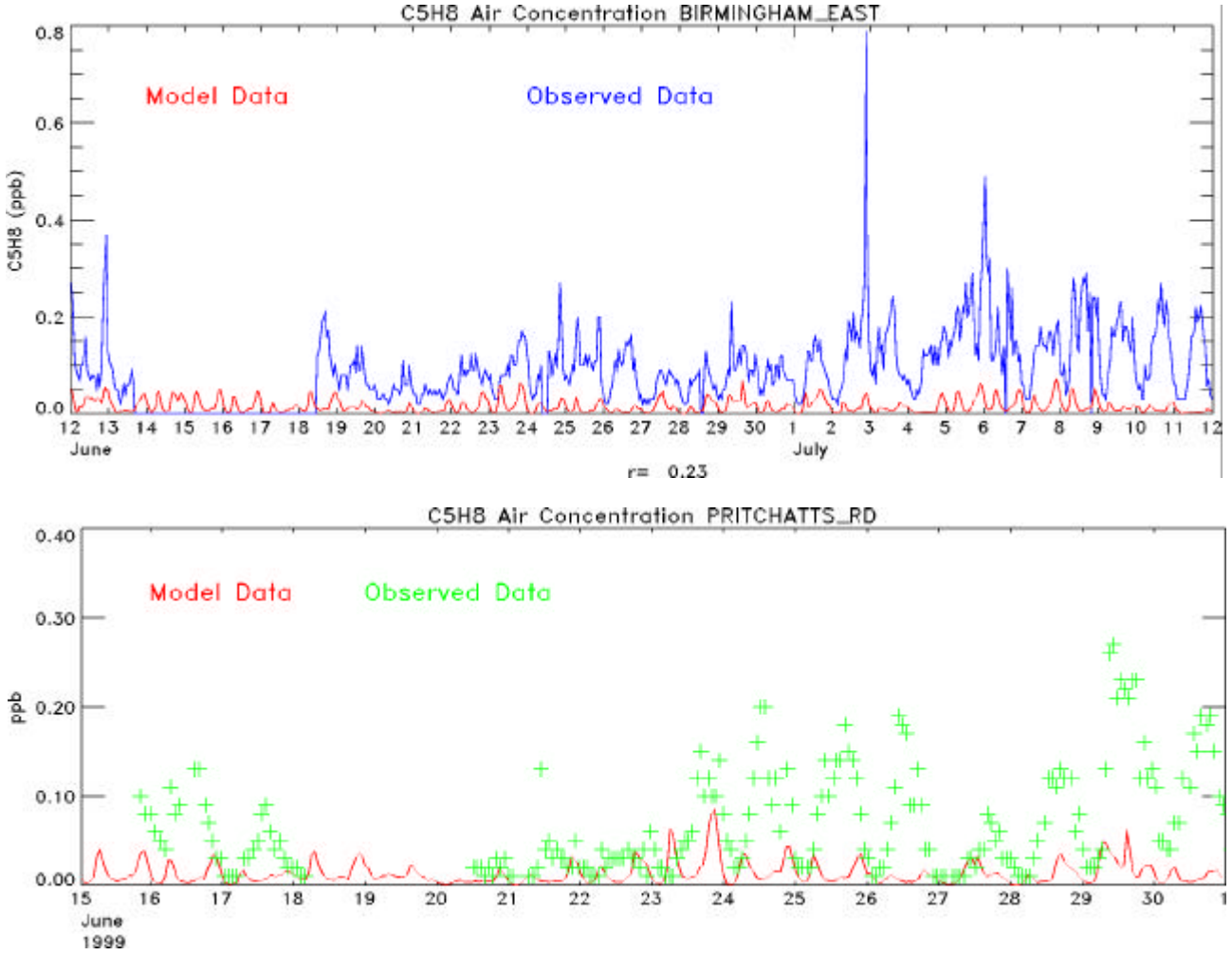

Figure 4.13 *Top*: model versus observed isoprene at Birmingham East. *Bottom*: Modelled and observed isoprene at Pritchatts Road.

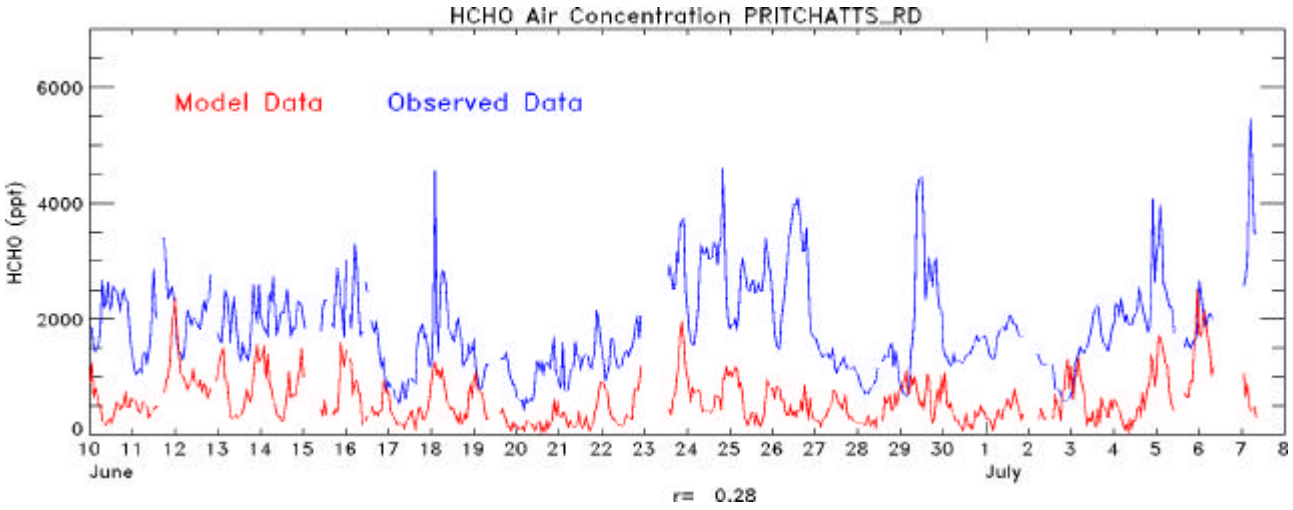

Figure 4.14 Modelled versus observed formaldehyde at Pritchatts Road.

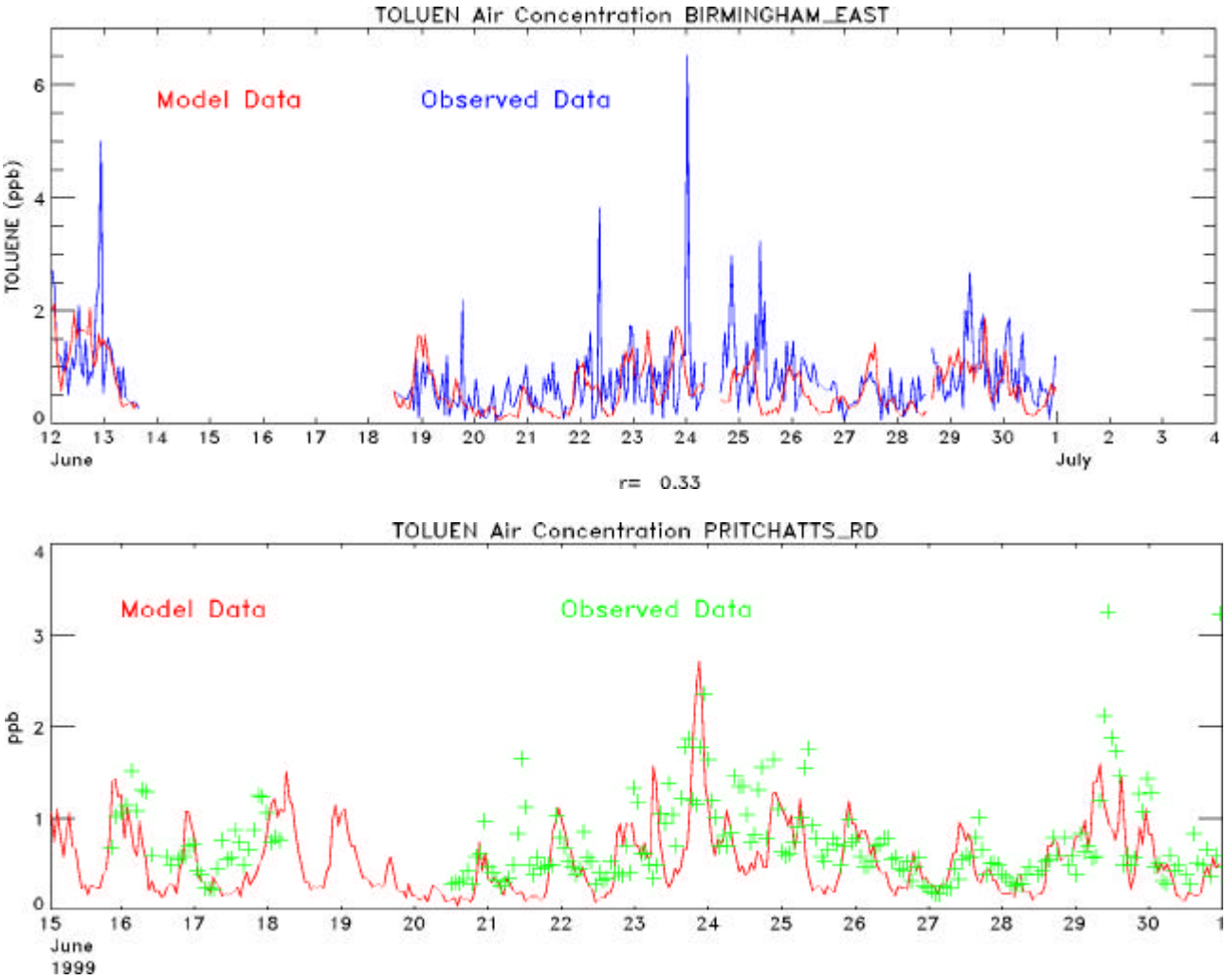

Figure 4.15 *Top*: modelled versus observed toluene at Birmingham East. *Bottom*: model toluene data and observed data at Pritchatts road.

4.5 Nitrate Aerosol, HNO_3 & NH_3

Figures 4.16 - 4.18 show nitrate aerosol, nitric acid and ammonia concentrations respectively. Nitrate aerosol is modelled as uptake of NO_3^- to aerosol and formation of ammonium nitrate from the equilibrium reaction with ammonia and nitric acid. The daily averaged model nitrate aerosol (red) is too low compared with measurements (blue), the nitric acid is reasonable but a bit low and the ammonia too high. The balance between the amount of ammonium nitrate and the amount of nitric acid can be controlled by applying a kinetic constraint to the formation of the equilibrium. In previous model runs without the kinetic constraint, both nitric acid and nitrate aerosol were low, the implementation of the constraint has adjusted the balance between them in favour of the nitric acid, but the sum of nitric acid and nitrate aerosol is still too low. The ammonia emission information is of poor resolution (50km) and it is therefore not surprising that this species does not compare very well with that observed.

A dotted red line is also plotted on figure 4.16 which is an attempt to account for the contribution to the modelled nitrate aerosol from long range transport. This amount has been calculated by running a simplified version of the chemistry scheme over a European wide domain. The Lagrangian nature of the model allows us to label each released model particle with its place of origin, so that we can sort the particles arriving at a particular receptor location (eg Birmingham) into those originating from inside the UK and those from outside. As the chemistry scheme used is different than that used in the model described here, it was not thought appropriate to add the actual amount of aerosol generated from Europe in the simpler model, but instead the daily average percentage of nitrate aerosol from Europe (excluding the UK) has been calculated for the summer campaign period. (The total amount of aerosol calculated in the European wide model is shown as the pink dashed line that can be seen to greatly overpredict during the summer.) The daily percentages of European import vary from 15-30% and the appropriate amount has been calculated from the model data shown in red and has been added to it to result in the red dotted line. Whilst the European import of aerosol is obviously contributing to that measured in Birmingham, it is not dominating over the locally formed aerosol over this period, and it therefore seems unlikely that it is the reason for the large model underprediction seen.

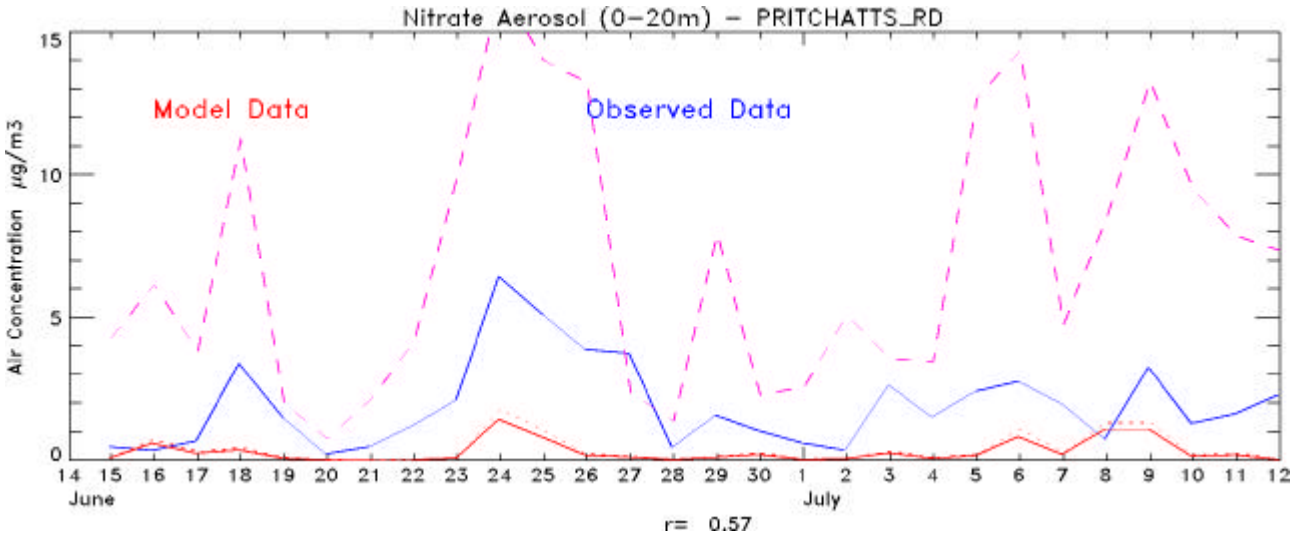

Figure 4.16 Modelled versus observed daily average nitrate aerosol at Pritchatts Road.

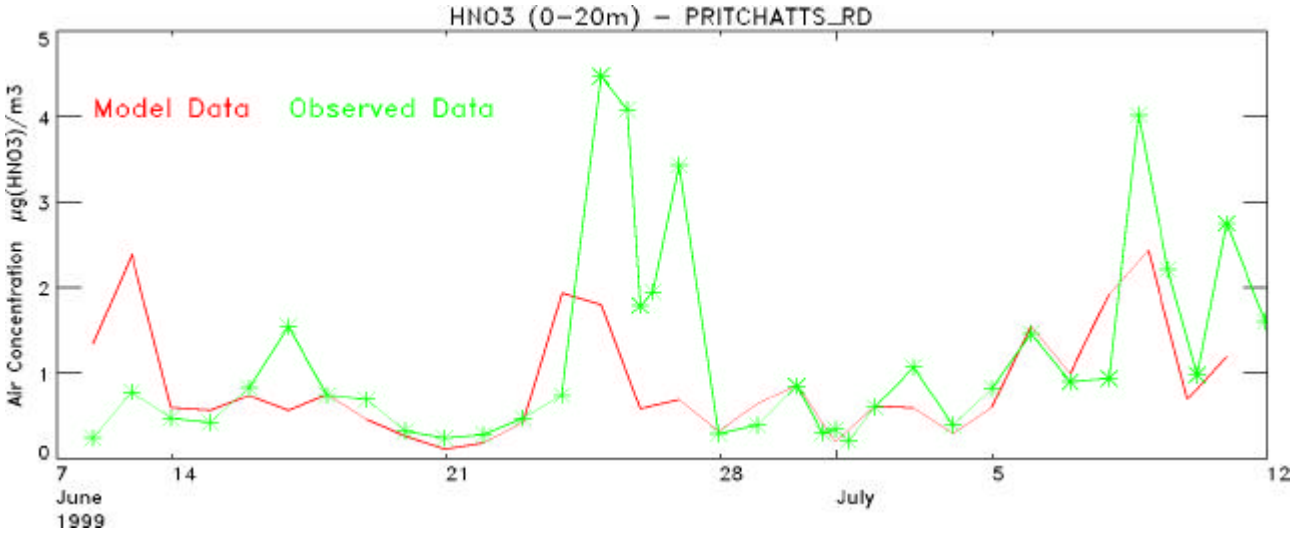

Figure 4.17 Daily average model nitric acid overplotted with observed nitric acid at Pritchatts Road.

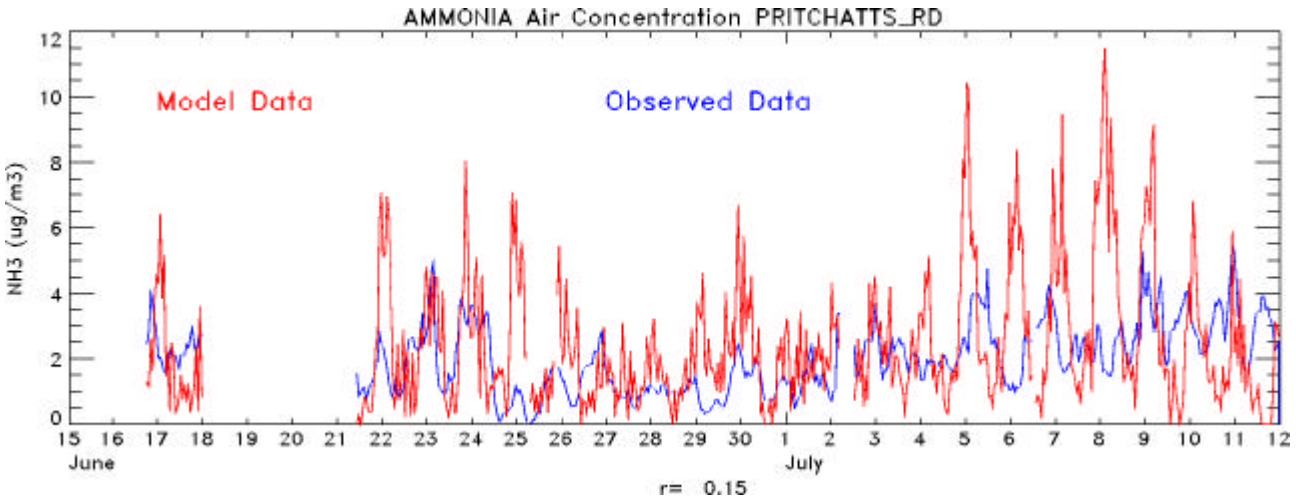

Figure 4.18 Model versus observed ammonia at Pritchatts Road.

4.6 HONO

Figure 4.19 shows modelled nitrous acid concentration plotted with measured data at Pritchatts road. In order to best display the data the two highest values measured are off the vertical scale, these are 1.75µ/m^3 and 4.32µ/m^3 in time order. The modelled daily average is consistently low and does not compare well with most of the measured data, failing to capture in any way the two highest values recorded.

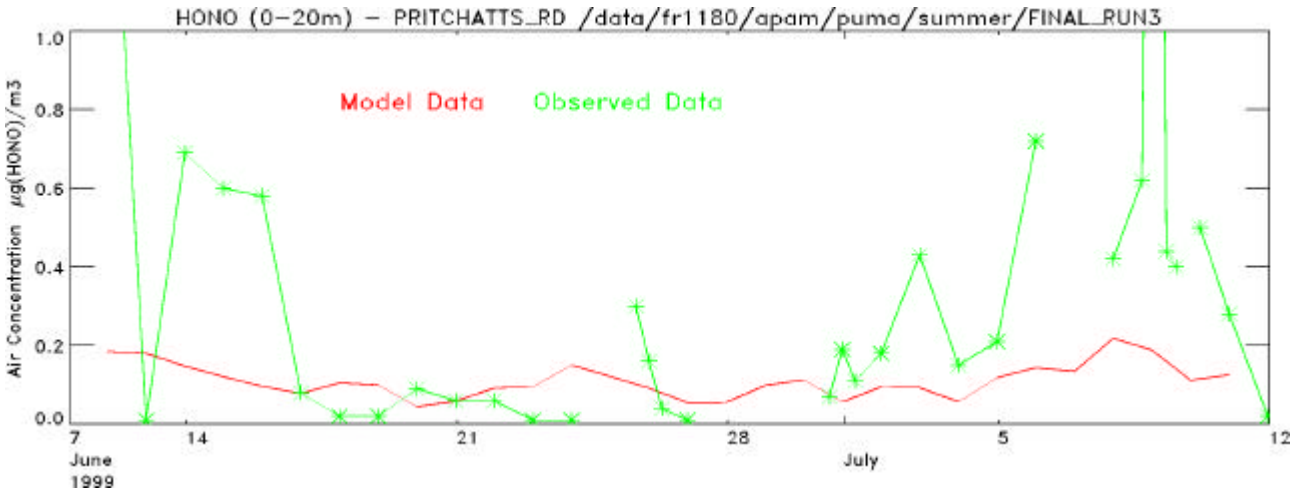

Figure 4.19 Daily average model HONO over plotted with measurement data from Pritchatts Road.

4.7 PAN

Figure 4.20 shows the modelled and measured PAN concentrations. The model has performed poorly and does not exhibit any skill in predicting this species. The bulk of the PAN is expected to be carried into the model domain from the regional background, and this contribution has not been modelled.

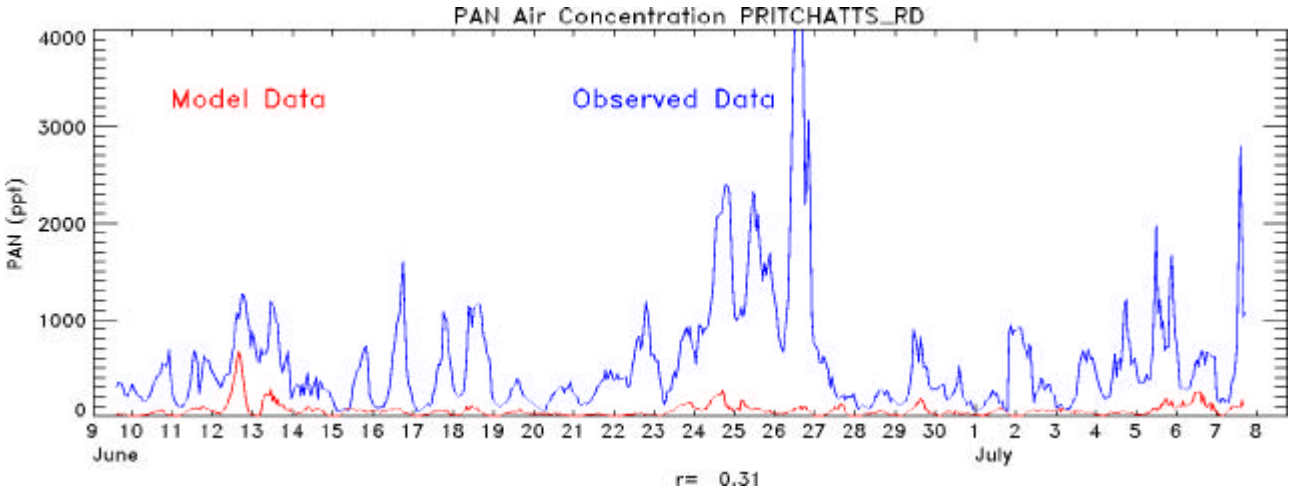

Figure 4.20 Modelled versus observed PAN at Pritchatts Road.

4.8 CO

Figures 4.21 and 4.22 show modelled and observed concentration data for CO at Birmingham and Birmingham East. The correlation at both sites is approximately 0.4, however the magnitudes are low, most notably at Birmingham Centre. Again much of CO (certainly up to 0.1-0.2 ppm) is expected to come from the regional background.

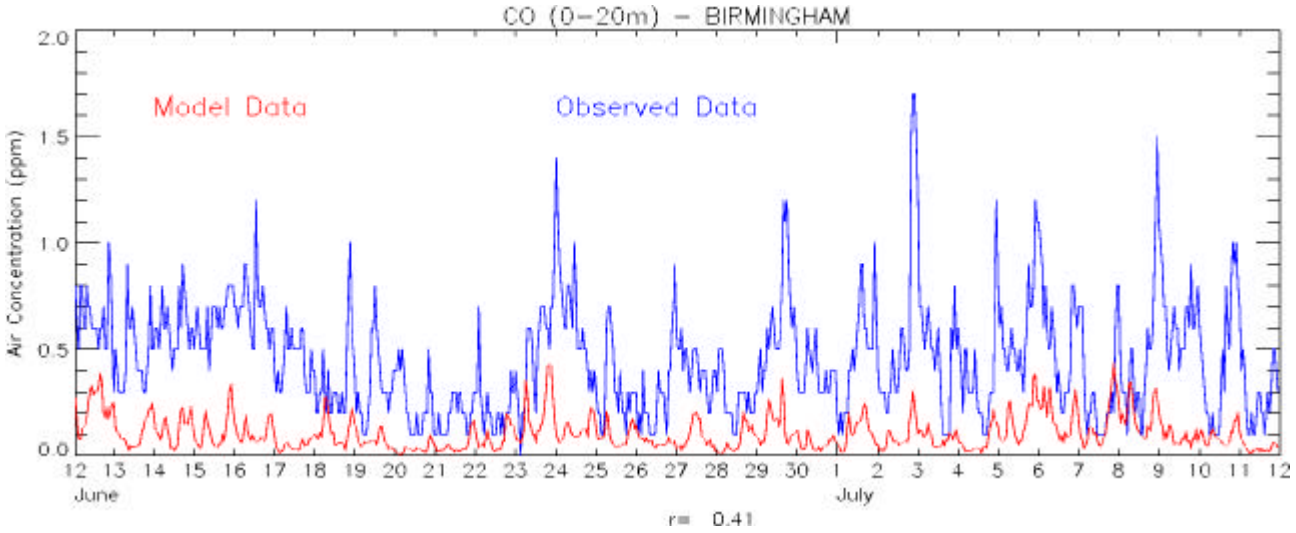

Figure 4.21 Modelled versus observed CO at Birmingham Centre.

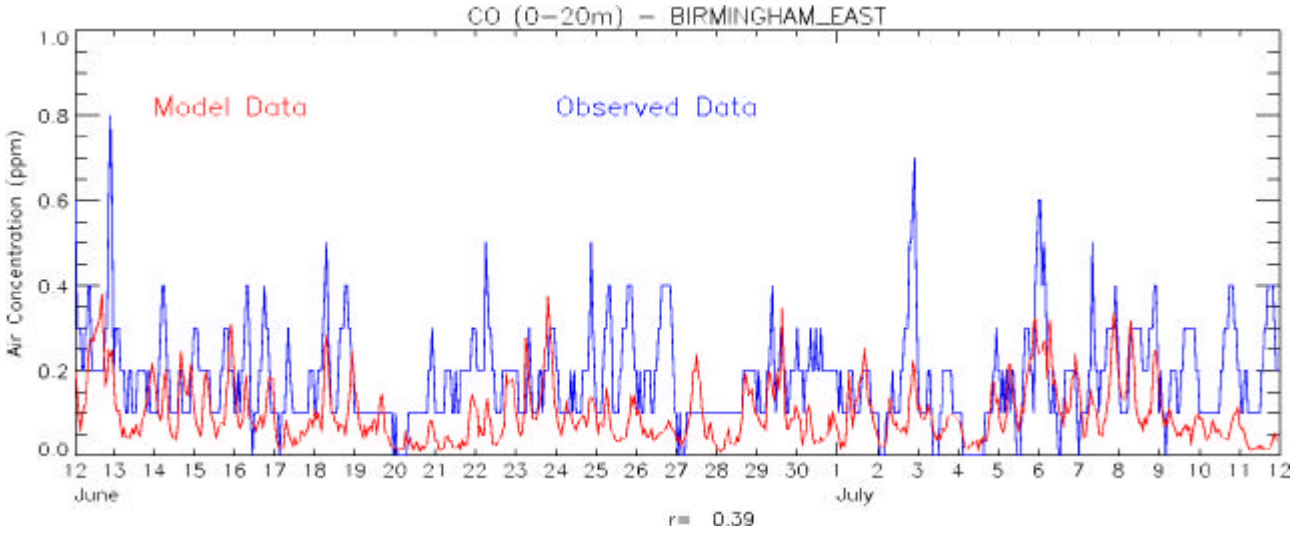

Figure 4.22 Modelled versus observed CO at Birmingham East.

4.9 SO_2

Figures 4.23 – 4.25 show sulphur dioxide concentration plots for Birmingham, Birmingham East and Ladybower. The agreement between the modelled and observed SO_2 is characteristically poor. Sulphur dioxide emissions are dominated by the large power stations, and without detailed hour-by-hour emissions data it is hard to generate accurate model predictions. The 1998 annual average emissions generally seem to overpredict slightly, which is in line with the declining emissions of sulphur dioxide.

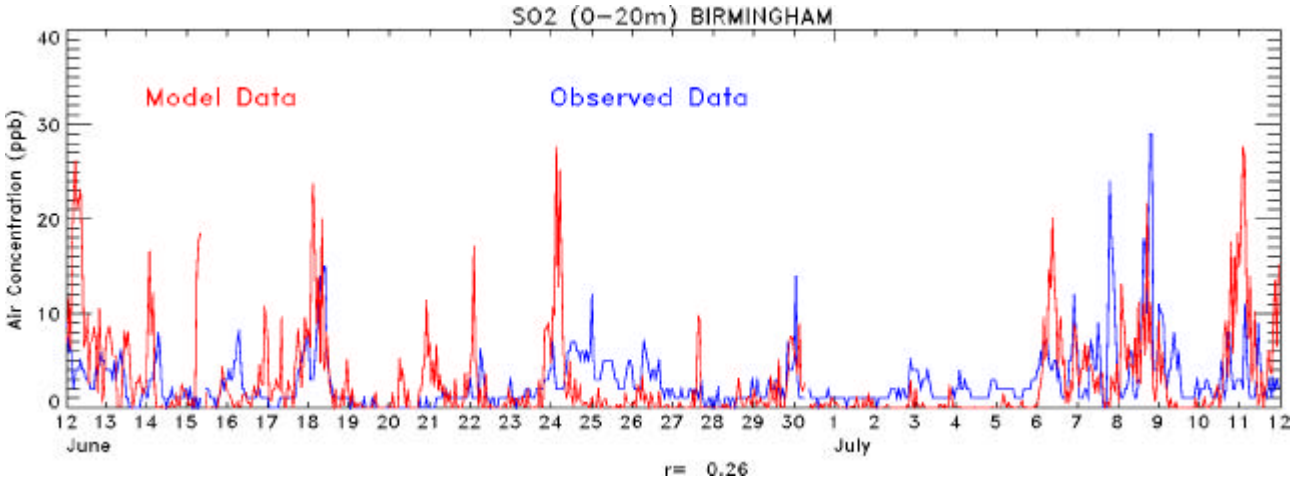

Figure 4.23 Modelled versus observed SO_2 at Birmingham Centre.

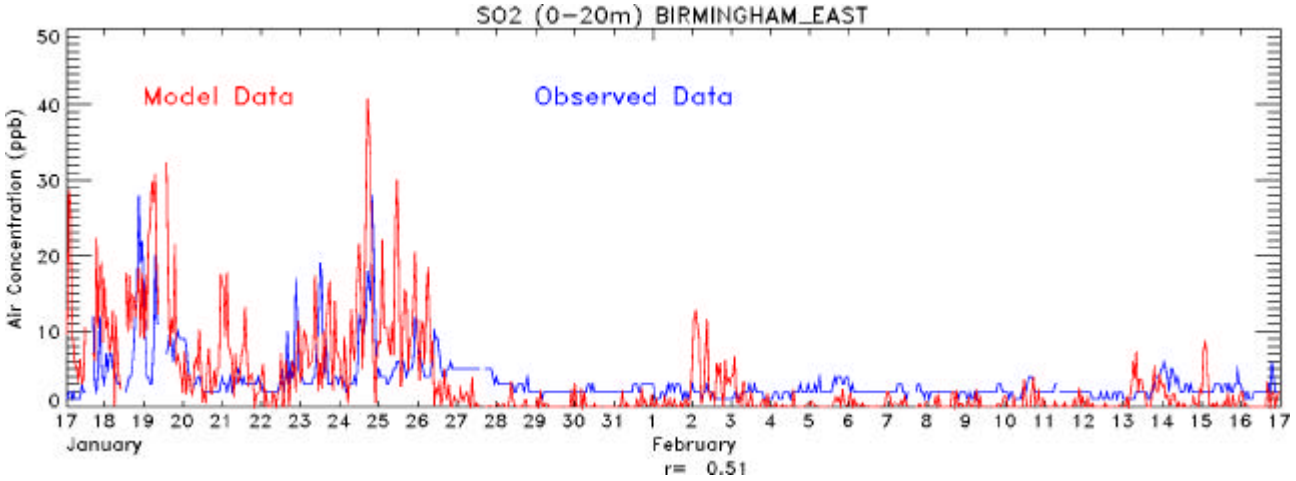

Figure 4.24 Modelled versus observed SO_2 at Birmingham East.

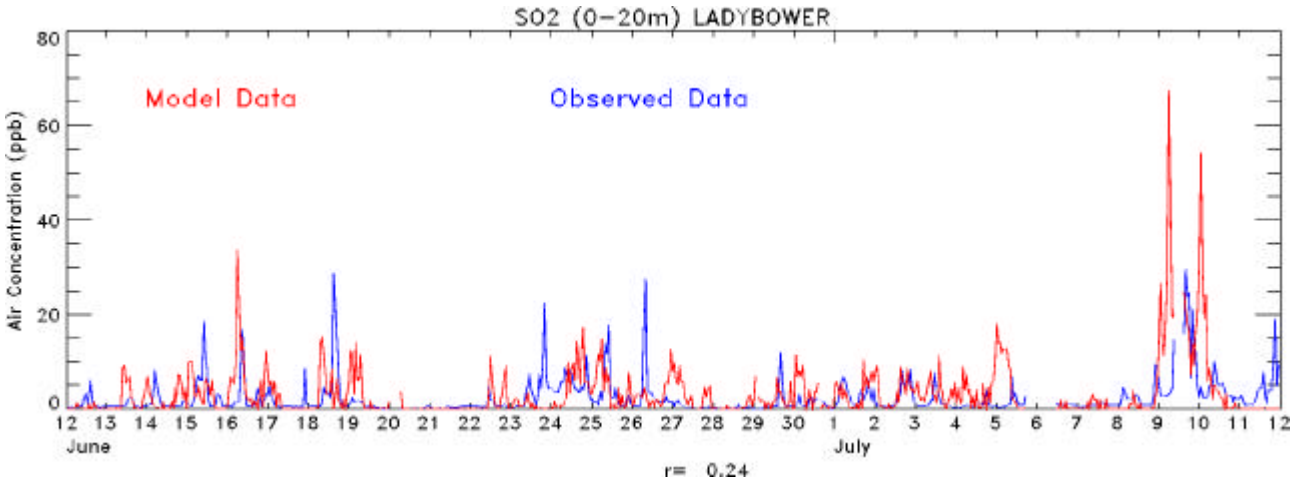

Figure 4.25 Modelled versus observed SO_2 at Ladybower.

4.10 Sulphate Aerosol

Figure 4.26 shows daily average modelled and measured sulphate aerosol concentrations at Pritchatts Road. The model is underpredicting virtually throughout the period, but not to as greater an extent as seen in the nitrate aerosol. A dotted red line is also shown to include the likely contribution from European sources over this period. This has been calculated using daily percentages in the same way as is described in section 4.5, and the actual modelled sulphate aerosol from the European run is shown as the pink dashed line. This model overpredicts sulphate aerosol in the summer. It would be preferable to be able to add in the actual amount of aerosol being imported, however due to the different chemistry schemes used this is not appropriate. Ideally the full chemistry scheme described here would be run over the European domain, but this is currently computationally prohibitive.

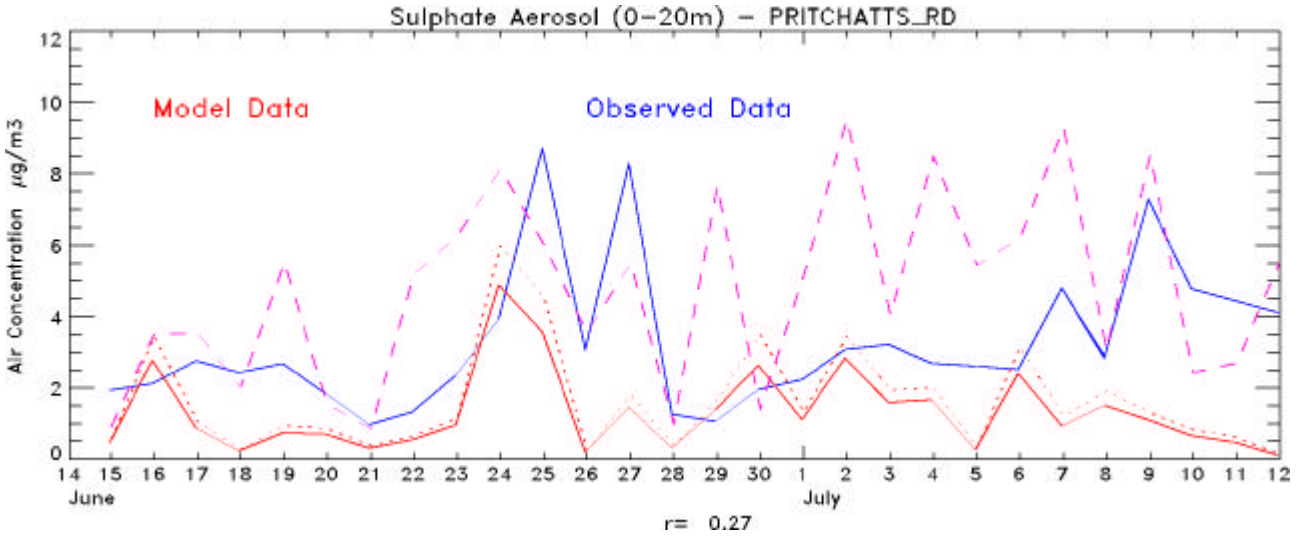

Figure 4.26 Daily average model versus observed sulphate aerosol at Pritchatts Road.

4.11 H_2O

Figure 4.27 shows model water vapour by % volume (extracted from the mesoscale meteorological data) plotted against measured data from Pritchatts Road. Except for the 16th June the model generally follows the pattern of the measured data, but is slightly lower than that measured.

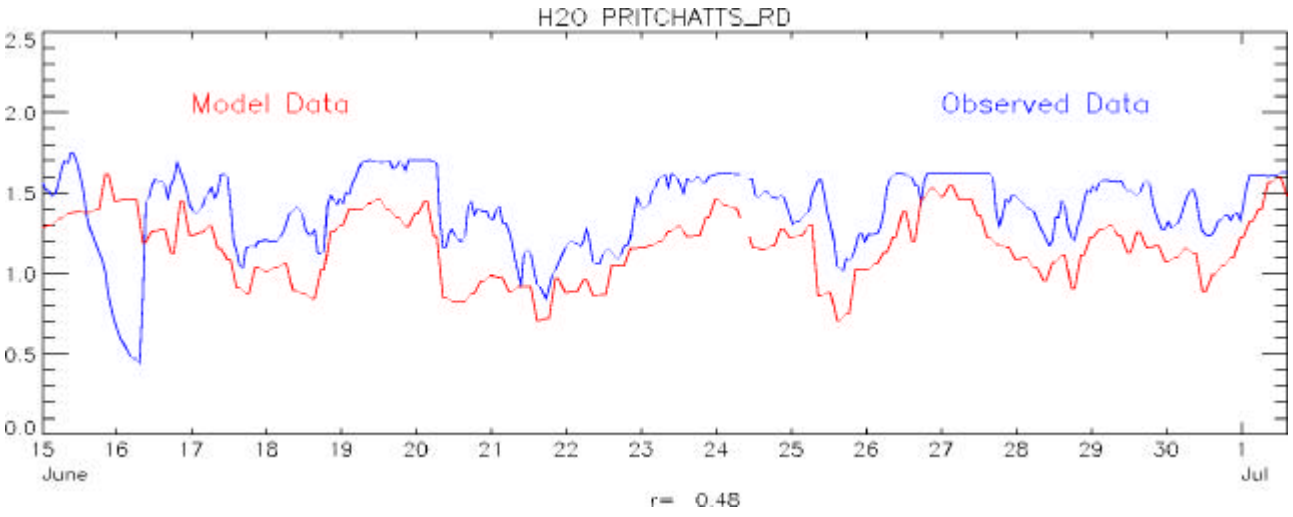

Figure 4.27 Model versus observed water vapour in % by volume at Pritchatts Road.

4.12 J O^1D

Figure 4.28 shows the value of the O_3 photolysis rate coefficient, J O^1D, used in the model and that which was measured at Pritchatts Road. It is disappointing to note that the rate used in the model does not seem to be varying with the cloud column, and thus remains at a constant value throughout. The code that was implemented to alter the rates in the presence of cloud must be checked.

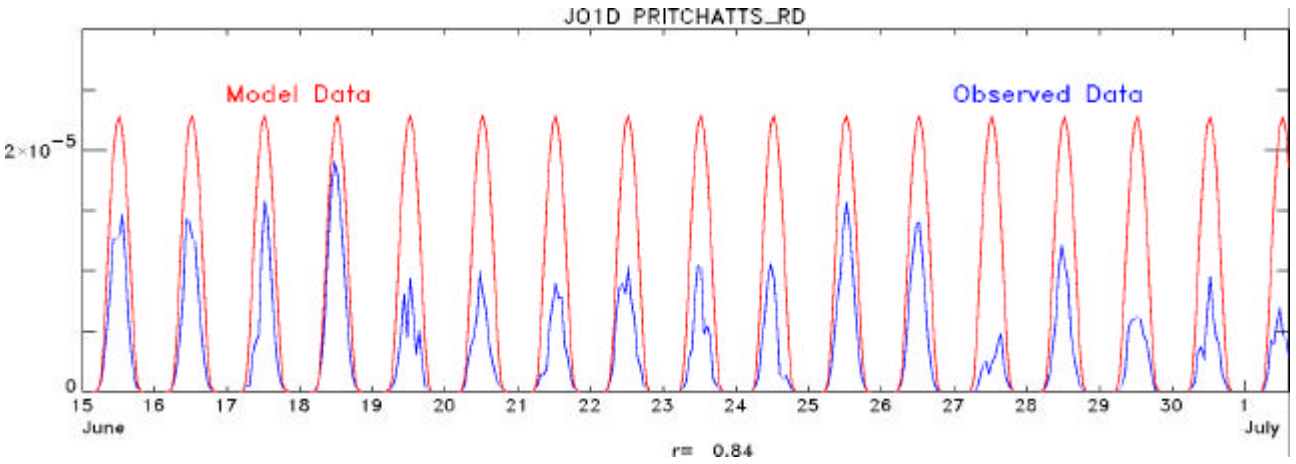

Figure 4.28 Modelled versus observed J O^1D values (s^{-1}) at Pritchatts Road.

4.13 PM_{10}

Figure 4.29 shows modelled versus measured PM_{10} concentrations at Birmingham Centre. The model underpredicts by as much as 20 µg/m^3 at times and shows no particular skill with a correlation of just 0.17. The modelled PM_{10} is comprised of primary, sulphate aerosol and nitrate aerosol and these components are shown separately in figure 4.30. Given that it is not likely that the TEOM measurement device at Birmingham Centre will be measuring the nitrate aerosol component of PM_{10} it is debatable whether it is correct to include nitrate aerosol in the modelled value, however as demonstrated in figure 4.16 the modelled nitrate aerosol is rather lower than that observed so its impact will not be great anyway. The model sulphate aerosol is also underpredicted in the summer but it still contributes quite substantially to the overall modelled PM_{10}. The estimated European contributions have not been added in, thus the increase in sulphate aerosol seen in figure 4.26 will increase the modelled PM_{10} magnitude as would including any primary PM_{10} that is imported from Europe. Previous work modelling PM_{10} over a European wide domain with the NAME model (Malcolm & Manning 2001) has also shown a consistent underprediction of the model compared with measured values, so the poor results seen here were largely as expected.

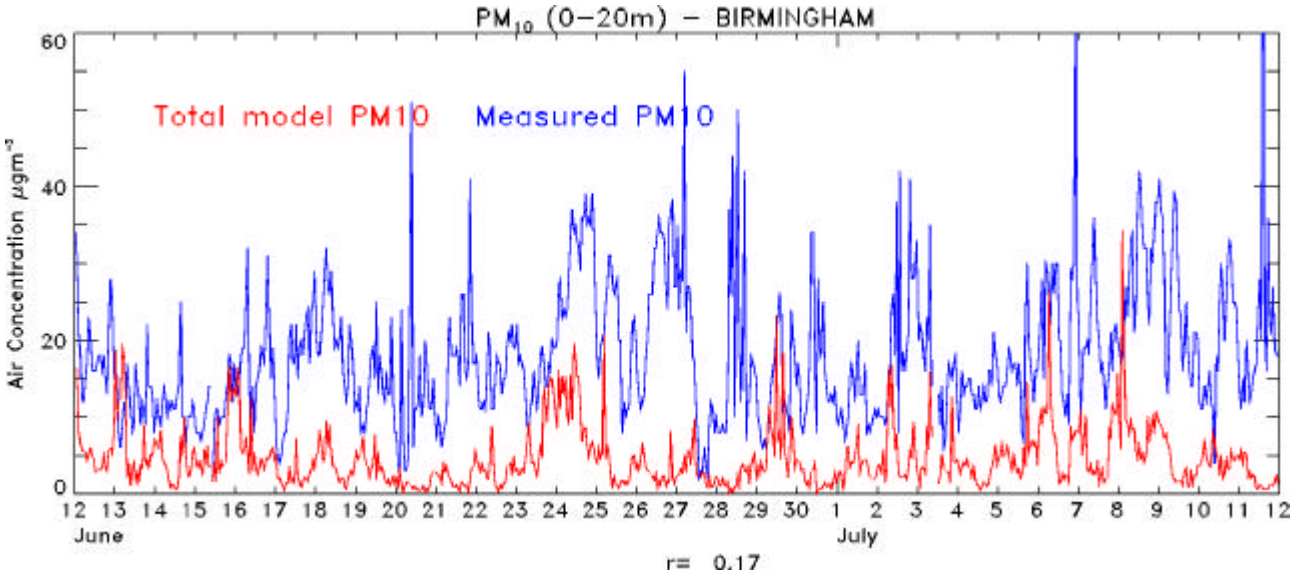

Figure 4.29 Modelled versus observed PM_{10} at Birmingham Centre.

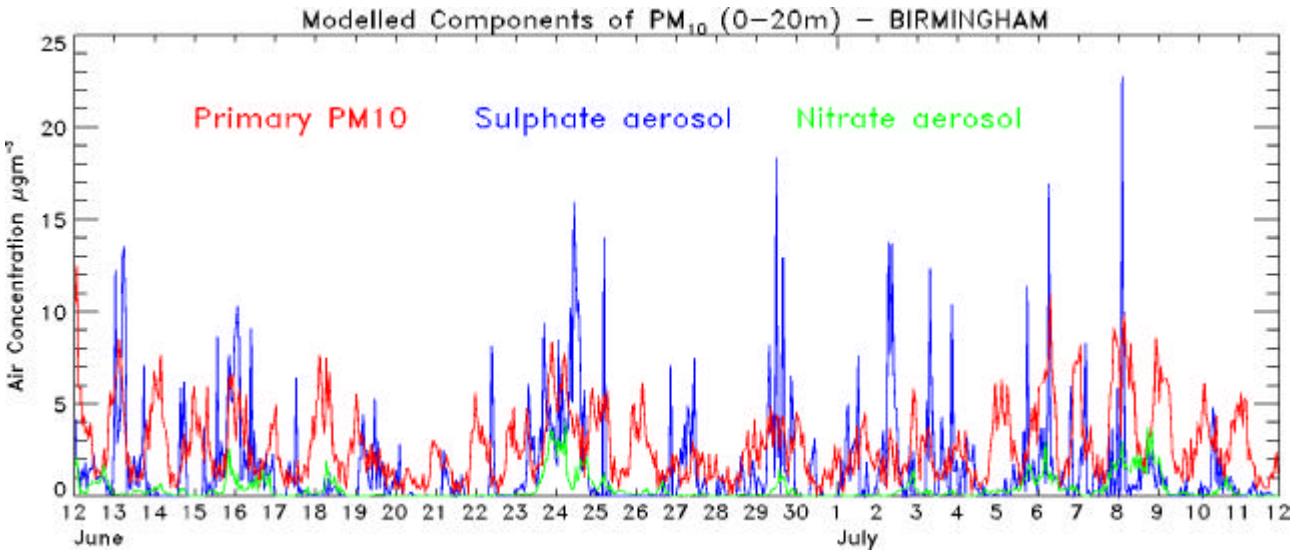

Figure 4.30 The three components of the modelled PM_{10}: sulphate aerosol, nitrate aerosol and primary PM_{10} at Birmingham Centre.

5.0 The Winter Campaign

The winter campaign was from 17th January – 17th February 2000. The wind directions were predominantly northwestlerly or westerly during the campaign, with the exception of 27th-29th January, 31st January – 2nd February and 4th – 6th February where there were easterly and southerly components. Appendix A shows plots of where the air has originated from that is arriving in Birmingham over 24 hour periods throughout the campaign.

5.1 NO, NO_2, NO_X

Figures 5.1 - 5.3 show plots of modelled and observed NO, NO_2 and NO_X concentrations for the Birmingham Centre, Birmingham East and Ladybower sites. The model predictions at Birmingham Centre are good, with the only problems being that the full extent of the NO peaks on the 25th January and 14th February were not captured, being about a factor of three too low. At Birmingham East, again the predictions are good, particularly of NO_2, however the model has again failed to capture the full extent of some of the measured peaks in NO. The peaks on 24/25/26th January are too low by approximately a factor of two, however the peak on 19/20th and 13/14th were much greater than those measured at Birmingham Centre by several hundred ppb. Given the proximity of these two locations it is concluded that it is perhaps a local source (either not included in the emissions inventory or a known source emitting at a rate significantly above the annual average) is causing these high spikes seen at Birmingham East. At Ladybower the NO levels are generally very low throughout as would be expected for a rural location, but with a peak of 20ppb on the 18/19th and 80ppb on 25/26th. In the first half of the period the modelled NO is almost completely flat, which is probably because the wind direction is north-westerly throughout this period and as Ladybower is close to the edge of the domain, NO is not being advected into the domain. This obviously impacts the amount of NO_2 generated in the model in this area.

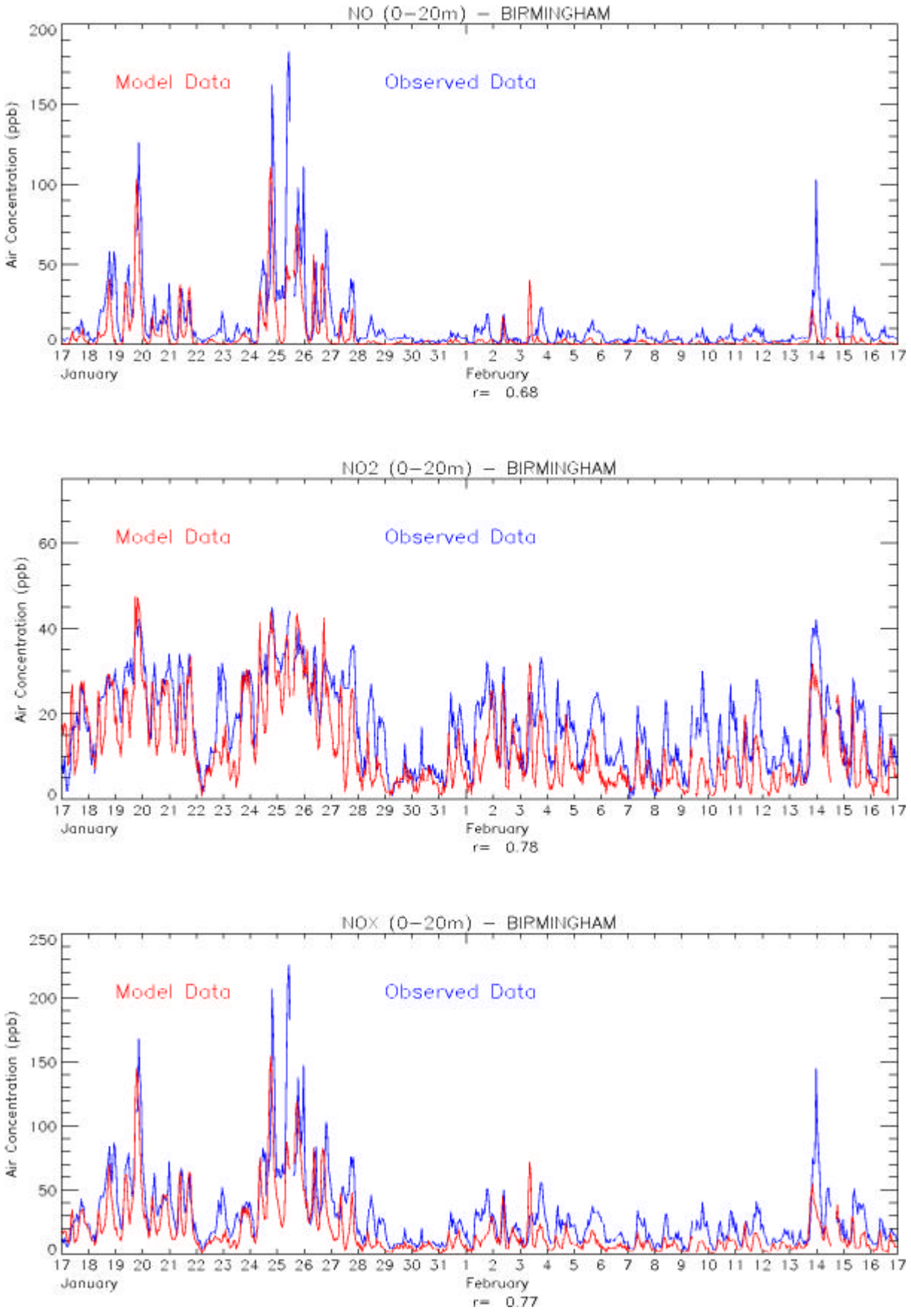

Figure 5.1 Modelled versus observed concentrations of NO, NO_2 and NO_X at Birmingham Centre.

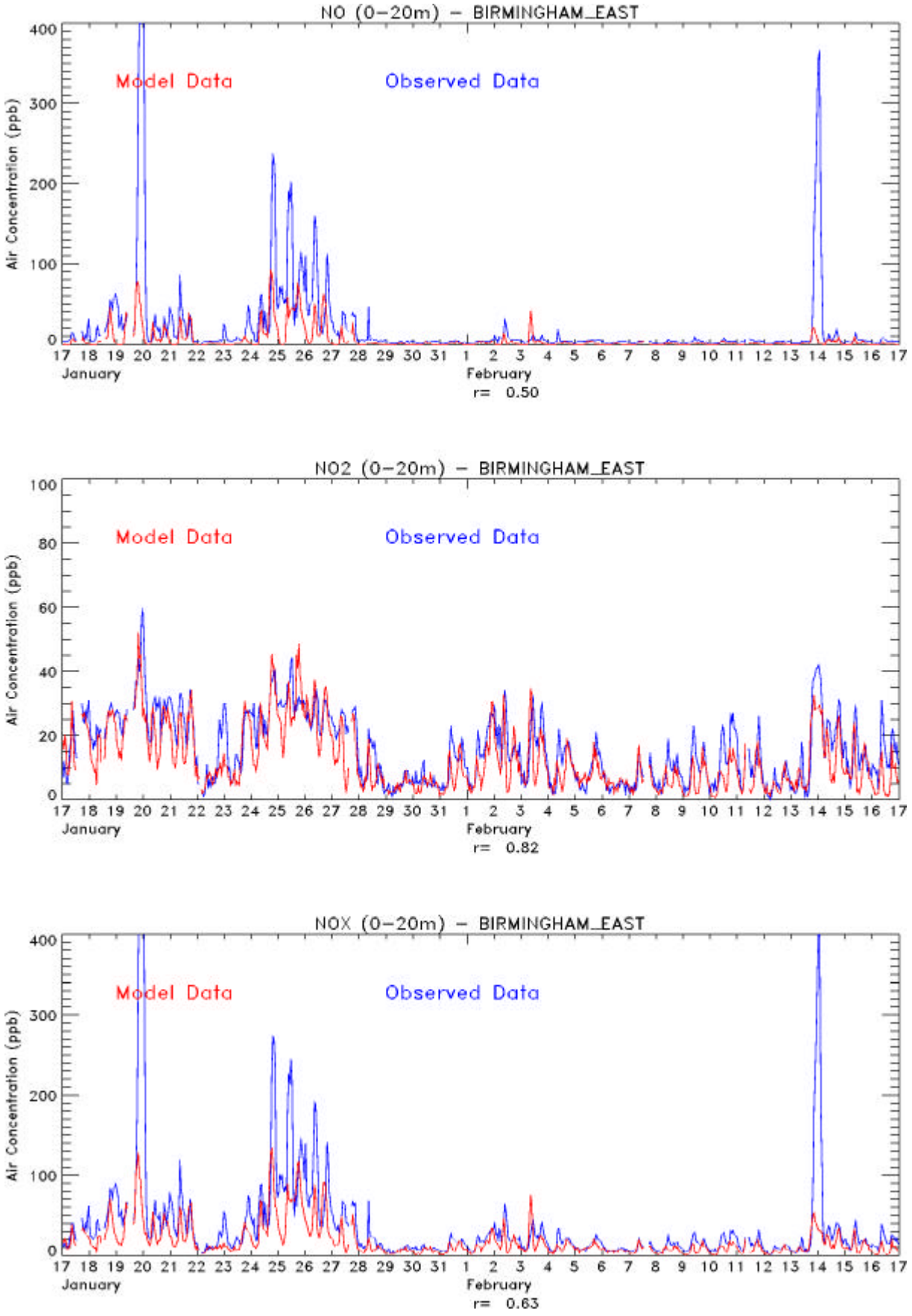

Figure 5.2 Modelled versus observed concentrations of NO, NO_2 and NO_X at Birmingham East.

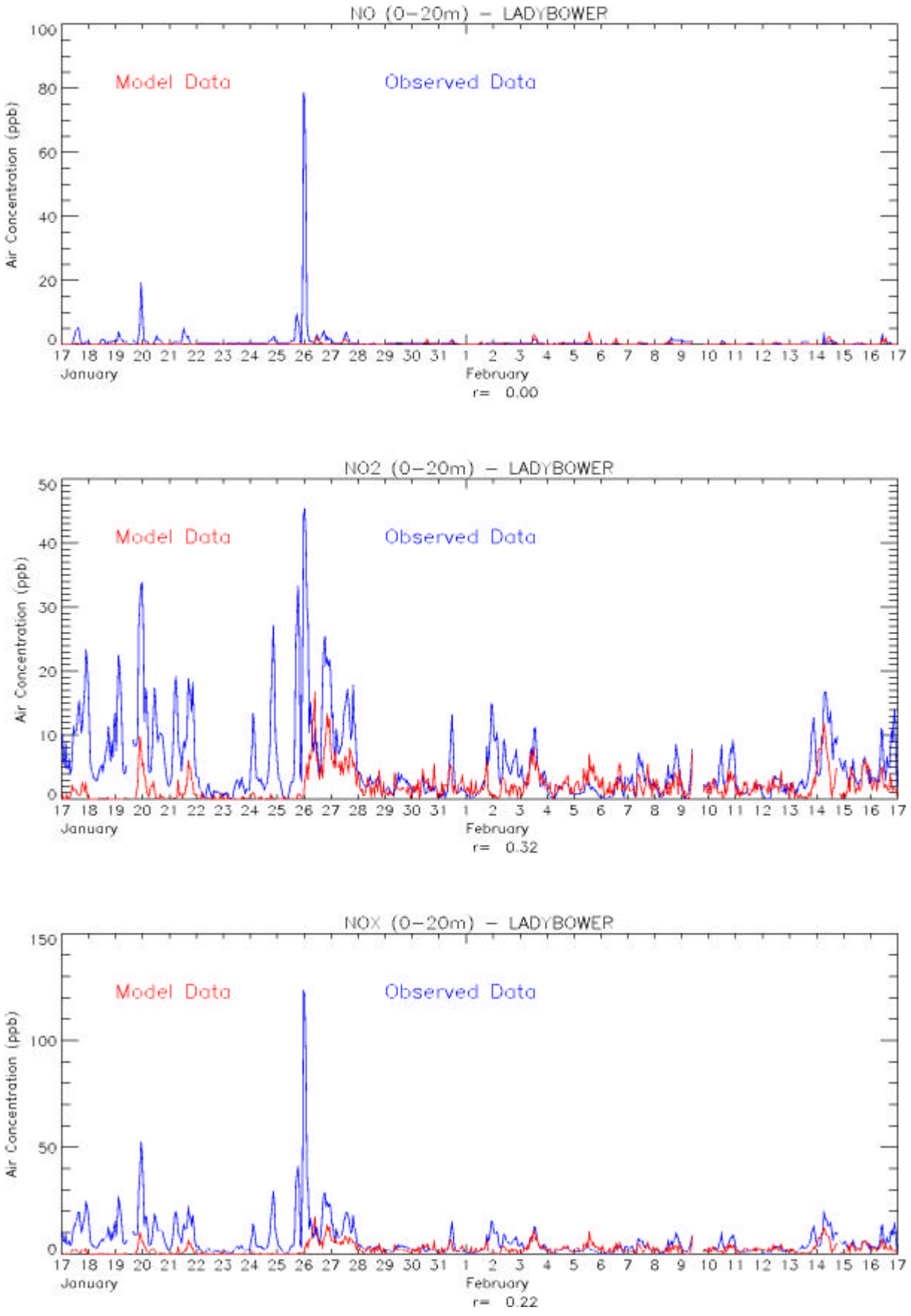

Figure 5.3 Modelled versus observed concentrations of NO, NO_2 and NO_X at Ladybower.

5.2 O_3

Figures 5.4-5.7 show plots of the model background ozone concentration plotted against measured ozone at Birmingham, Birmingham East, Ladybower and Bottesford and also the model local production of ozone carried by the particle plume at each location. The approximate method for calculating the model background ozone appears to perform better in the winter than in the summer, giving a much better match to the observed data at Birmingham and Birmingham East. Ladybower performs least well, which is due to the poor representation of NO_2 at this site for the reasons outlined above.

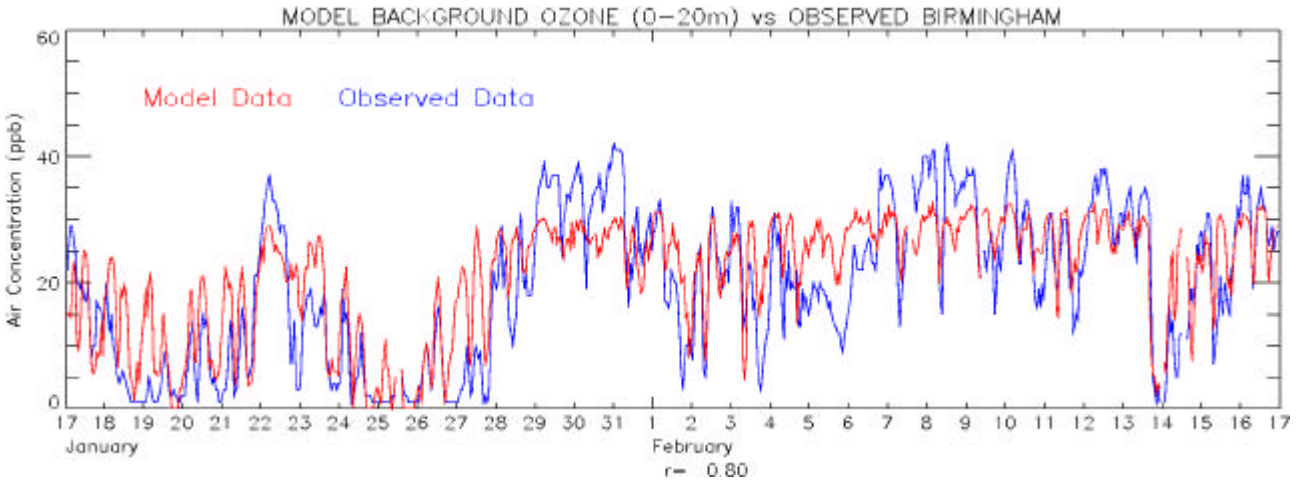

Figure 5.4 Model background ozone plotted against observed ozone at Birmingham Centre.

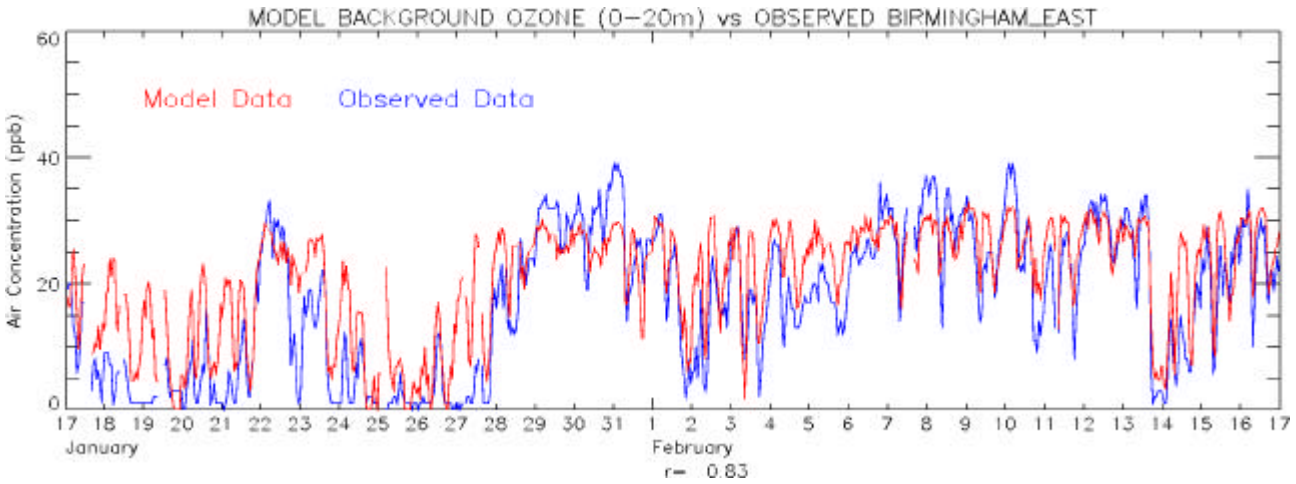

Figure 5.5 Model background ozone plotted against observed ozone at Birmingham East.

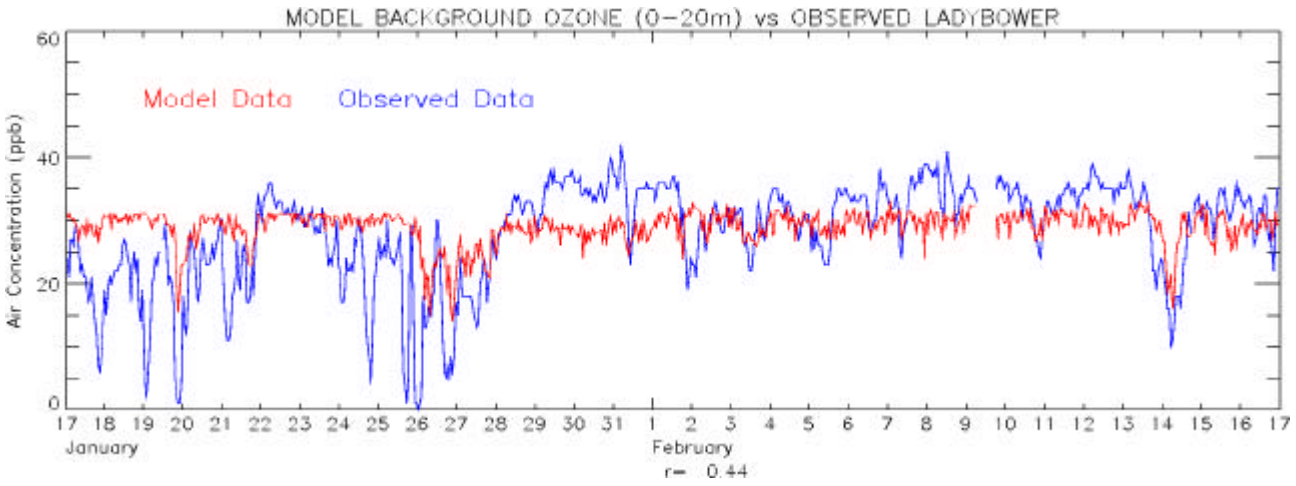

Figure 5.6 Model background ozone plotted against observed ozone at Ladybower.

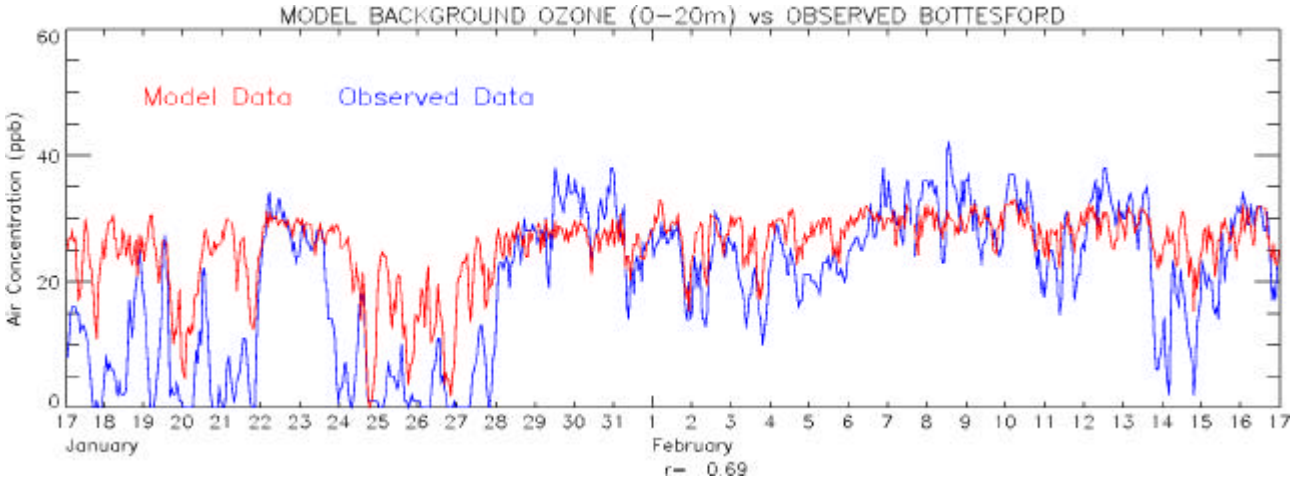

Figure 5.7 Model background ozone plotted against observed ozone at Bottesford.

Figure 5.8 shows the plots used to validate the ozone production term calculated by NAME for the winter period. As in the summer period, the wind direction is dominated by westerlies, therefore the Aston Hill ozone measurement data have been used again. The model production term is somewhat better in the winter, and although is still lower than that expected, is demonstrating some skill with a correlation of 0.5. The elevated levels on the 24th-27th January are clearly evident in the model results.

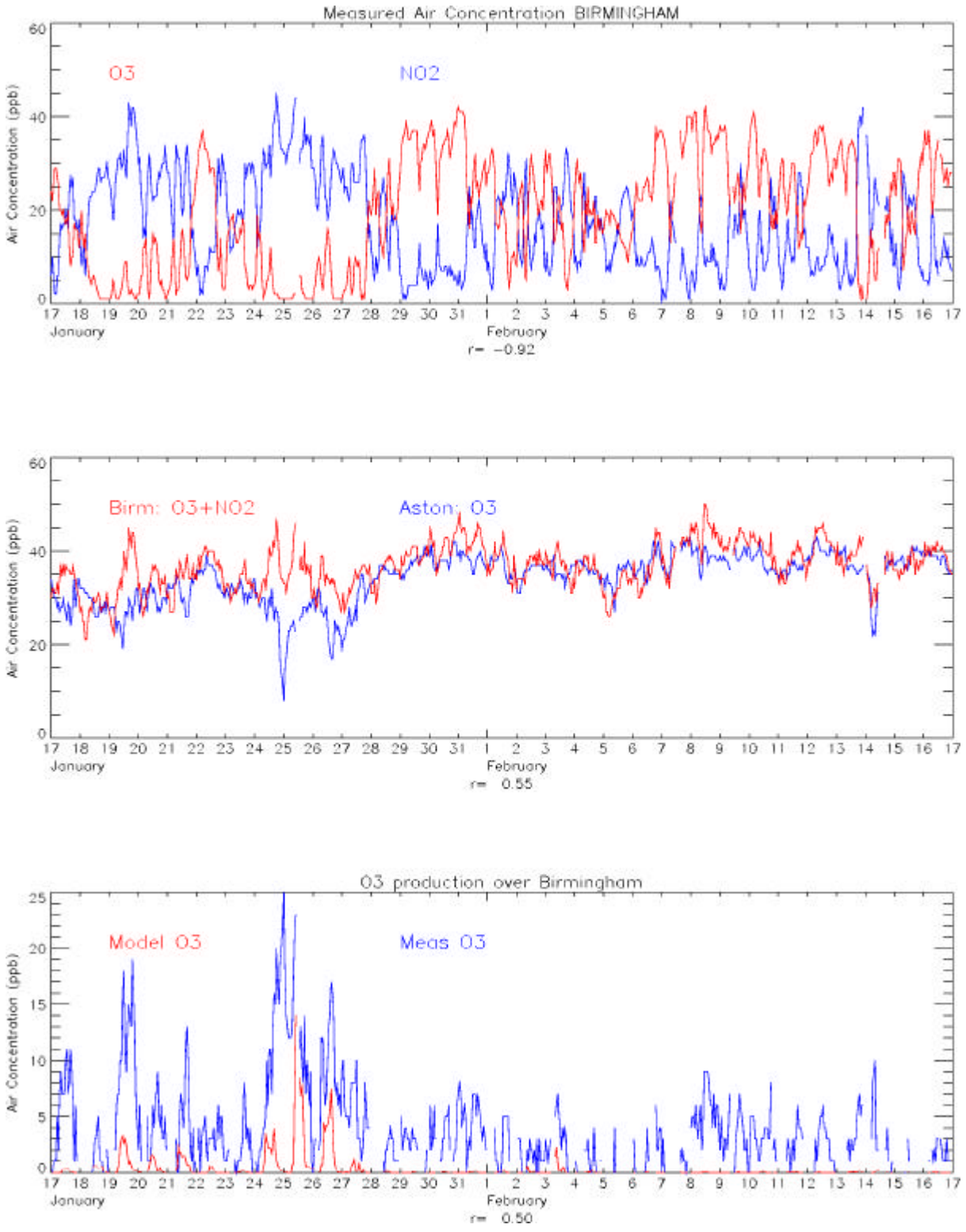

Figure 5.8 *Top*: observed O_3 and NO_2 air concentrations at Birmingham Centre. *Middle*: The sum of Birmingham Centre observed O_3 and NO_2 plotted against observed O_3 at Aston Hill. *Bottom*: Modelled ozone production at Birmingham plotted against the difference between the Birmingham oxidants (O_3 + NO_2) and the Aston Hill O_3 (which is labelled 'Meas O3').

5.3 OH, HO_2

Figures 5.9 and 5.10 show modelled OH and HO_2 concentrations plotted against measured data. The modelled OH data shows both a poorer correlation and a greater variance than the summer data. The model overpredicts that measured from the 21st – 28th January and then for the remainder of the period under predicts. As in the summer campaign, the winter HO_2 values are substantially lower than those measured, being at maximum only $1x10^8$ molecules/cm^3 compared with a measured maximum of $1.4x10^9$ molecules/cm^3 as an hourly average.

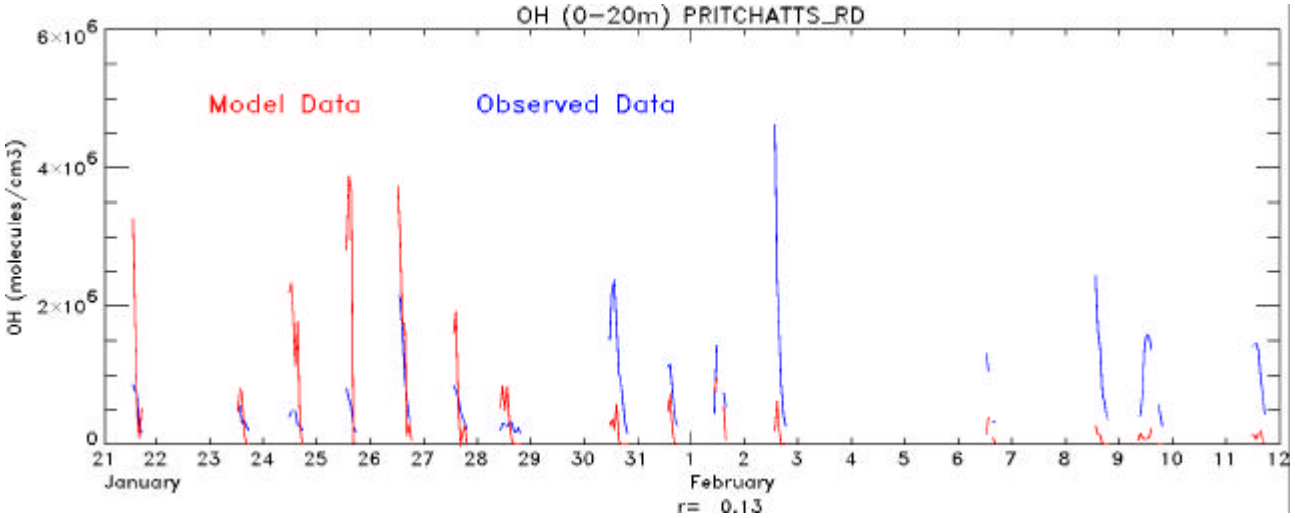

Figure 5.9 Modelled versus observed OH in molecule/cm^3 at Pritchatts Road.

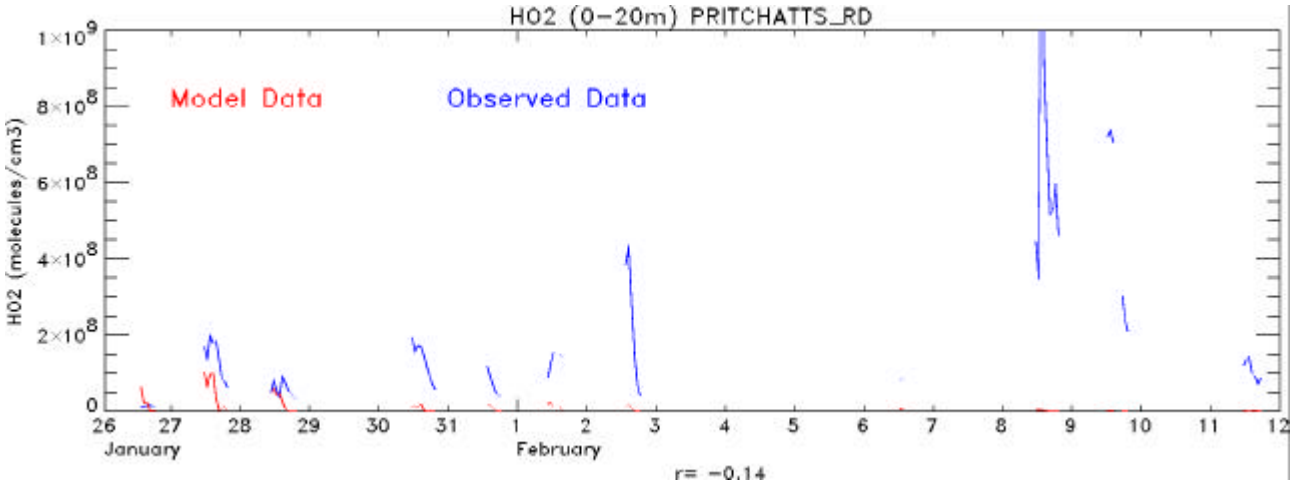

Figure 5.10 Modelled versus observed HO_2 in molecule/cm^3 at Pritchatts Road.

5.4 VOC

Figures 5.11 - 5.13 show plots of the 1,3 butadiene, isoprene and toluene concentrations respectively. No measurement data were available for ethylene and formaldehyde for the winter period. 1,3 butadiene shows an excellent match with the measured data at Birmingham East and Pritchatts Road. It is interesting to note that the only exception to this is seen at Birmingham East on 19/20th January and 13/14th February where the model fails to capture the full extent of the measured peaks which rise to almost 3ppb on each occasion. The peak on 19/20th January is not evident in the measured data at Pritchatts Road but unfortunately no data is available for the second peak on the 13/14th February. Peaks at these times were also evident in the NO at Birmingham East, but not at Birmingham.

The comments above also apply to the isoprene data, where again the model gives a good match to the measurement data at both sites, except for the peaks of 1.5ppb seen on the 19/20th January and 13/14th February. The fact that the magnitude of the winter isoprene (with the exception of the two peaks) agrees well with the measured data shows that we are estimating the anthropogenic emission accurately, as there will be little or no biogenic emissions at this time of year.

The modelled toluene data again shows a good match with the measured data with the exception of the peaks mentioned above. The only additional information is the evidence of a peak (which is small relative to those at Birmingham East) in the measured data at Pritchatts Road on the 9th February which does not appear in the modelled data nor in the measured data at Birmingham East. As in the summer case, the model and the inventory provide a reasonable description of the VOC levels in the West Midlands during the winter.

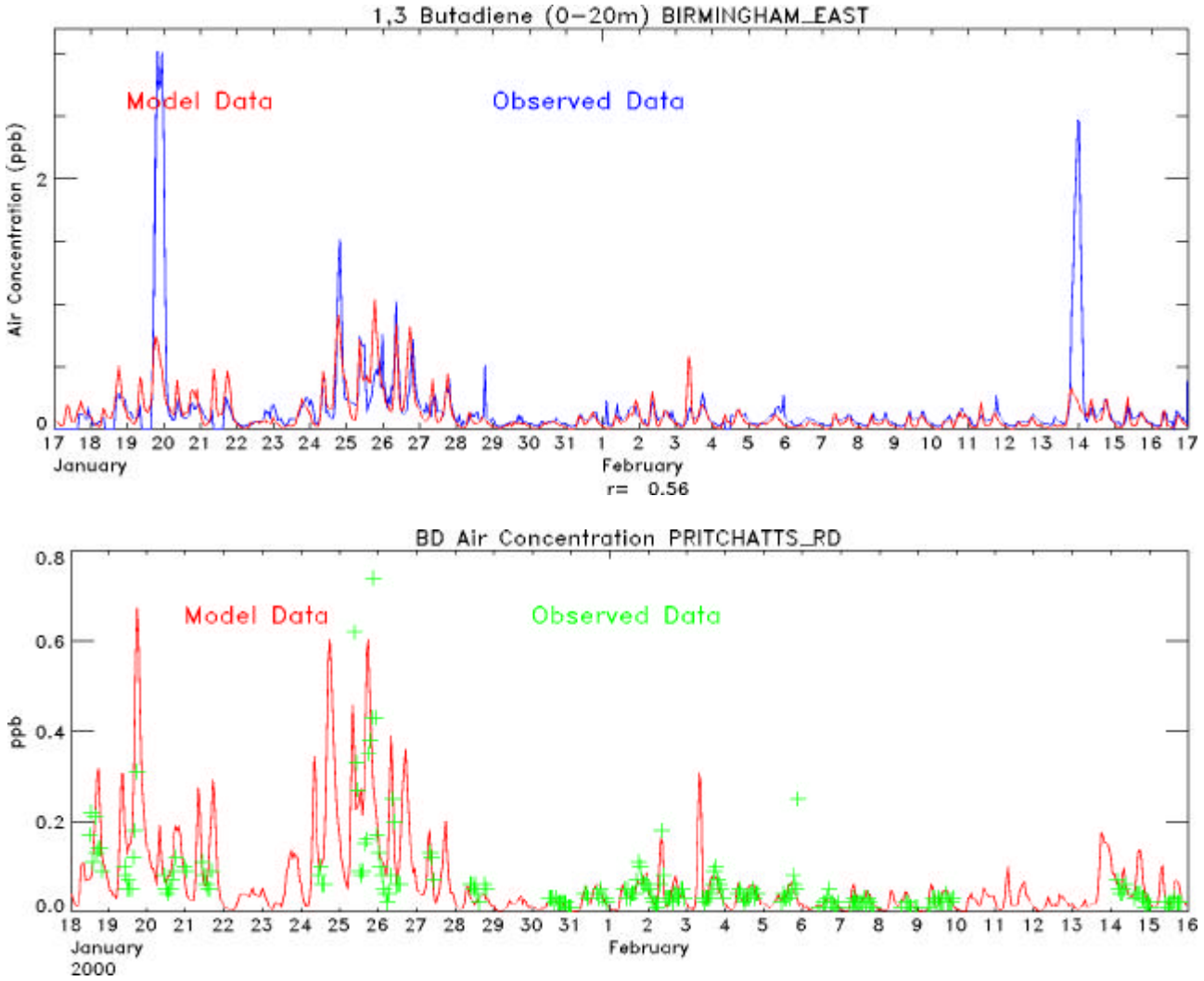

Figure 5.11 *Top*: Modelled versus observed 1,3 butadiene at Birmingham East. *Bottom*: Modelled and observed 1,3 butadiene at Pritchatts Road.

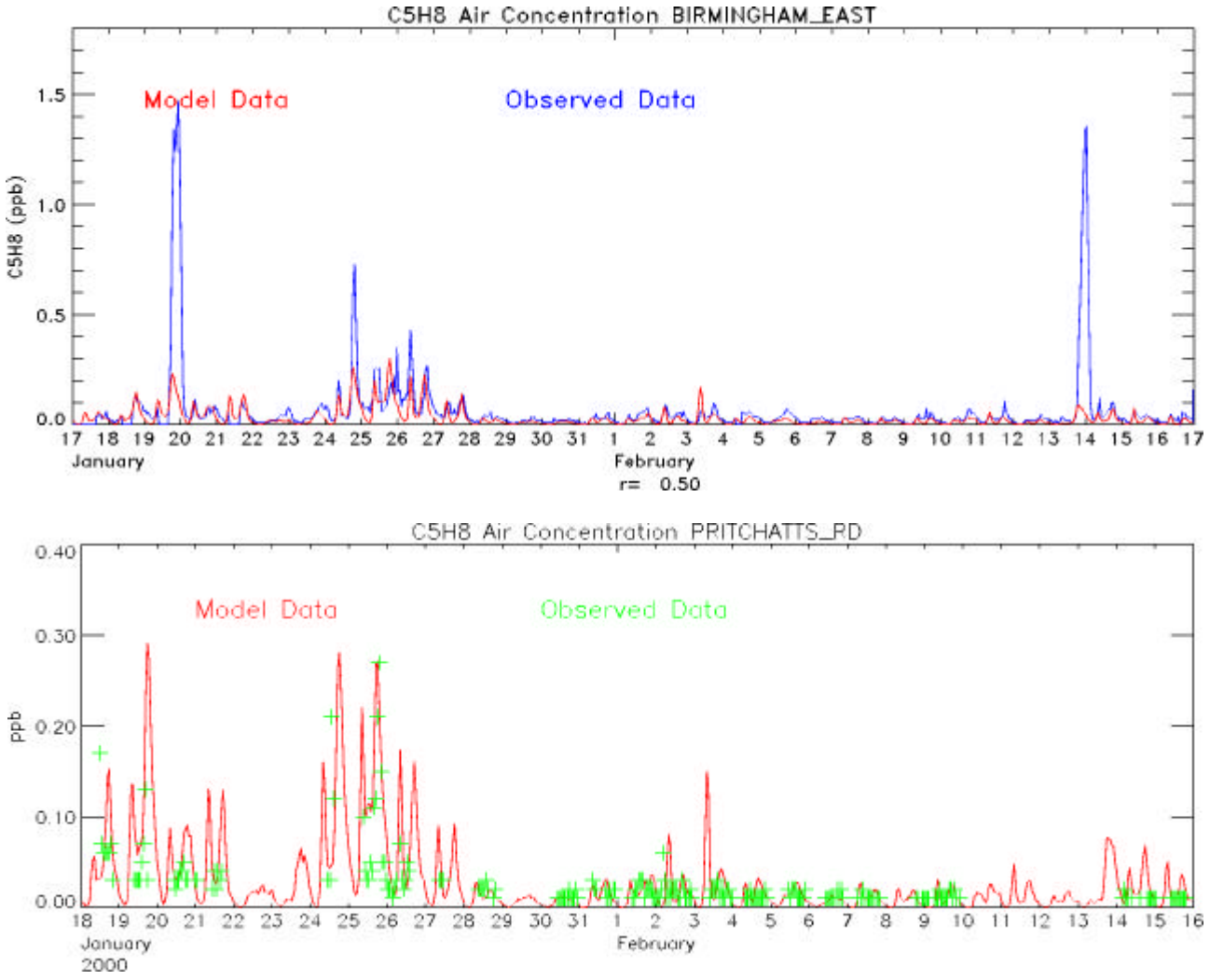

Figure 5.12 *Top*: model versus observed isoprene at Birmingham East. *Bottom*: Modelled and observed isoprene at Pritchatts Road.

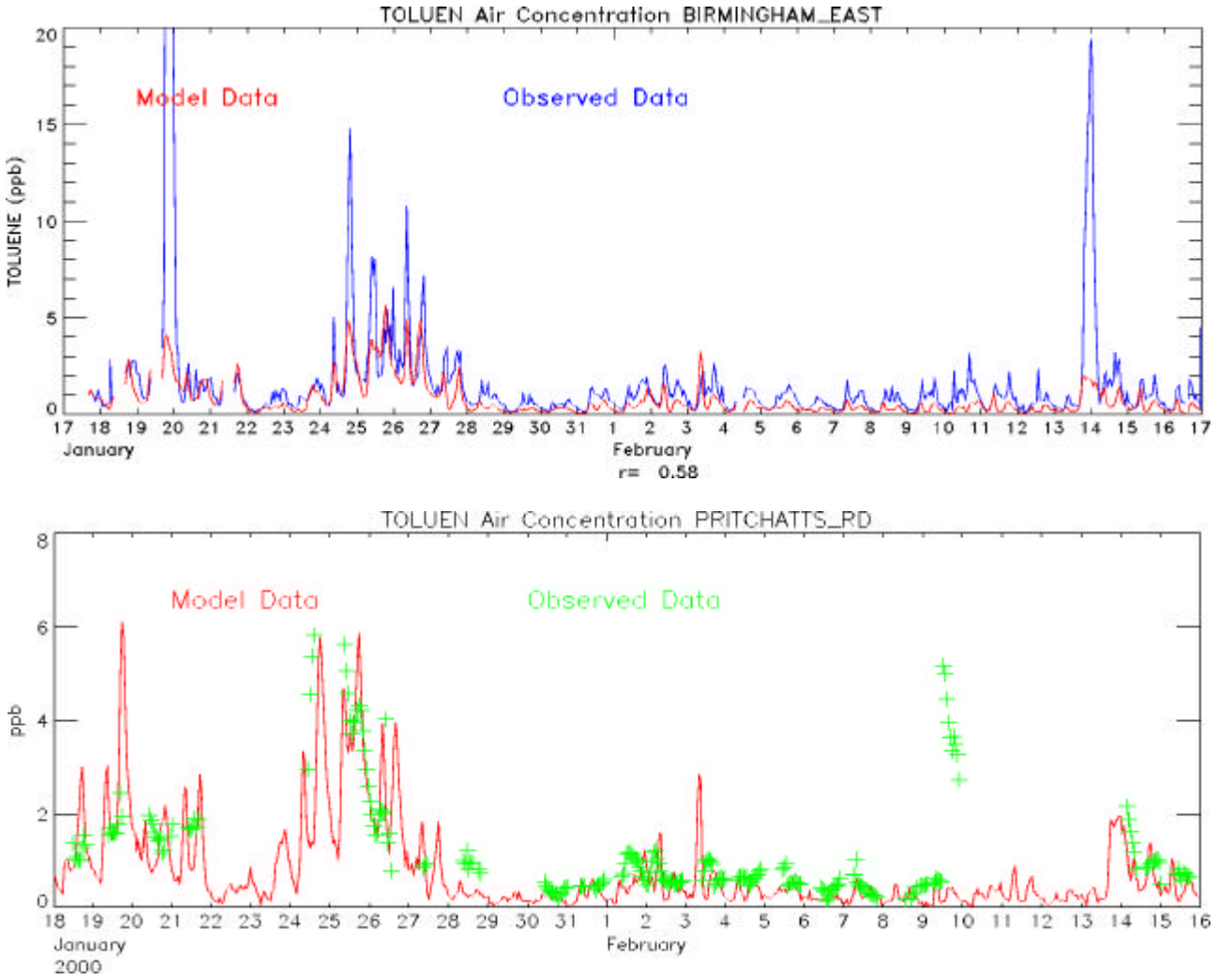

Figure 5.13 *Top*: modelled versus observed toluene at Birmingham East. *Bottom*: model toluene data and observed data at Pritchatts road.

5.5 Nitrate Aerosol, HNO3 & NH3

Figures 5.14 - 5.16 show nitrate aerosol, nitric acid and ammonia concentrations respectively. The wintertime nitrate aerosol is even more suppressed than the summer time results. The modelled nitric acid is generally lower then that measured, though not greatly so, except for the large model peak of around 2 µg/m^3 over the 25th –26th period. It seems likely that this nitric acid should really be converted to aerosol so that it could contribute to the large peak in nitrate aerosol seen at this time. As with the summer case the estimated contribution from long range transport has been included by calculating daily percentages from the European wide run, (which were between 15-30%), and are plotted as a dotted red line. The nitrate aerosol modelled by the European wide model run is shown as a dashed pink line. In the winter case the simpler chemistry model performs slightly better, producing greater amounts of aerosol, though still much less than that observed. As seen in the summer, the ammonia does not correlate very well with the observed values, however it is generally of the correct order of magnitude.

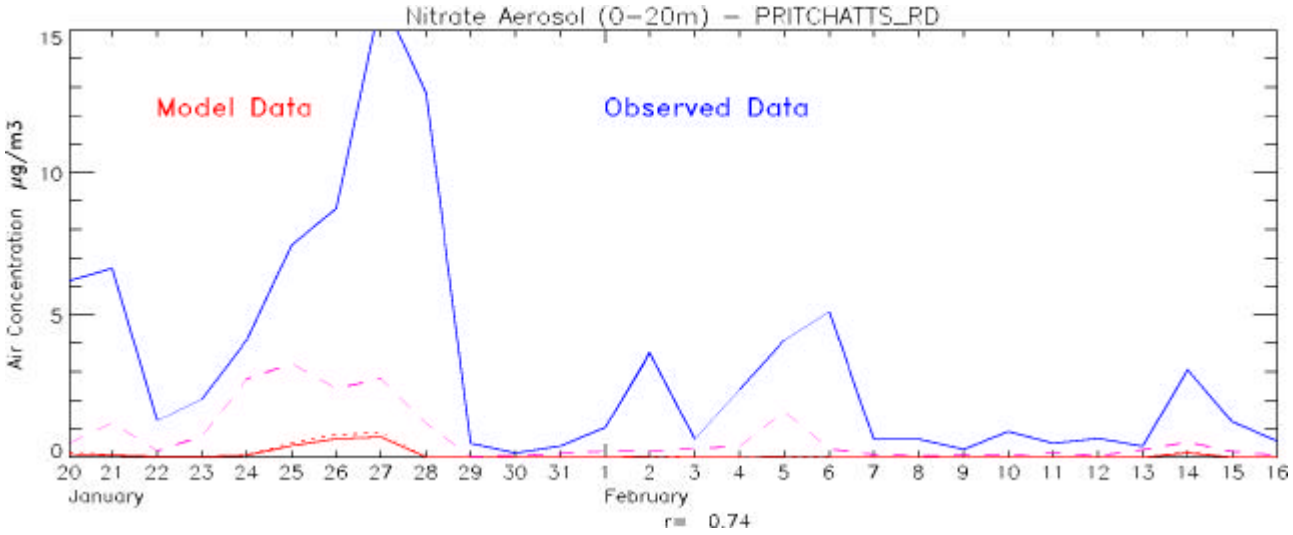

Figure 5.14 Modelled versus observed daily average nitrate aerosol.

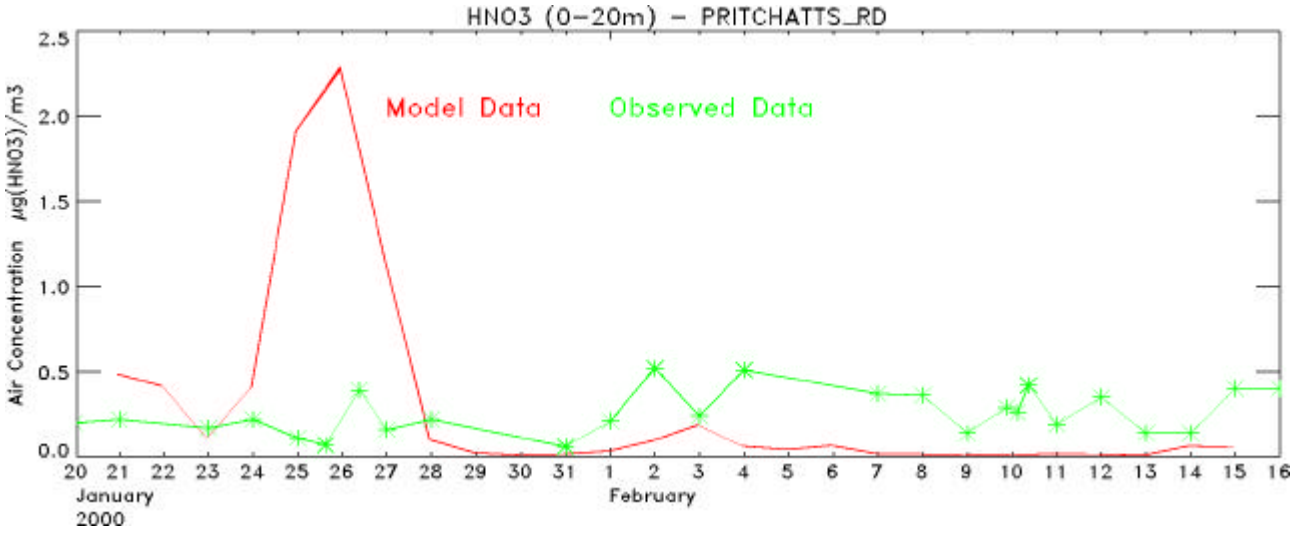

Figure 5.15 Daily average model nitric acid overplotted with observed nitric acid at Pritchatts Road.

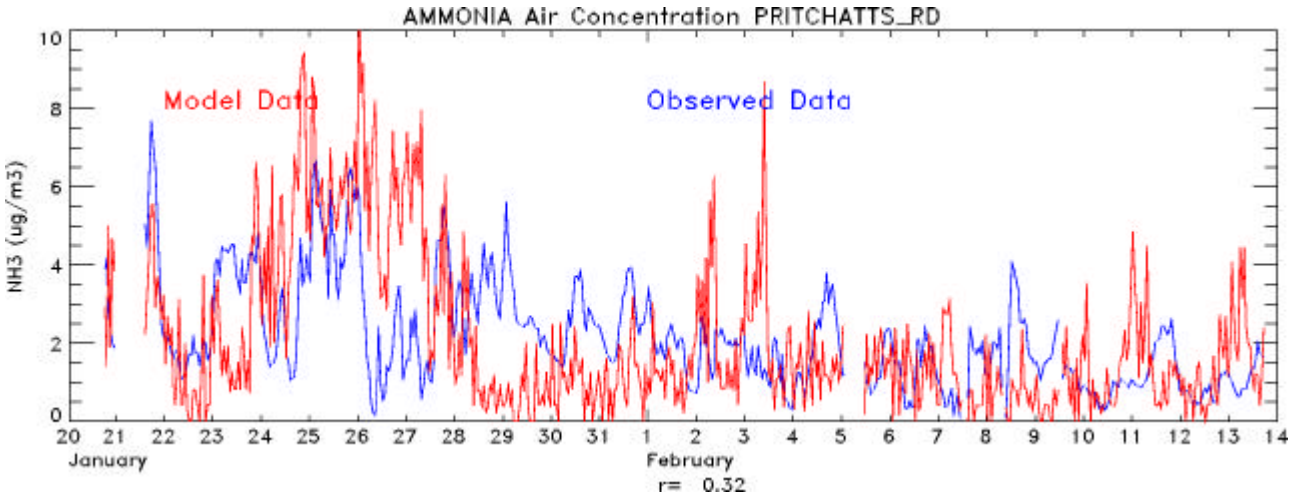

Figure 5.16 Model versus observed ammonia at Pritchatts Road.

5.6 HONO

Figure 5.17 shows modelled nitrous acid concentrations plotted with measured data at Pritchatts road. Unlike the summer period where the model shows little skill in comparison with measured data, the winter time daily average follows the pattern seen in the measured data quite well, though does not reach the full magnitude seen. It should be noted that the measured data are daily averages with the exception of 25th-26th January and 9th-10th February where additional data at 15.00, 21.00, 3.00 and 9.00 hrs are plotted. This may explain in part the high measurement recorded at 21.00hrs on 25th as the HONO exhibits a pronounced diurnal cycle with night-time peaks which this measurement is capturing.

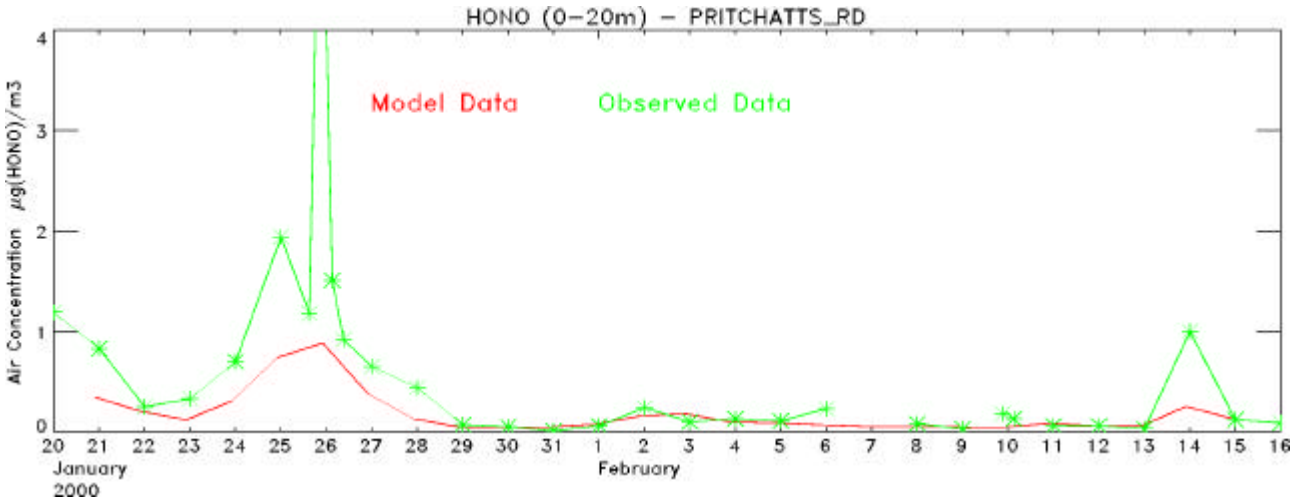

Figure 5.17 Daily average model HONO over plotted with measurement data from Pritchatts Road.

5.7 PAN

Figure 5.18 shows the modelled and measured PAN concentrations. In contrast to the summer situation, the model PAN in winter greatly overpredicts that measured, at least for the first half of the period, with daytime peaks far exceeding both the measured wintertime values and indeed the modelled values for the summertime period. For the second half of the period the modelled concentration is low, as is that measured.

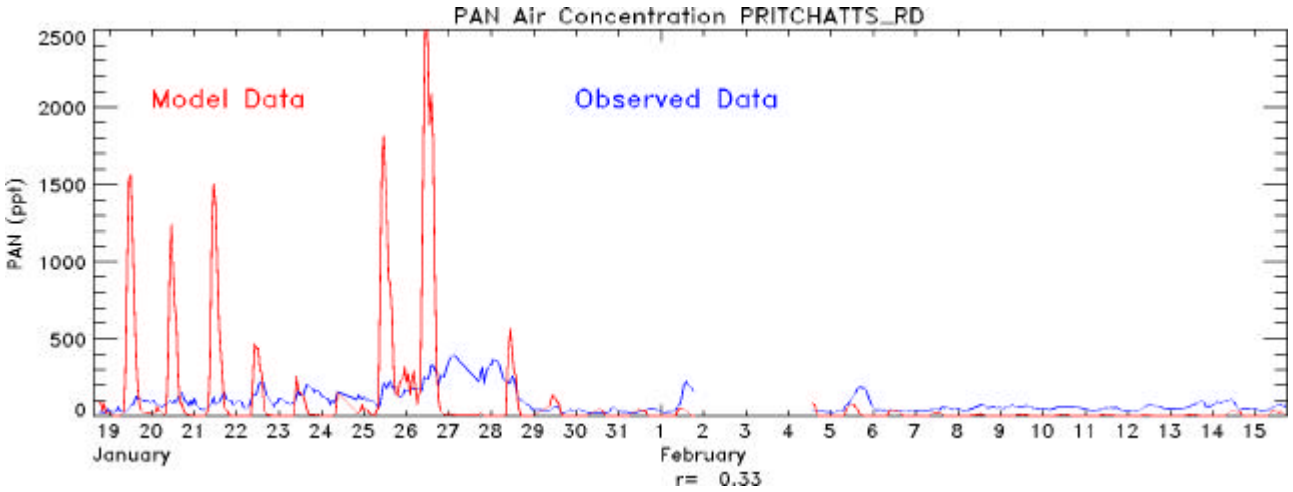

Figure 5.18 Modelled versus observed PAN at Pritchatts Road.

5.8 CO

Figures 5.19 and 5.20 show modelled and observed concentration data for CO at Birmingham and Birmingham East. The results are similar to the summer situation in that the correlation is again around 0.4 and the model underpredicts the measured values at both sites but much less so at Birmingham East. It is also interesting to note that there are peaks on the 19/20th January and 13/14th February in the measured data at Birmingham East which are not picked up by the model which correspond to those seen in the NO and VOC measurements.

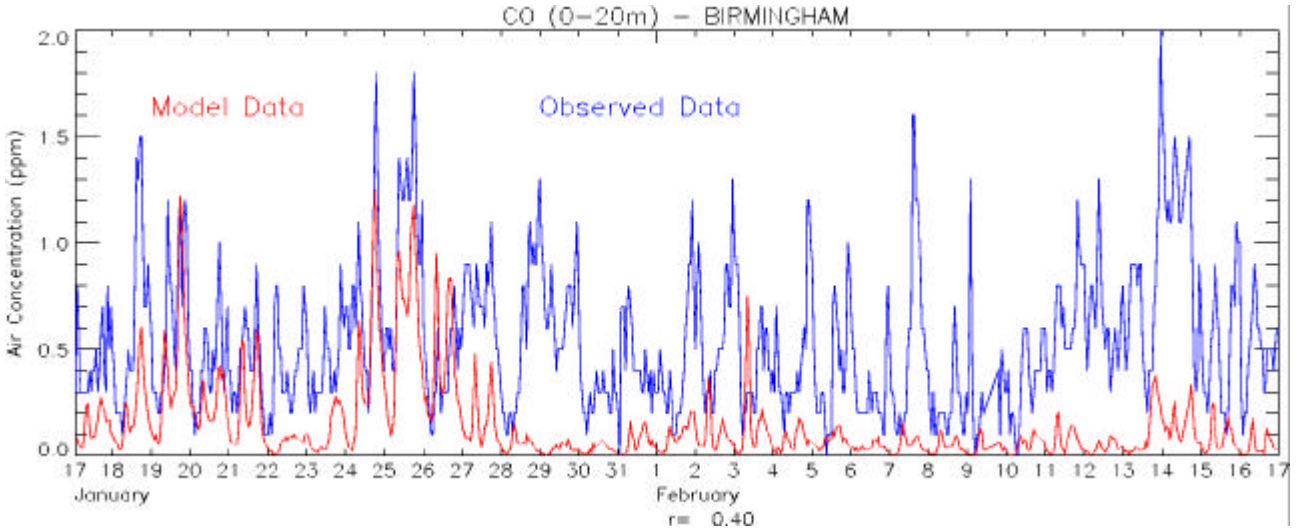

Figure 5.19 Modelled versus observed CO at Birmingham Centre.

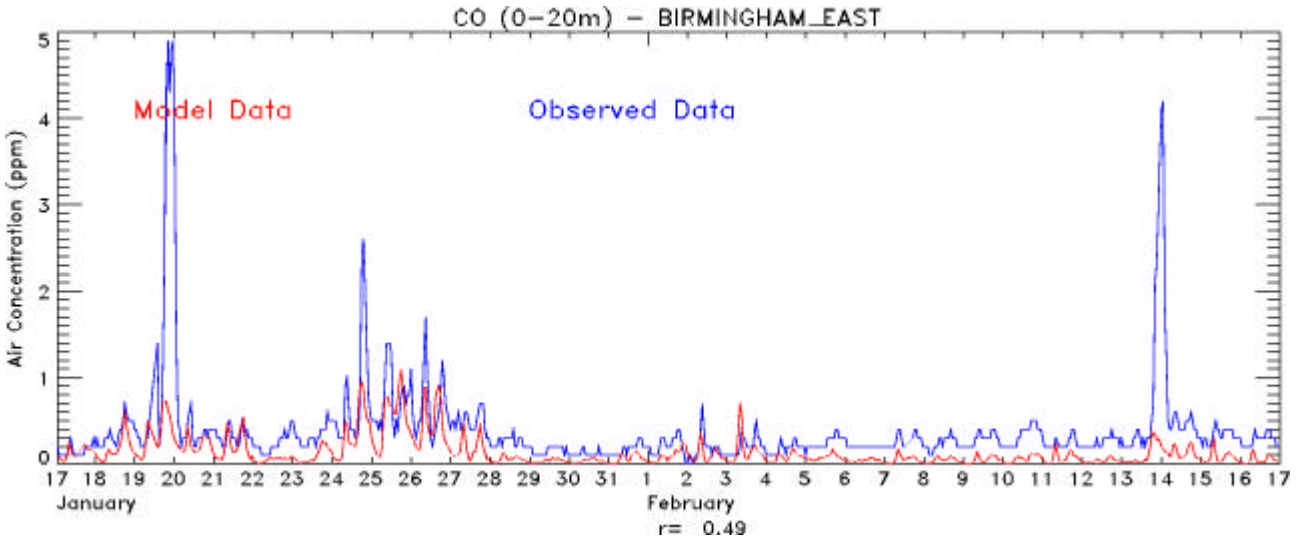

Figure 5.20 Modelled versus observed CO at Birmingham East.

5.9 SO_2

Figures 5.21 – 5.23 show sulphur dioxide concentration plots for Birmingham, Birmingham East and Ladybower. The model has performed better over the winter period than the summer, giving higher correlations at all three sites. The model appears to overpredict at Ladybower, but the magnitudes are quite reasonable at Birmingham and Birmingham East, although there are model peaks not seen in the observed data.

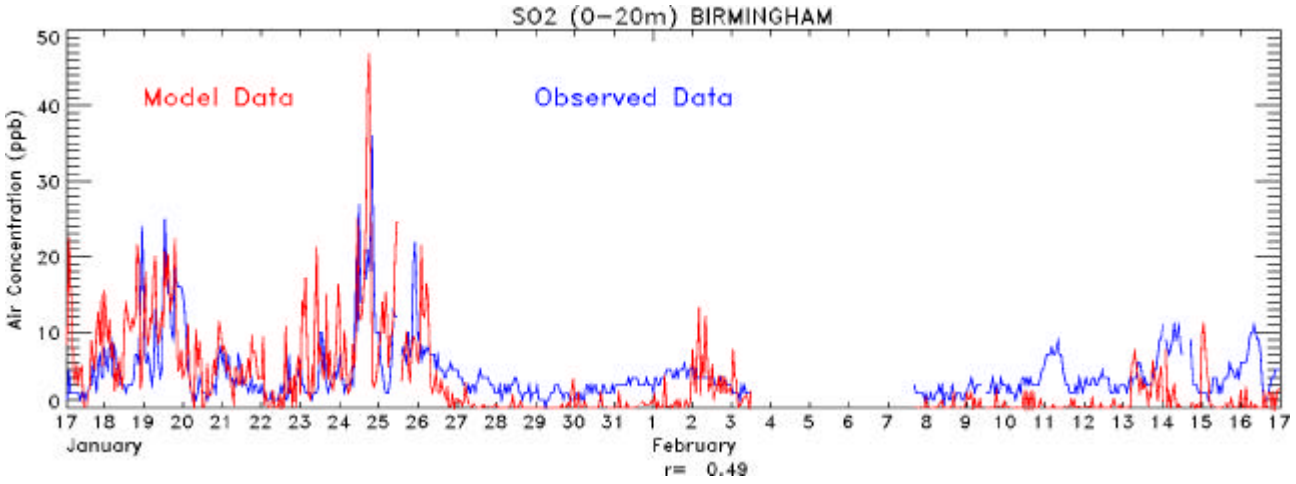

Figure 5.21 Modelled versus observed SO_2 at Birmingham Centre.

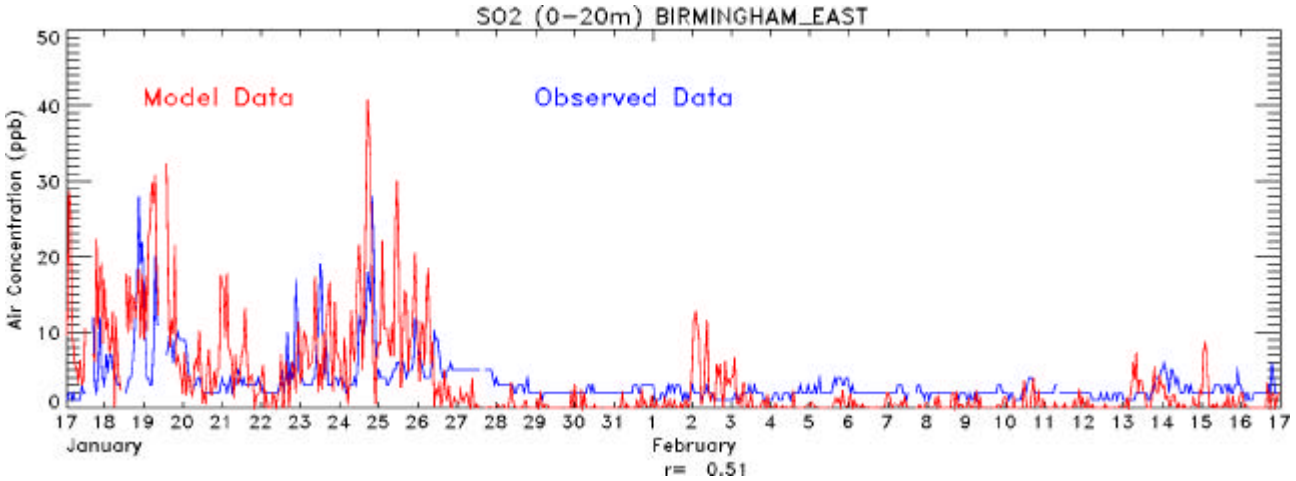

Figure 5.22 Modelled versus observed SO_2 at Birmingham East.

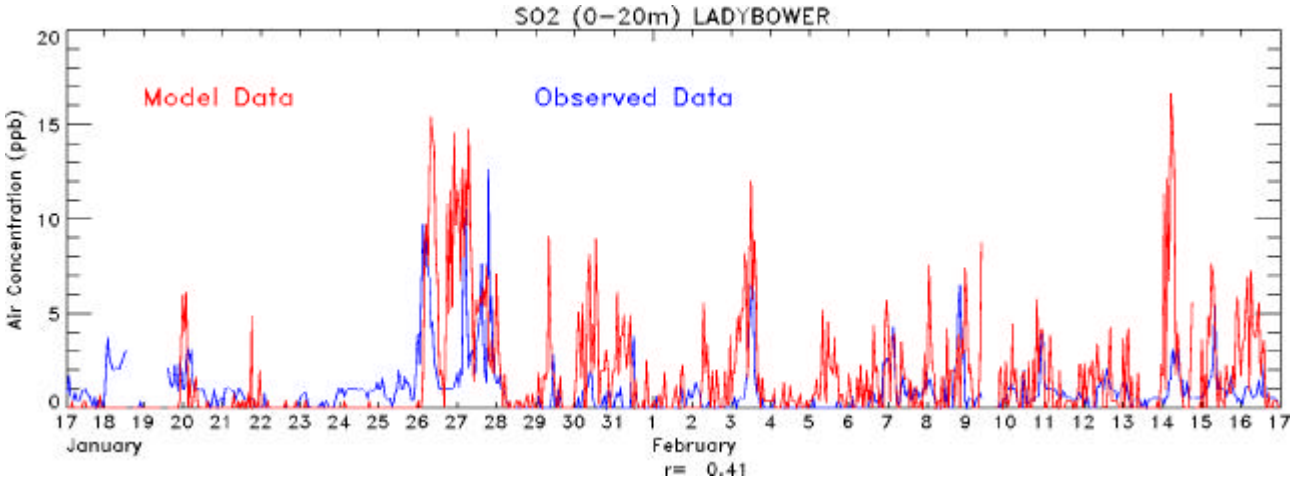

Figure 5.23 Modelled versus observed SO_2 at Ladybower.

5.10 Sulphate Aerosol

Figure 5.24 shows daily averaged modelled and measured sulphate aerosol concentrations at Pritchatts Road. The model performs better over the winter period than the summer. The model captures the peak at the beginning of February very well, but overpredicts the January peaks. In between these elevated levels the model tends to underpredict the background sulphate aerosol by about 1µg/m^3. Again, the estimated European component has been added in and is shown as a dotted red line. The modelled sulphate aerosol from the European run is shown as a dashed pink line. This model underpredicts the first peak in January, captures the second quite well but then overpredicts the peak in February.

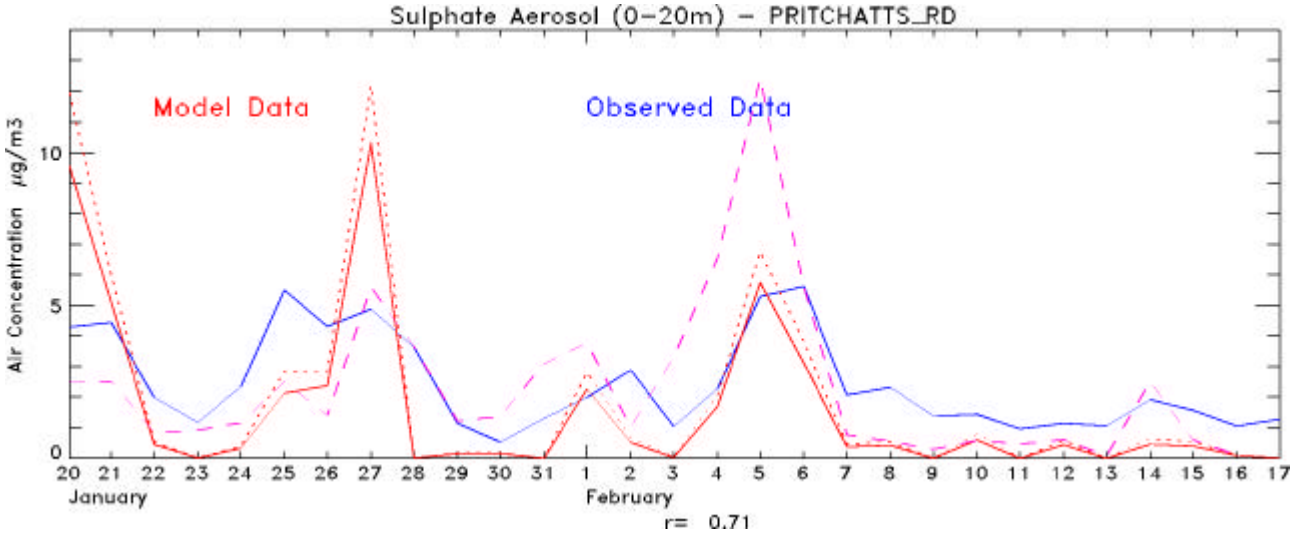

Figure 5.24 Daily average model versus observed sulphate aerosol at Pritchatts Road.

5.11 H_2O

Figure 5.25 shows model water vapour concentrations in % by volume (extracted from the mesoscale meteorological data) plotted against measured data from Pritchatts Road. As with the summer period the model tends to underpredict that measured slightly but does follow the general pattern observed.

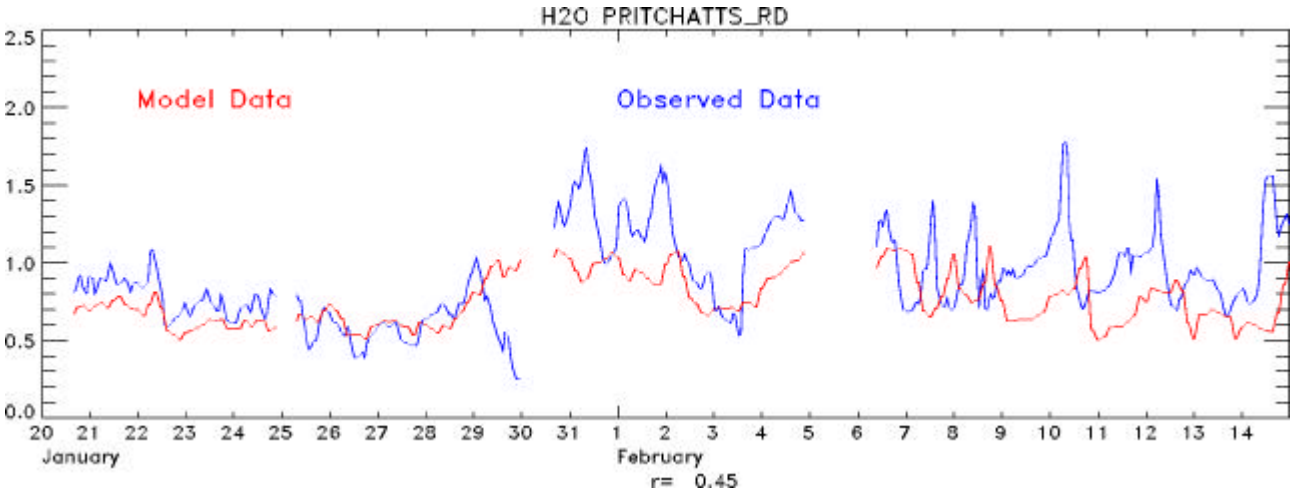

Figure 5.25 Model versus observed water vapour by % volume at Pritchatts Road.

5.12 J O^1D

Figure 5.26 shows the value of J O^1D used in the model and that which was measured at Pritchatts Road. The model is making a good approximation to the measured values, however as with the summer case the model value does not capture the reduced values seen for example on 28th January and 14th February.

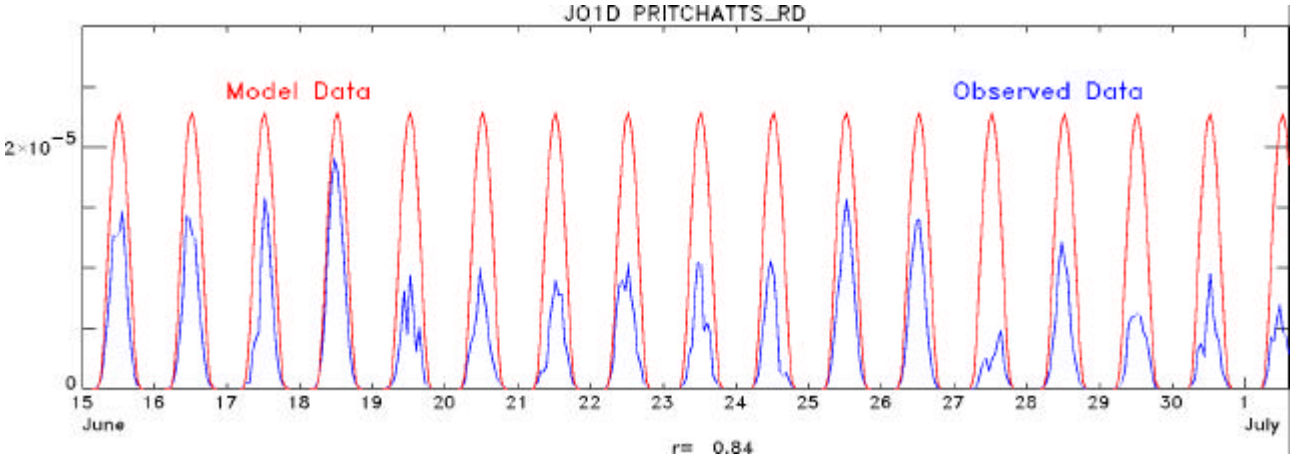

Figure 5.26 Modelled versus observed J O^1D values (s^{-1}) at Pritchatts Road

5.13 PM_{10}

Figure 5.27 shows model PM_{10} concentration against measured data at Birmingham Centre. The model performs much better over the winter period with a correlation of 0.49. The magnitude modelled is still too low, particularly for the period 7th-17th February, however 18th-22nd January and the 24th-27th January are captured quite well. This to some extent is reflecting the fact that the magnitude of modelled sulphate aerosol is better in the winter (Figure 5.24). Figure 5.28 shows the three components of the model PM_{10}. The model nitrate aerosol is very low in winter and is therefore contributing little. The total modelled PM_{10} overpredicts that measured on the 26th January and this overprediction is also seen in the sulphate aerosol on this day. The contribution from Europe is not included in these plots.

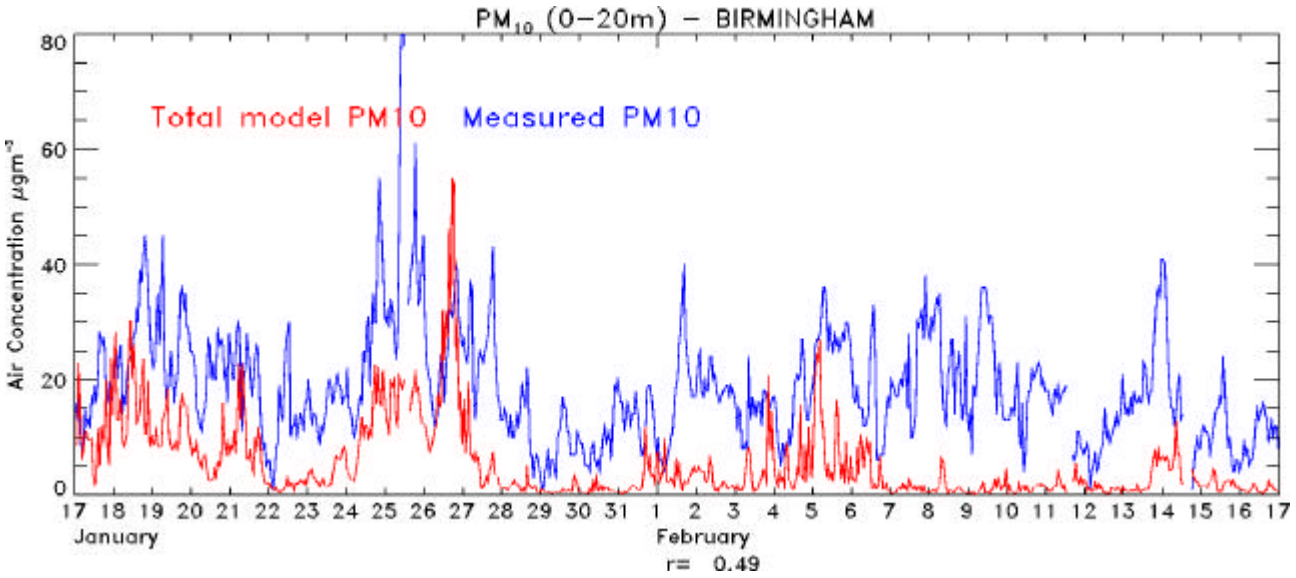

Figure 5.27 Modelled versus observed PM_{10} at Birmingham Centre.

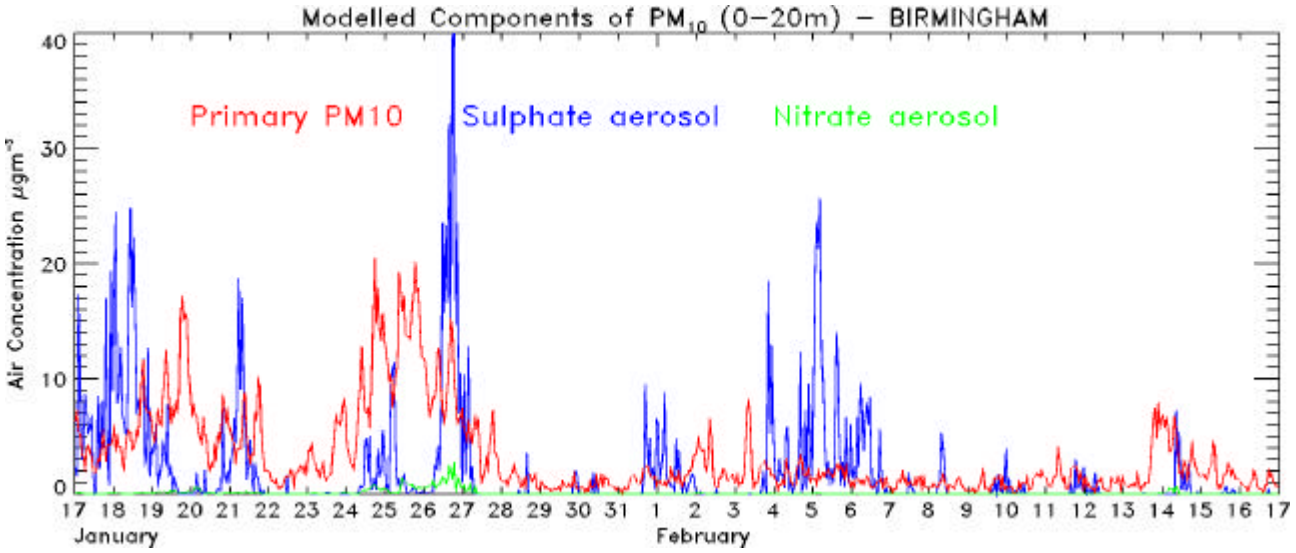

Figure 5.28 The three components of the modelled PM_{10}: sulphate aerosol, nitrate aerosol and primary PM_{10} at Birmingham Centre.

6.0 Maps of modelled ozone production and nitrogen dioxide

Appendix B shows modelled ozone production and nitrogen dioxide as maps over the modelled domain. The maps are one hour averages (plotted at hour ending) and are given every six hours for both species throughout the campaign periods. These plots have been included to complete the set of model output presented. No validation of these maps has been carried out as yet, however a high density network of ozone sensors were collecting data throughout the campaigns so it is hoped that some comparison work will be possible when these data are available.

7.0 Discussion and Conclusions

The aim of this part of the PUMA project was to develop an urban airshed model capable of producing urban background concentrations of key atmospheric pollutants. The NAME model has been developed to include the release of thirteen primary species and contains 100+ reactions for over 30 species.

In order to assess the optimum source of meteorology for input into NAME, an analysis of the met data available (RAMS (2km x 2km resolution), Met Office mesoscale (12km x 12km resolution) and Met Office global (60km x 60km resolution) data) has been carried out. Section 2 of this report presents a comparison of the three sets of data with meteorological measurements at Coleshill (a rural site) and Pritchatts Road (an urban site). The dispersion model has been adapted to run using the RAMs data and then run on the three different sets of meteorological data to assess the potential differences; this was done without using the chemical scheme for simplicity. The differences in performance between the three models were found to be small. From this it was concluded that increasing the resolution from 60 km to 2 km provided little extra information over the periods studied. It was decided to use the mesoscale data for the detailed chemistry model runs as this met input has both the benefit of a continuous assimilation cycle and the moisture parameters required to simulate the aqueous phase chemistry and wet deposition.

A recent paper by Hogrefe et al 2001 evaluates the performance of the RAMS3b and MM5 meteorological models by comparison against observed temperature, water vapour and wind speed over a variety of timescales using both traditional statistics, as presented here, and using a method of spectral decomposition. The findings were consistant with the conclusions drawn in this work, showing that the features with longer temporal and larger spatial scales were captured well by the models, but that there was a lack of agreement in the intra-day and diurnal timescales. The

finest grid resolution used in their study was 12km x 12km, which did show improvement over the same model at 36km x 36km resolution. Theoretically the model should continue to give improved results as the grid resolution is increased, as the amount of inherent uncertainty due to sub grid scale fluctuations would be reduced (assuming that a perfect formulation of the model dynamics is possible at all scales). However it is pointed out that unless continuous assimilation of observational data is also carried out at this increased resolution, this will not necessarily improve the overall model performance.

The other part of this project was to take an existing three dimensional Lagrangian dispersion model, NAME, and introduce a detailed chemical scheme that could output key atmospheric species for validation against an extensive set of measurements in Birmingham over summer-time and winter-time conditions. This has been achieved and the results for NO, NO_2, NO_x, O_3, OH, HO_2, 1,3 butadiene, ethylene, isoprene, formaldehyde, toluene, nitrate aerosol, nitric acid, ammonia, nitrous acid, PAN, CO, SO_2, sulphate aerosol, H_2O, JO1D and PM_{10} have been compared with measured data and presented. The development of such a chemistry scheme within the Lagrangian framework has presented many challenges and inevitably made necessary some assumptions and approximations. As with all models there is still considerable room for improvement in many different areas, and which of these will yield the greatest improvements is hard to say. Undoubtedly, there are problems still to be solved within the current chemistry scheme, for example, the aerosol production, HO_2 and PAN.

A sub-set of the more reactive VOCs are emitted in the model, and scaled up to try to represent the full ozone producing potential of the atmosphere. The inclusion of more species and their associated reactions would improve the chemical representation. The lack of any speciated spatial distribution for the VOCs is a problem, especially for biogenic species such as isoprene, for which it was felt more appropriate to only model the anthropogenic part of the emission. Inclusion of the biogenic emissions will undoubtedly have an impact on the chemistry.

As discussed in section 3.1, ideally all the chemical fields would be advected, preferably using a Lagrangian particle approach in keeping with the current model. This would be more beneficial to species with longer lifetimes; for those with short lifetimes such as the hydroxyl radical the current assumption is quite appropriate. This approach would allow us to model the regional ozone in addition to just the local production term in the NO_x plume. This would however also require a much larger domain to be modelled, to allow both re-circulation of air from the UK and import from Europe. The demand on computing resources required to achieve this is currently prohibitive.

The question of how to use the existing computing resources continues to be a crucial issue. If there is no apparent benefit in using meteorological data at finer resolution, it is debatable whether or not there would be any gain in calculating the chemistry scheme at finer scales, unless there is sufficient spatial detail in the emissions data that could then be resolved. If the model is run at a finer resolution, then it is necessary to increase the numbers of particles released to represent the emissions so that a statistically significant number of particles will be in each grid box to provide a smooth output. This would be more expensive to run and the domain size would have to be reduced in order to keep the total numbers of modelled particles at a workable level.

The emissions side of the modelling process could also be improved. Time dependent releases for power station emissions, for example, would be of benefit for sulphur dioxide in particular. For other species such as VOCs, seasonal cycles could be implemented, and traffic cycles that represent the local area could be constructed. Another point for consideration is the representativeness of observed data. Measurement sites may not always be ideally placed to record the modelled ‘background’ concentrations and may be influenced unduly by local sources. Models provide volume average concentrations, but observations will reflect the fluctuations that occur in reality and that are not possible to resolve in the model.

The underlying model physics also requires attention, as previous work (Manning 1999) has shown that NAME over-emphasises the diurnal cycle. This could be due to a systematic error in the model boundary layer height, due to a too rapid transition between stable nighttime conditions to unstable daytime conditions, or the extent of vertical mixing could be too rapid. In an area such as Birmingham, urban effects will alter the local dispersion; currently these are poorly accounted for in the meteorological models. These questions are the subject of current research. A further area which warrents investigation is to consider adapting the model to allow assimulation of measurement data in the same manner as is carried out in meteorological models.

In light of the previous comments, we might now conclude that the model results seem surprisingly good in some cases. It is clear that much further work is required and that substantial improvements ought to be possible in the future. It is important however, that all aspects of the modelling process continue to be evaluated, not just the chemistry scheme, if the potential for model improvement is to be maximised.

References

Collins, W.J., Stevenson, D.S., Johnson, C.E. and Derwent, R.G. (1997) Tropospheric ozone in a global scale three dimensional Lagrangian Model and its response to NO_x emission controls; J of Atmospheric Chemistry, 26, 223-274

Cullen, M.J.P. (1993) The Unified Forecast/Climate Model; Meteorological Magazine, (U.K.), 1449, 81-94

DeMore, W.B. et al 1997 Chemical Kinetics and photochemical data for use in stratospheric modelling. Evaluation no 12, JPL Publ., 97-4 Pasadena, Califorina.

Derwent, R.G. and Malcolm, A.L. 2000. Photochemical generation of secondary particulates in the United Kingdom. Phil. Trans. R. Soc. Lond. A, vol.358, 1-15

Derwent, R.G. et al 2000 Analysis and interpretation of the continuous hourly monitoring data for 26 C_2-C_8 hydrocarbons at 12 UK sites during 1996. Atmospheric Environment 34, 297-312

Ellis, N.L. and Middleton, D.R. Field measurements and modelling of urban meteorology in Birmingham, UK. Met Office Turbulence and Diffusion Note No. 268.

EMEP MSC-W Status Report 1989 Norwegian Meteorological Institute EMEP/MSC-W Report 2/89

Harrison, R.M., Peak, J.P., Collins, G.M. 1996 Tropospheric cycle of nitrous acid. J Geophys. Res. Vol.101, 14429-144439.

Harrison, R.M. and MacKenzie, A.R. 1990 A numerical simulation of kinetic constraints upon achievement of the ammonium nitrate dissociation equilibrium in the troposphere. Atmospheric Environment 24A, 91-102

Hogrefe, C., Roa, S.T., Kasibhatla, P. et al 2001 Evaluating the performance of regional-scale photochemical modeling systems: Part 1 – meteorological predicitions. Atmospheric Environment 35, 4159-4174.

Hough, A.M., 1988 The calculation of photolysis rates for use in global tropospheric modelling studies. United Kingdom Atomic Energy Authority Report AERE-R 13259

Kurtenbach, R., Becker, K.H., Gomes, J.A.G., Kleffmann,J.K., Lorzer, J.C., Spittler, M. Wiesen, P., Ackermann, R., Geyer, A. & Platt, U. 2001 Investigations of emissions and heterogeneous formation of hono in a road traffic tunnel. Atmospheric Environment 35, 3385-3394.

Malcolm, A.L. and Manning, A.J. 2001 Testing the skill of a Lagrangian Dispersion Model at estimating Primary and Secondary Particulates. Atmospheric Environment, 35,1677-1685

Malcolm A. L., Derwent R. G. and Maryon R. H. (2000) Modelling the long range transport of secondary PM_{10} to the UK. Atmospheric Environment 34, 881-894

Manning, A.J. 1999 Predicting NO_X levels in urban areas using two different dispersion models. Proceedings of the 6th International conference on harmonisation within atmospheric dispersion modelling for regulatory purposes, Rouen, France. (Accepted for publication in the Int. J. of Environment & Pollution.)

PORG 1997 Ozone in the United Kingdom. Fourth Report of the Photochemical Oxidants Review Group. Prepared at the request of the Air and Environmental Quality Division, Department of the Environment, Transport and the Regions.

Russell, A. and Dennis, R. 2000 NARSTO critical review of photochemical models and modelling. Atmospheric Environment 34, 2283-2324

Ryall, D.B., Derwent, R.G., Manning, A.J., Simmonds, P.G., O'Doherty, S. 2001 Estimating source regions of European emissions of trace gases from observations at Mace Head. Atmospheric Environment 35, 2507-2523.

Appendix A

Back trajectory analysis is traditionally used to determine the likely origin of airmasses. One disadvantage of this approach is that a back trajectory can only represent one of the many possible routes that an air parcel could take en-route to a receptor. Another disadvantage is that the technique does not provide any quantitative information about the relative contribution of possible sources. In reality vertical and horizontal mixing will result in air from a wide area contributing at a given point. In order to generate a more complete and quantitative picture of possible sources, we utilise the NAME model to predict the transport of surface emissions throughout Europe (Ryall et al 2001). The model is run using a uniform surface emission rate throughout the domain, to predict concentrations at a given receptor. We can then quantify the relative contribution from all sources at any given time. In the following plots we show maps of possible sources for each of the PUMA campaign days. (The darker colour indcates more trajectories arriving from that location.)

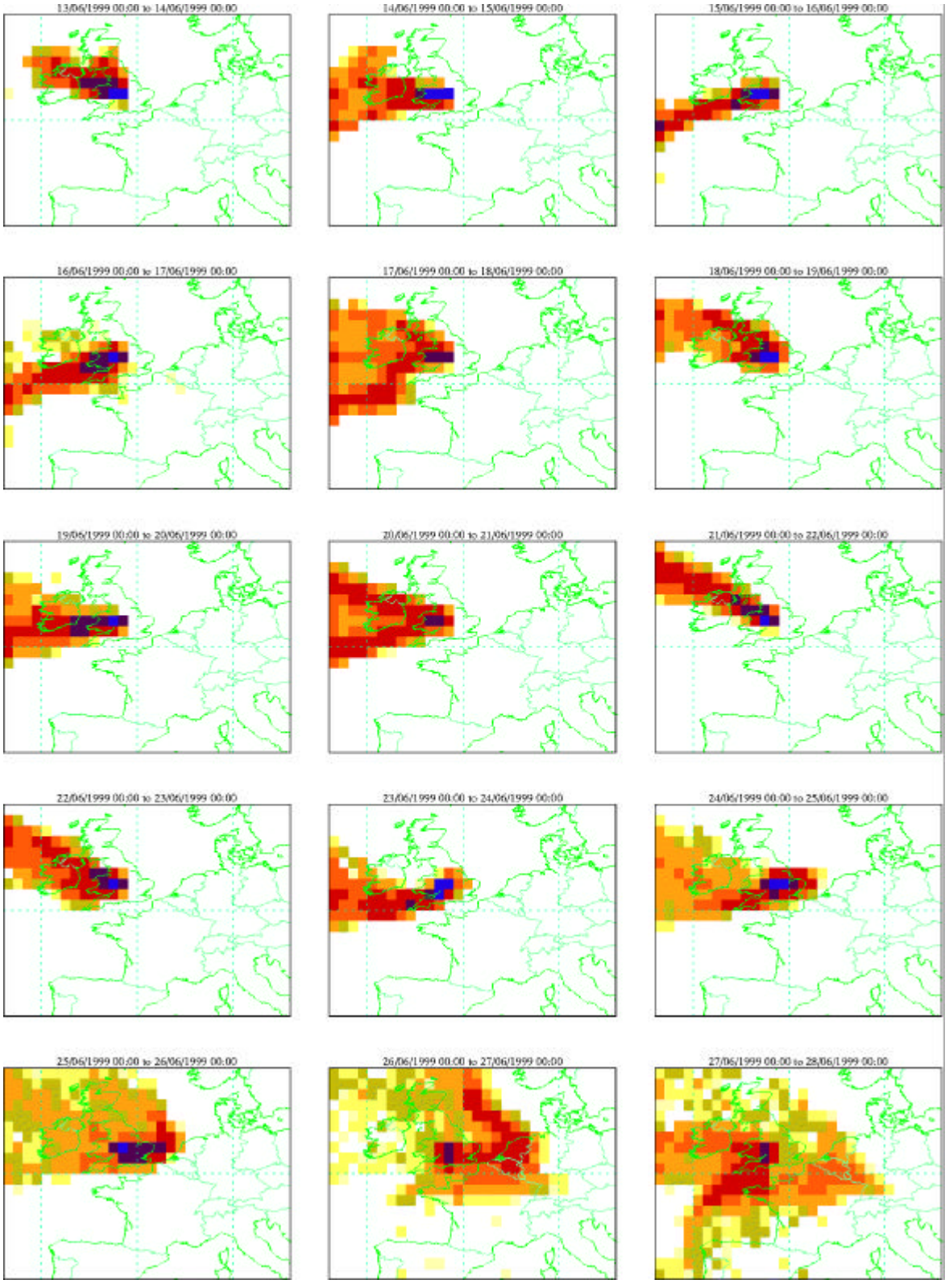
13/06/1999 00:00 to 14/06/1999 00:00
14/06/1999 00:00 to 15/06/1999 00:00
15/06/1999 00:00 to 16/06/1999 00:00
16/06/1999 00:00 to 17/06/1999 00:00
17/06/1999 00:00 to 18/06/1999 00:00
18/06/1999 00:00 to 19/06/1999 00:00
19/06/1999 00:00 to 20/06/1999 00:00
20/06/1999 00:00 to 21/06/1999 00:00
21/06/1999 00:00 to 22/06/1999 00:00
22/06/1999 00:00 to 23/06/1999 00:00
23/06/1999 00:00 to 24/06/1999 00:00
24/06/1999 00:00 to 25/06/1999 00:00
25/06/1999 00:00 to 26/06/1999 00:00
26/06/1999 00:00 to 27/06/1999 00:00
27/06/1999 00:00 to 28/06/1999 00:00

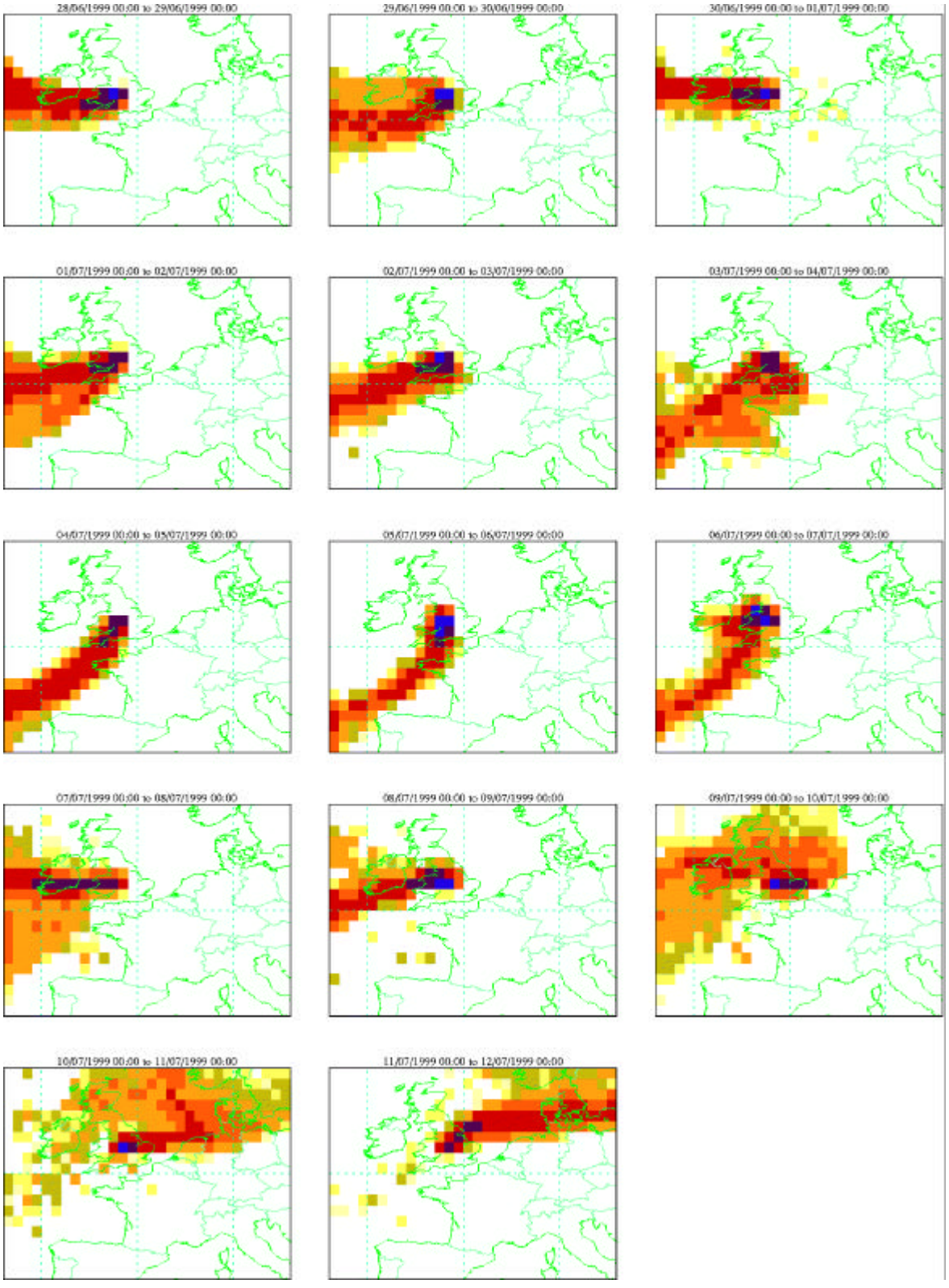
28/06/1999 00:00 to 29/06/1999 00:00
29/06/1999 00:00 to 30/06/1999 00:00
30/06/1999 00:00 to 01/07/1999 00:00
01/07/1999 00:00 to 02/07/1999 00:00
02/07/1999 00:00 to 03/07/1999 00:00
03/07/1999 00:00 to 04/07/1999 00:00
04/07/1999 00:00 to 05/07/1999 00:00
05/07/1999 00:00 to 06/07/1999 00:00
06/07/1999 00:00 to 07/07/1999 00:00
07/07/1999 00:00 to 08/07/1999 00:00
08/07/1999 00:00 to 09/07/1999 00:00
09/07/1999 00:00 to 10/07/1999 00:00
10/07/1999 00:00 to 11/07/1999 00:00
11/07/1999 00:00 to 12/07/1999 00:00

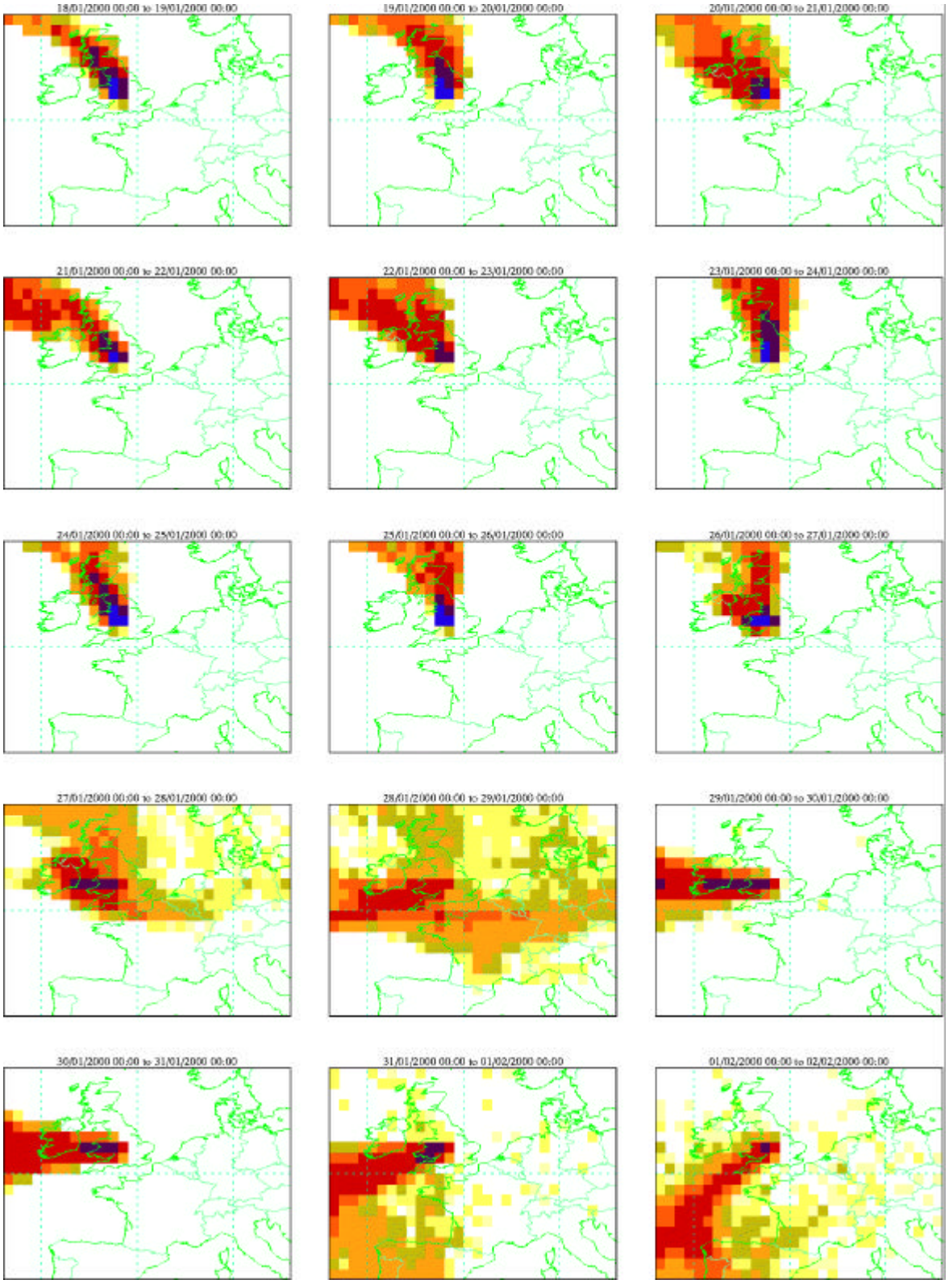
18/01/2000 00:00 to 19/01/2000 00:00
19/01/2000 00:00 to 20/01/2000 00:00
20/01/2000 00:00 to 21/01/2000 00:00
21/01/2000 00:00 to 22/01/2000 00:00
22/01/2000 00:00 to 23/01/2000 00:00
23/01/2000 00:00 to 24/01/2000 00:00
24/01/2000 00:00 to 25/01/2000 00:00
25/01/2000 00:00 to 26/01/2000 00:00
26/01/2000 00:00 to 27/01/2000 00:00
27/01/2000 00:00 to 28/01/2000 00:00
28/01/2000 00:00 to 29/01/2000 00:00
29/01/2000 00:00 to 30/01/2000 00:00
30/01/2000 00:00 to 31/01/2000 00:00
31/01/2000 00:00 to 01/02/2000 00:00
01/02/2000 00:00 to 02/02/2000 00:00

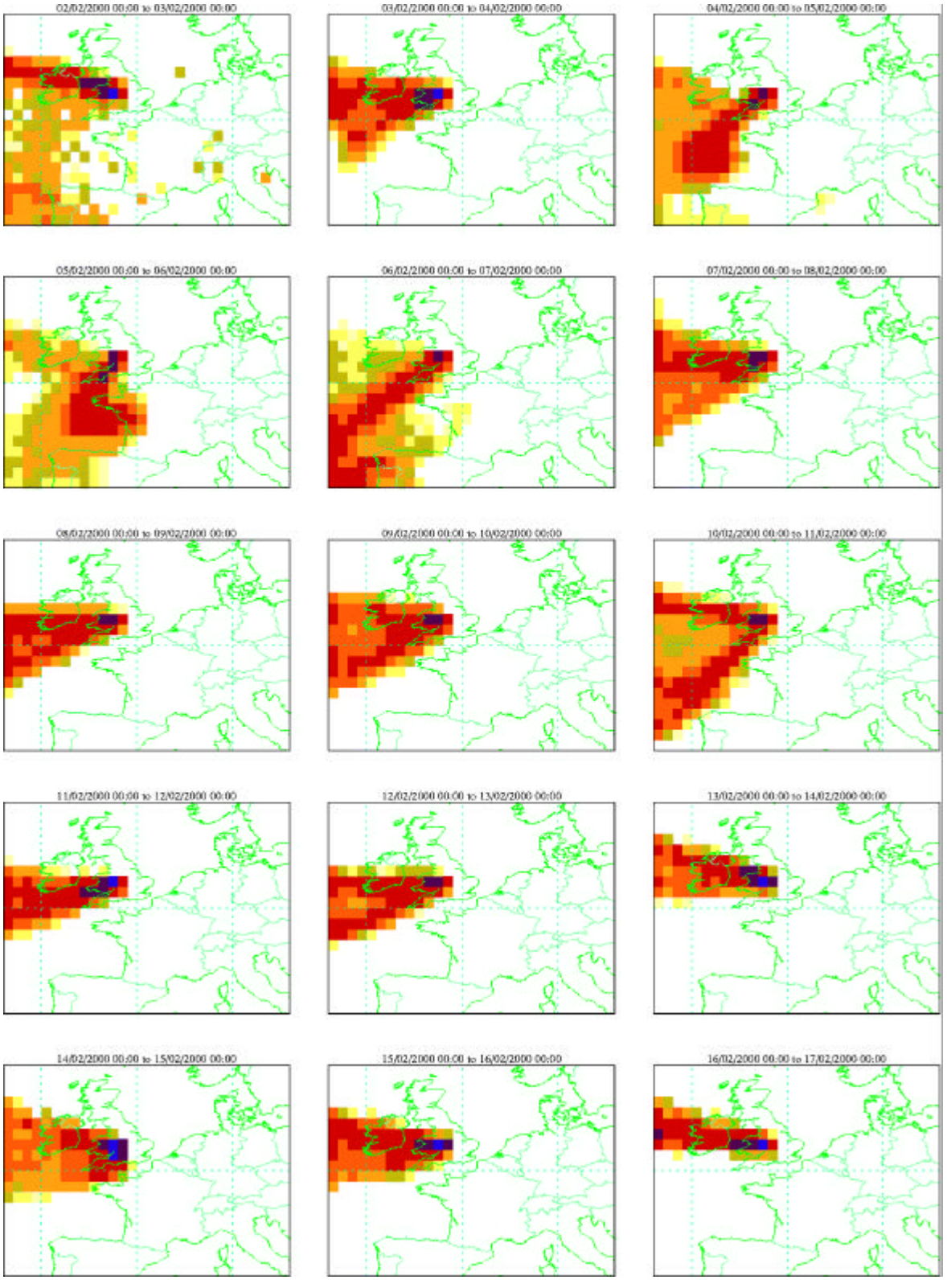
02/02/2000 00:00 to 03/02/2000 00:00
03/02/2000 00:00 to 04/02/2000 00:00
04/02/2000 00:00 to 05/02/2000 00:00
05/02/2000 00:00 to 06/02/2000 00:00
06/02/2000 00:00 to 07/02/2000 00:00
07/02/2000 00:00 to 08/02/2000 00:00
08/02/2000 00:00 to 09/02/2000 00:00
09/02/2000 00:00 to 10/02/2000 00:00
10/02/2000 00:00 to 11/02/2000 00:00
11/02/2000 00:00 to 12/02/2000 00:00
12/02/2000 00:00 to 13/02/2000 00:00
13/02/2000 00:00 to 14/02/2000 00:00
14/02/2000 00:00 to 15/02/2000 00:00
15/02/2000 00:00 to 16/02/2000 00:00
16/02/2000 00:00 to 17/02/2000 00:00

Appendix B

Modelled ozone production - summer campaign: One hour average concentrations (ppb) from 0-20 m, plotted every 6 hours. Birmingham is marked (+). Occasionally the concentration exceeds the top of the scale and is plotted in pink; the maximum value is indicated.

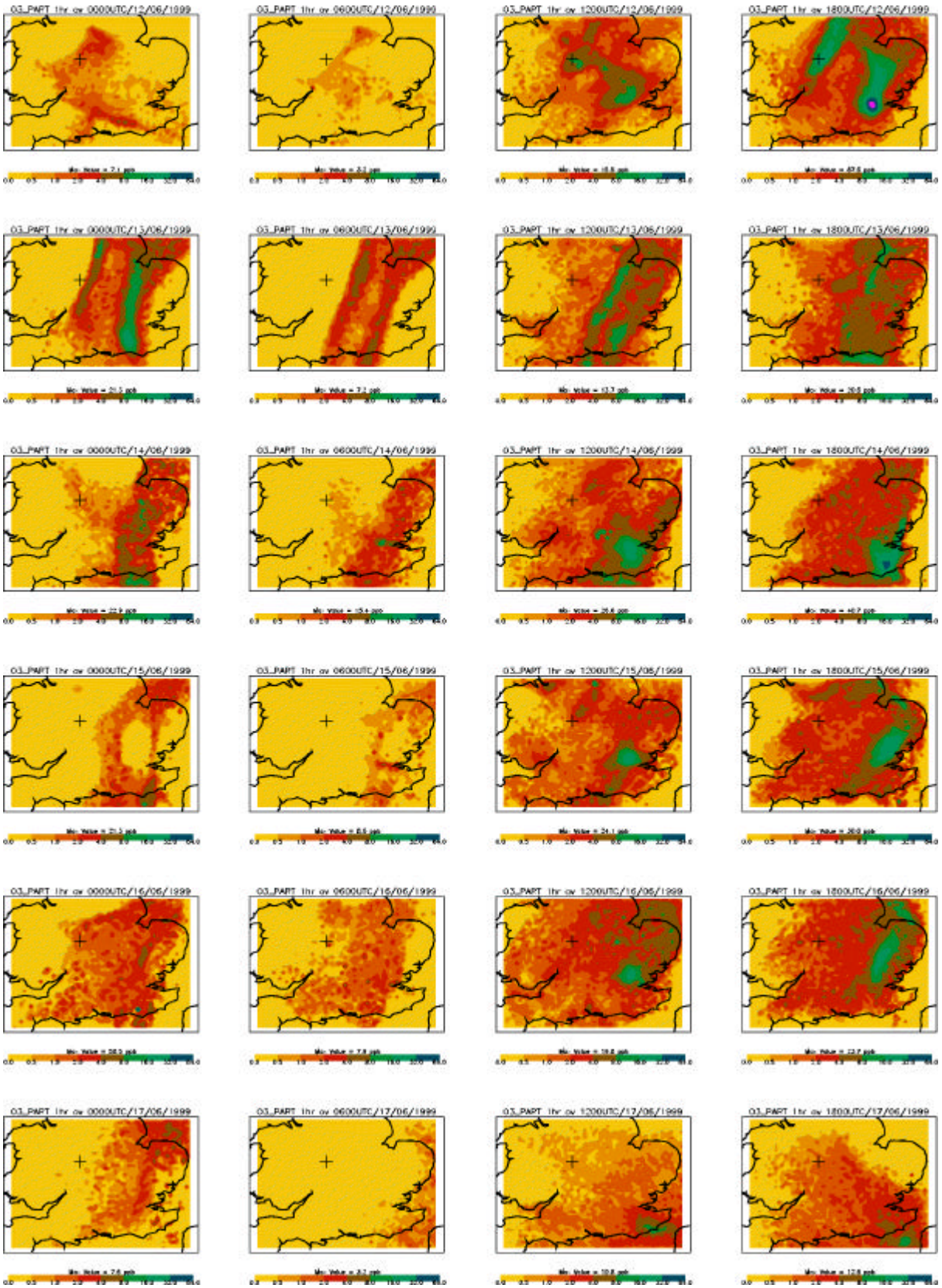

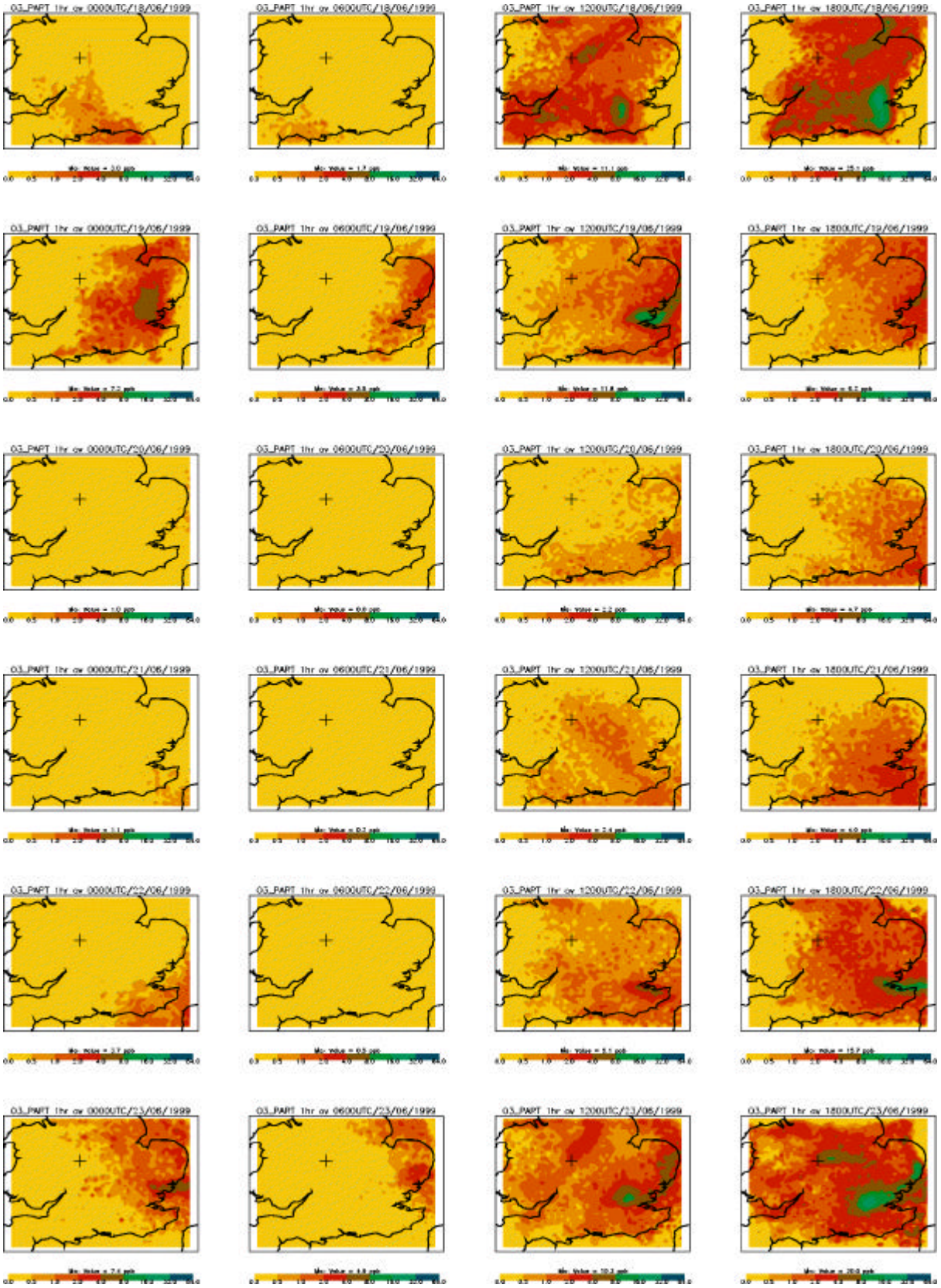
O3_PART 1hr av 0000UTC/18/06/1999
O3_PART 1hr av 0600UTC/18/06/1999
O3_PART 1hr av 1200UTC/18/06/1999
O3_PART 1hr av 1800UTC/18/06/1999
O3_PART 1hr av 0000UTC/19/06/1999
O3_PART 1hr av 0600UTC/19/06/1999
O3_PART 1hr av 1200UTC/19/06/1999
O3_PART 1hr av 1800UTC/19/06/1999
O3_PART 1hr av 0000UTC/20/06/1999
O3_PART 1hr av 0600UTC/20/06/1999
O3_PART 1hr av 1200UTC/20/06/1999
O3_PART 1hr av 1800UTC/20/06/1999
O3_PART 1hr av 0000UTC/21/06/1999
O3_PART 1hr av 0600UTC/21/06/1999
O3_PART 1hr av 1200UTC/21/06/1999
O3_PART 1hr av 1800UTC/21/06/1999
O3_PART 1hr av 0000UTC/22/06/1999
O3_PART 1hr av 0600UTC/22/06/1999
O3_PART 1hr av 1200UTC/22/06/1999
O3_PART 1hr av 1800UTC/22/06/1999
O3_PART 1hr av 0000UTC/23/06/1999
O3_PART 1hr av 0600UTC/23/06/1999
O3_PART 1hr av 1200UTC/23/06/1999
O3_PART 1hr av 1800UTC/23/06/1999

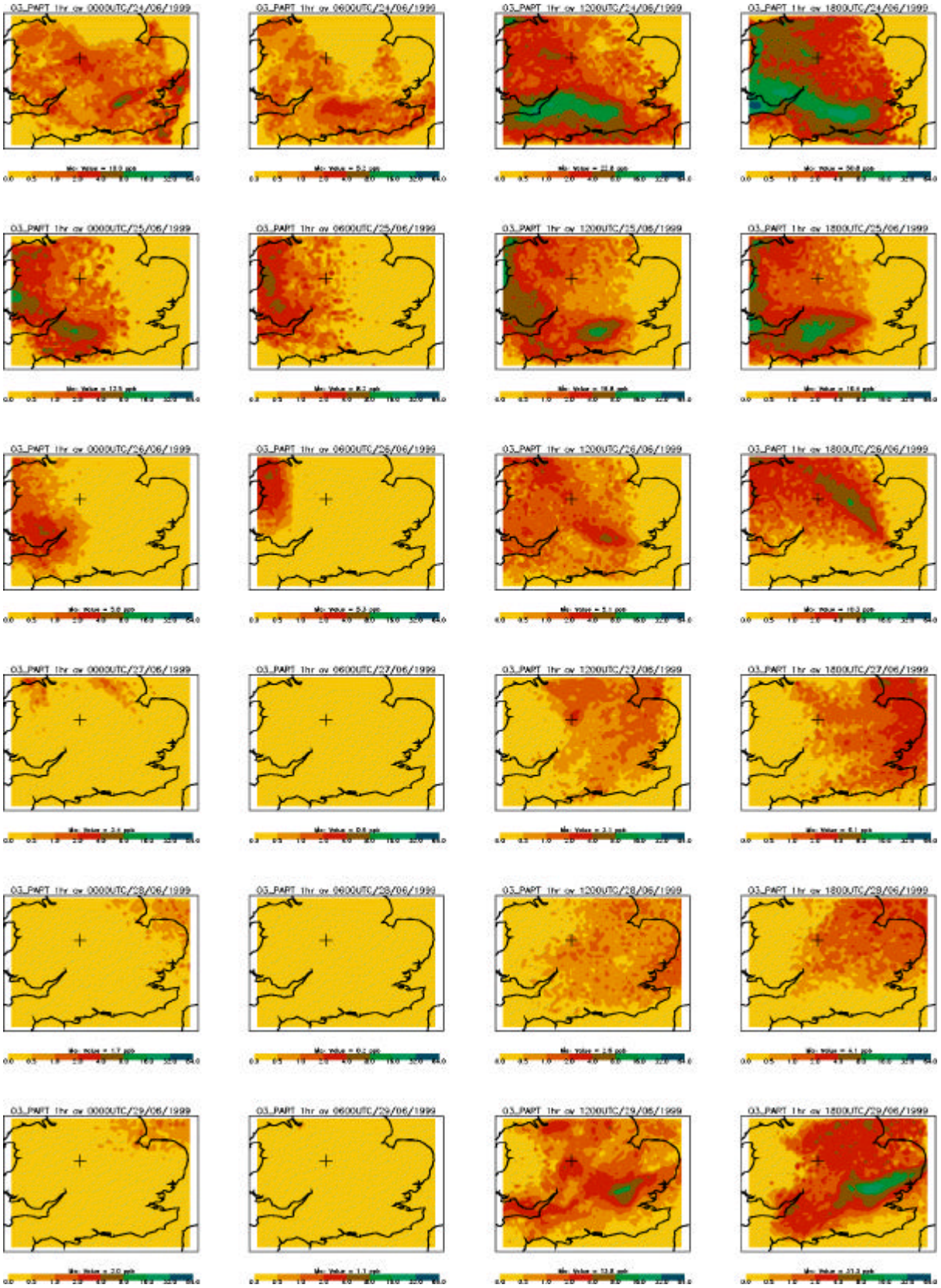
O3_PART 1hr av 0000UTC/24/06/1999
O3_PART 1hr av 0600UTC/24/06/1999
O3_PART 1hr av 1200UTC/24/06/1999
O3_PART 1hr av 1800UTC/24/06/1999
O3_PART 1hr av 0000UTC/25/06/1999
O3_PART 1hr av 0600UTC/25/06/1999
O3_PART 1hr av 1200UTC/25/06/1999
O3_PART 1hr av 1800UTC/25/06/1999
O3_PART 1hr av 0000UTC/26/06/1999
O3_PART 1hr av 0600UTC/26/06/1999
O3_PART 1hr av 1200UTC/26/06/1999
O3_PART 1hr av 1800UTC/26/06/1999
O3_PART 1hr av 0000UTC/27/06/1999
O3_PART 1hr av 0600UTC/27/06/1999
O3_PART 1hr av 1200UTC/27/06/1999
O3_PART 1hr av 1800UTC/27/06/1999
O3_PART 1hr av 0000UTC/28/06/1999
O3_PART 1hr av 0600UTC/28/06/1999
O3_PART 1hr av 1200UTC/28/06/1999
O3_PART 1hr av 1800UTC/28/06/1999
O3_PART 1hr av 0000UTC/29/06/1999
O3_PART 1hr av 0600UTC/29/06/1999
O3_PART 1hr av 1200UTC/29/06/1999
O3_PART 1hr av 1800UTC/29/06/1999

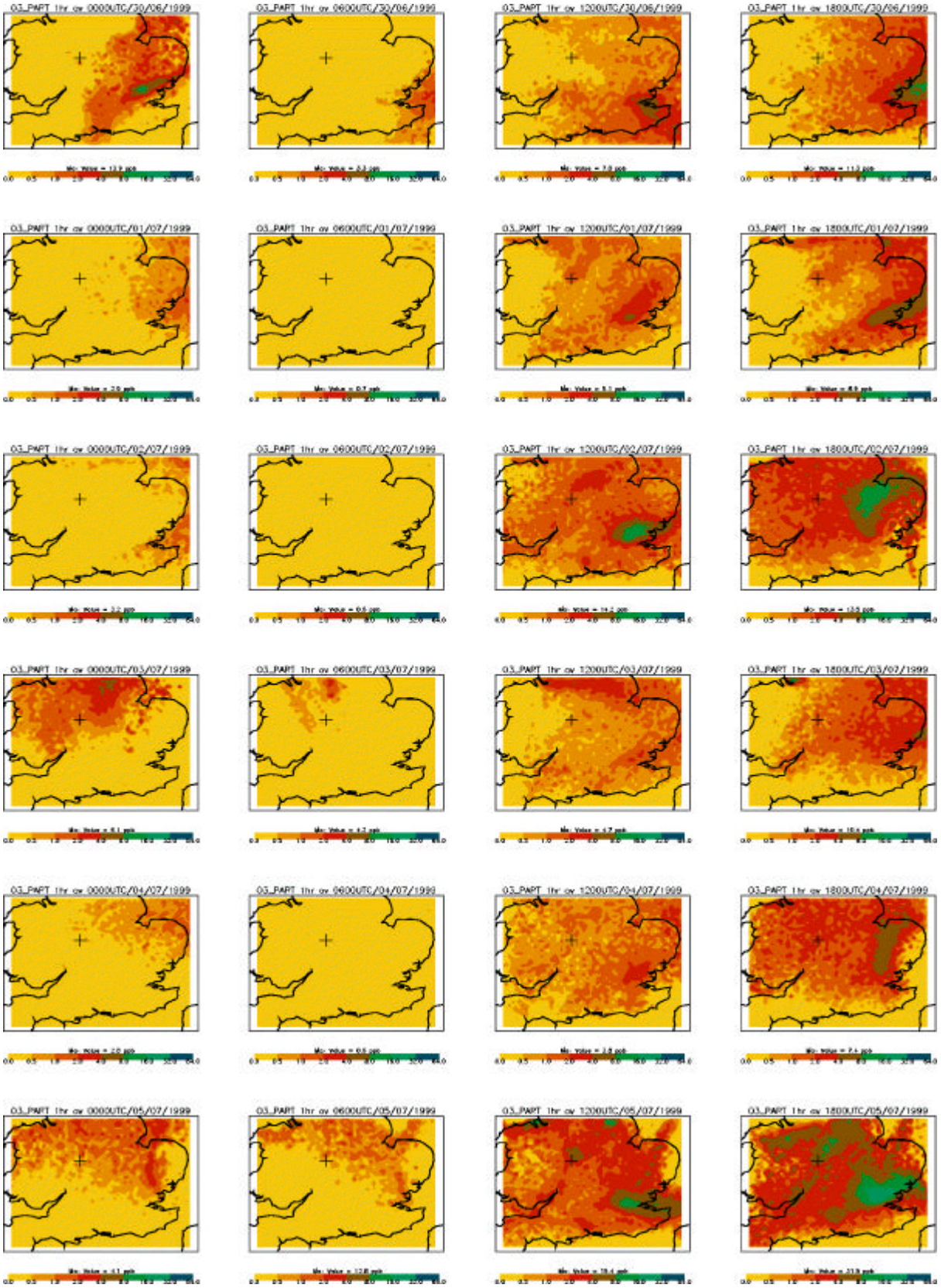
O3_PART 1hr av 0000UTC/30/06/1999
O3_PART 1hr av 0600UTC/30/06/1999
O3_PART 1hr av 1200UTC/30/06/1999
O3_PART 1hr av 1800UTC/30/06/1999
O3_PART 1hr av 0000UTC/01/07/1999
O3_PART 1hr av 0600UTC/01/07/1999
O3_PART 1hr av 1200UTC/01/07/1999
O3_PART 1hr av 1800UTC/01/07/1999
O3_PART 1hr av 0000UTC/02/07/1999
O3_PART 1hr av 0600UTC/02/07/1999
O3_PART 1hr av 1200UTC/02/07/1999
O3_PART 1hr av 1800UTC/02/07/1999
O3_PART 1hr av 0000UTC/03/07/1999
O3_PART 1hr av 0600UTC/03/07/1999
O3_PART 1hr av 1200UTC/03/07/1999
O3_PART 1hr av 1800UTC/03/07/1999
O3_PART 1hr av 0000UTC/04/07/1999
O3_PART 1hr av 0600UTC/04/07/1999
O3_PART 1hr av 1200UTC/04/07/1999
O3_PART 1hr av 1800UTC/04/07/1999
O3_PART 1hr av 0000UTC/05/07/1999
O3_PART 1hr av 0600UTC/05/07/1999
O3_PART 1hr av 1200UTC/05/07/1999
O3_PART 1hr av 1800UTC/05/07/1999

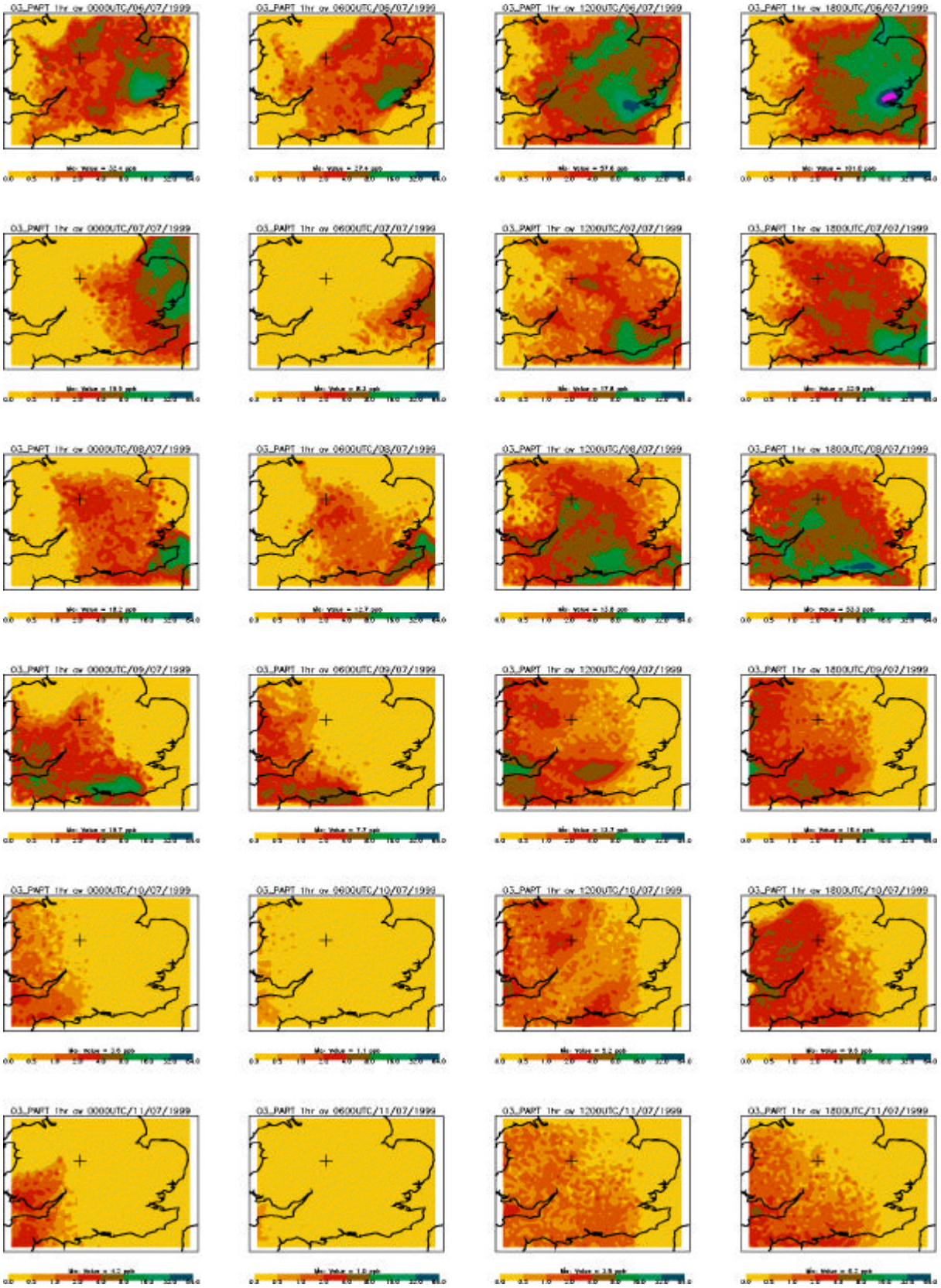
O3_PART 1hr av 0000UTC/06/07/1999
O3_PART 1hr av 0600UTC/06/07/1999
O3_PART 1hr av 1200UTC/06/07/1999
O3_PART 1hr av 1800UTC/06/07/1999
O3_PART 1hr av 0000UTC/07/07/1999
O3_PART 1hr av 0600UTC/07/07/1999
O3_PART 1hr av 1200UTC/07/07/1999
O3_PART 1hr av 1800UTC/07/07/1999
O3_PART 1hr av 0000UTC/08/07/1999
O3_PART 1hr av 0600UTC/08/07/1999
O3_PART 1hr av 1200UTC/08/07/1999
O3_PART 1hr av 1800UTC/08/07/1999
O3_PART 1hr av 0000UTC/09/07/1999
O3_PART 1hr av 0600UTC/09/07/1999
O3_PART 1hr av 1200UTC/09/07/1999
O3_PART 1hr av 1800UTC/09/07/1999
O3_PART 1hr av 0000UTC/10/07/1999
O3_PART 1hr av 0600UTC/10/07/1999
O3_PART 1hr av 1200UTC/10/07/1999
O3_PART 1hr av 1800UTC/10/07/1999
O3_PART 1hr av 0000UTC/11/07/1999
O3_PART 1hr av 0600UTC/11/07/1999
O3_PART 1hr av 1200UTC/11/07/1999
O3_PART 1hr av 1800UTC/11/07/1999

Modelled ozone production - winter campaign: One hour average concentrations (ppb) from 0-20 m, plotted every 6 hours. Birmingham is marked (+). Occasionally the concentration exceeds the top of the scale and is plotted in pink; the maximum value is indicated.

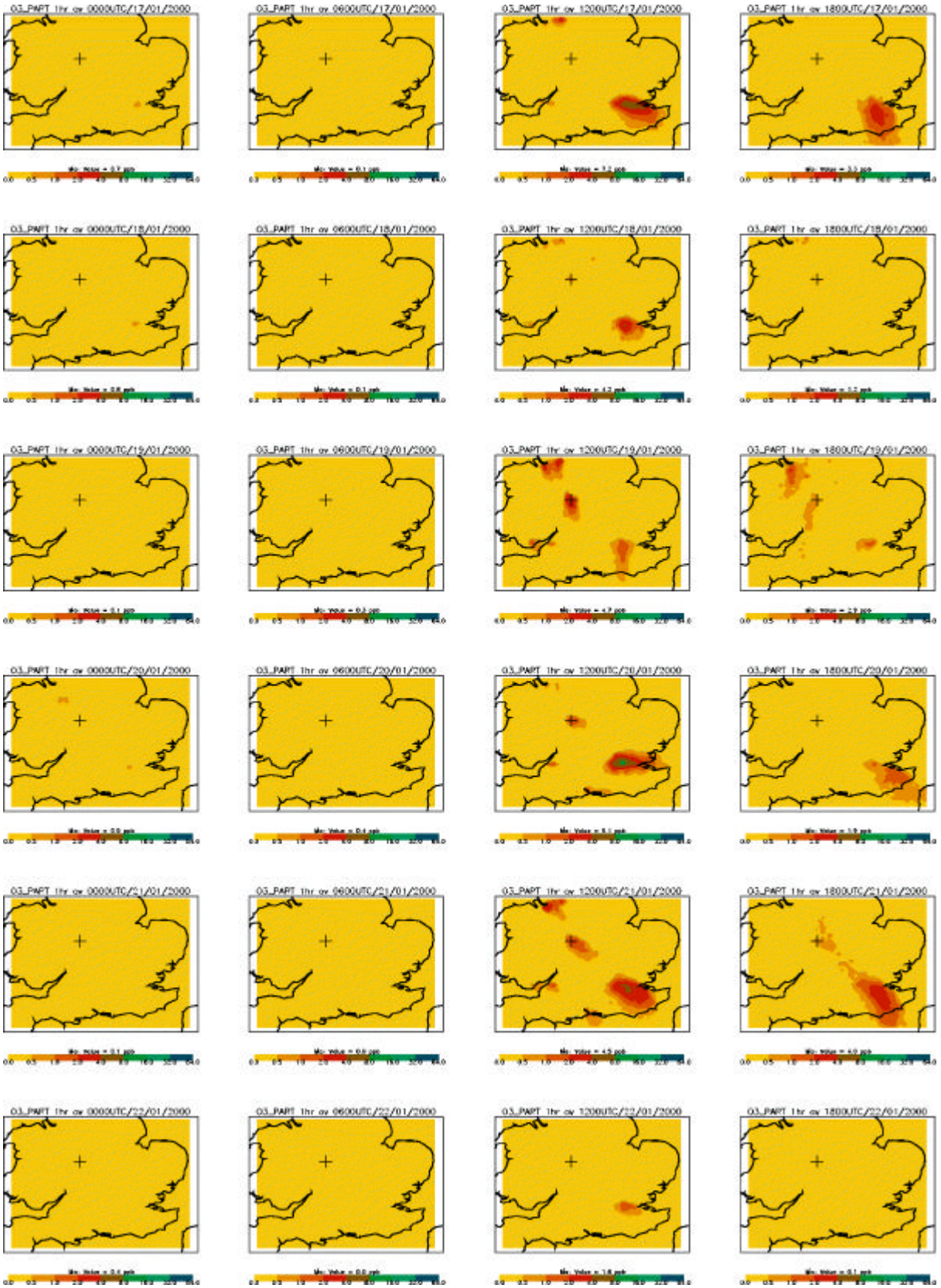

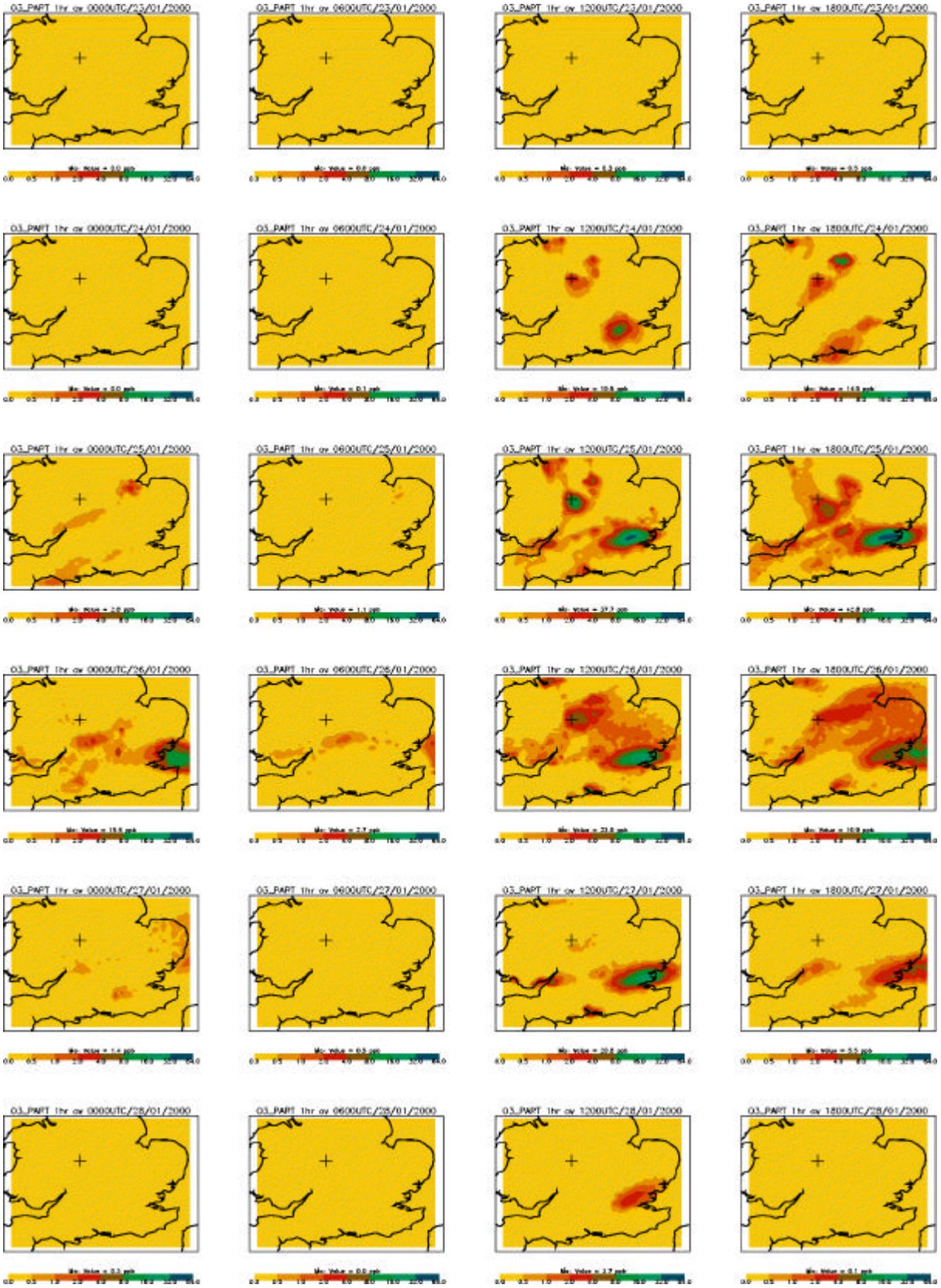
O3_PART 1hr av 0000UTC/23/01/2000
O3_PART 1hr av 0600UTC/23/01/2000
O3_PART 1hr av 1200UTC/23/01/2000
O3_PART 1hr av 1800UTC/23/01/2000
O3_PART 1hr av 0000UTC/24/01/2000
O3_PART 1hr av 0600UTC/24/01/2000
O3_PART 1hr av 1200UTC/24/01/2000
O3_PART 1hr av 1800UTC/24/01/2000
O3_PART 1hr av 0000UTC/25/01/2000
O3_PART 1hr av 0600UTC/25/01/2000
O3_PART 1hr av 1200UTC/25/01/2000
O3_PART 1hr av 1800UTC/25/01/2000
O3_PART 1hr av 0000UTC/26/01/2000
O3_PART 1hr av 0600UTC/26/01/2000
O3_PART 1hr av 1200UTC/26/01/2000
O3_PART 1hr av 1800UTC/26/01/2000
O3_PART 1hr av 0000UTC/27/01/2000
O3_PART 1hr av 0600UTC/27/01/2000
O3_PART 1hr av 1200UTC/27/01/2000
O3_PART 1hr av 1800UTC/27/01/2000
O3_PART 1hr av 0000UTC/28/01/2000
O3_PART 1hr av 0600UTC/28/01/2000
O3_PART 1hr av 1200UTC/28/01/2000
O3_PART 1hr av 1800UTC/28/01/2000

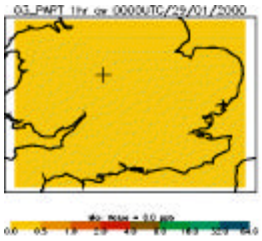
O3_PART 1hr av 0000UTC/29/01/2000
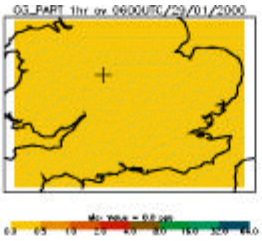
O3_PART 1hr av 0600UTC/29/01/2000
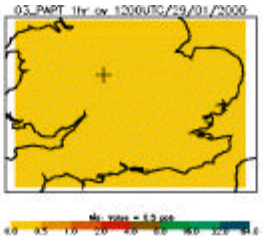
O3_PART 1hr av 1200UTC/29/01/2000
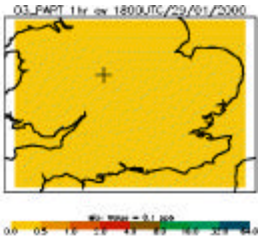
O3_PART 1hr av 1800UTC/29/01/2000
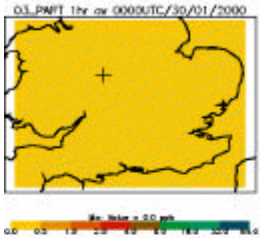
O3_PART 1hr av 0000UTC/30/01/2000
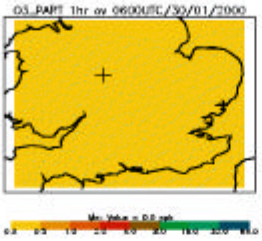
O3_PART 1hr av 0600UTC/30/01/2000
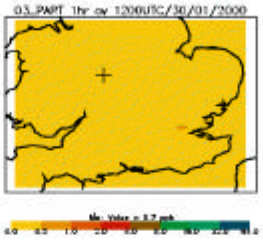
O3_PART 1hr av 1200UTC/30/01/2000
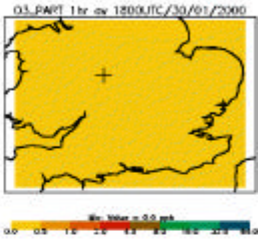
O3_PART 1hr av 1800UTC/30/01/2000
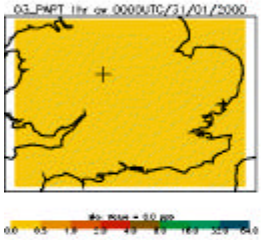
O3_PART 1hr av 0000UTC/31/01/2000
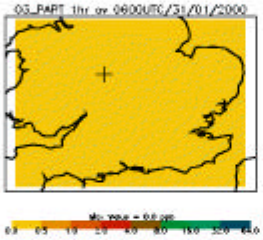
O3_PART 1hr av 0600UTC/31/01/2000
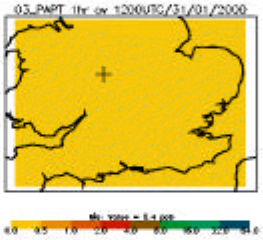
O3_PART 1hr av 1200UTC/31/01/2000
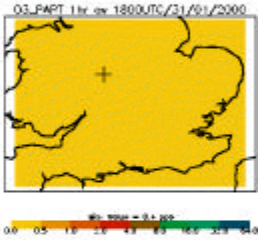
O3_PART 1hr av 1800UTC/31/01/2000
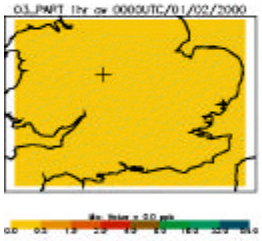
O3_PART 1hr av 0000UTC/01/02/2000
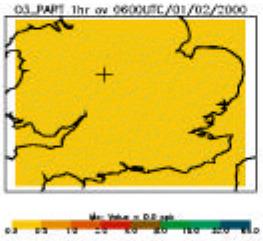
O3_PART 1hr av 0600UTC/01/02/2000
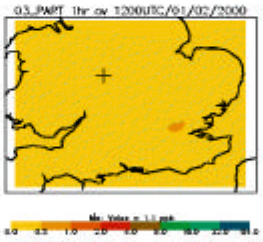
O3_PART 1hr av 1200UTC/01/02/2000
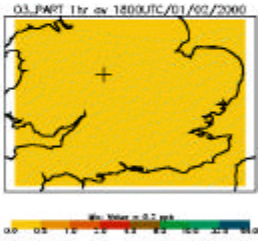
O3_PART 1hr av 1800UTC/01/02/2000
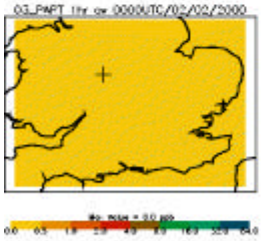
O3_PART 1hr av 0000UTC/02/02/2000
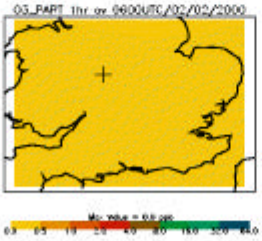
O3_PART 1hr av 0600UTC/02/02/2000
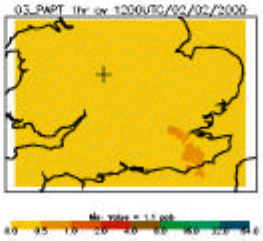
O3_PART 1hr av 1200UTC/02/02/2000
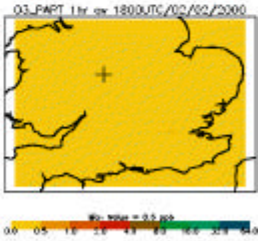
O3_PART 1hr av 1800UTC/02/02/2000
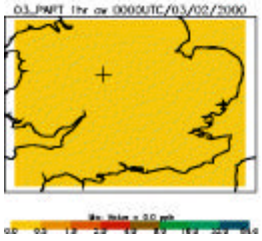
O3_PART 1hr av 0000UTC/03/02/2000
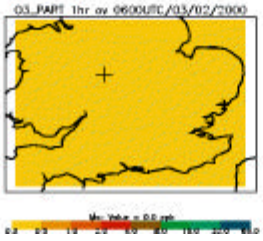
O3_PART 1hr av 0600UTC/03/02/2000
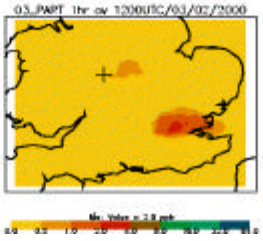
O3_PART 1hr av 1200UTC/03/02/2000
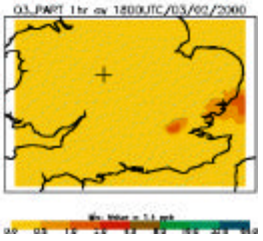
O3_PART 1hr av 1800UTC/03/02/2000

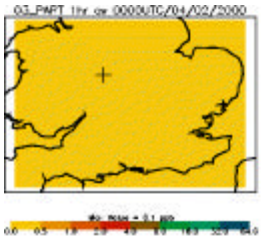
O3_PART 1hr av 0000UTC/04/02/2000
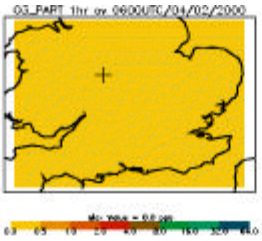
O3_PART 1hr av 0600UTC/04/02/2000
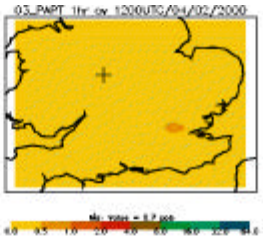
O3_PART 1hr av 1200UTC/04/02/2000
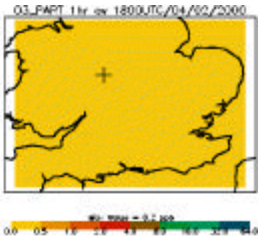
O3_PART 1hr av 1800UTC/04/02/2000
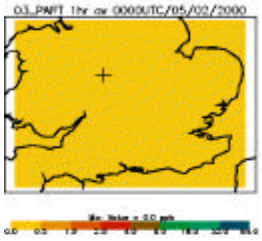
O3_PART 1hr av 0000UTC/05/02/2000
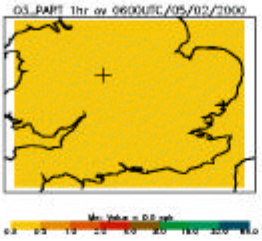
O3_PART 1hr av 0600UTC/05/02/2000
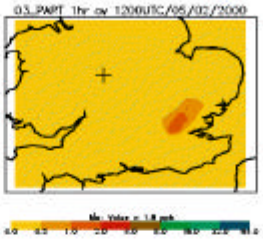
O3_PART 1hr av 1200UTC/05/02/2000
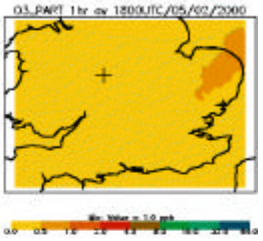
O3_PART 1hr av 1800UTC/05/02/2000
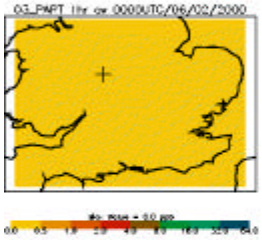
O3_PART 1hr av 0000UTC/06/02/2000
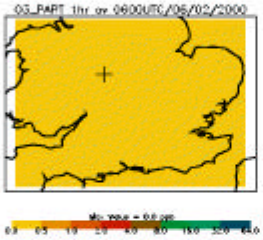
O3_PART 1hr av 0600UTC/06/02/2000
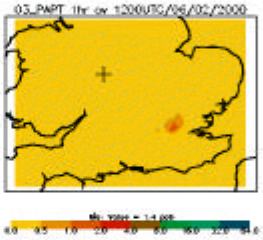
O3_PART 1hr av 1200UTC/06/02/2000
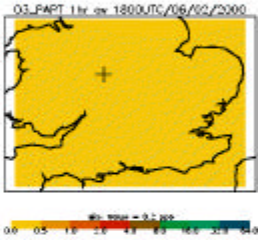
O3_PART 1hr av 1800UTC/06/02/2000
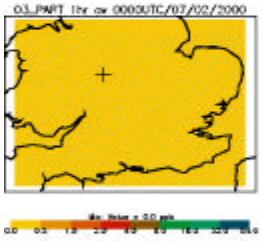
O3_PART 1hr av 0000UTC/07/02/2000
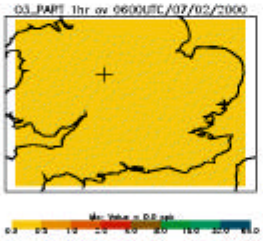
O3_PART 1hr av 0600UTC/07/02/2000
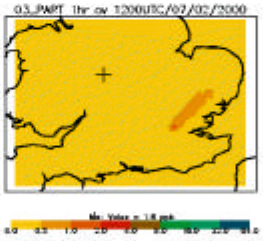
O3_PART 1hr av 1200UTC/07/02/2000
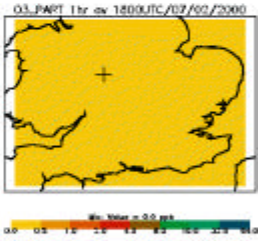
O3_PART 1hr av 1800UTC/07/02/2000
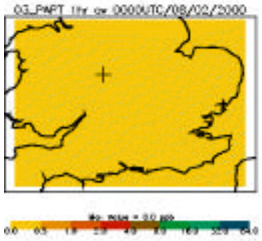
O3_PART 1hr av 0000UTC/08/02/2000
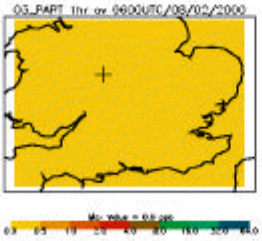
O3_PART 1hr av 0600UTC/08/02/2000
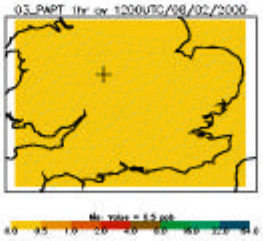
O3_PART 1hr av 1200UTC/08/02/2000
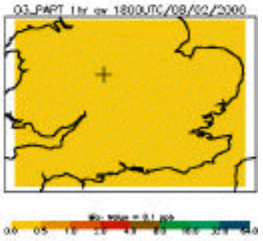
O3_PART 1hr av 1800UTC/08/02/2000
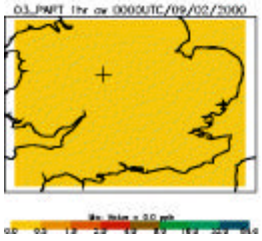
O3_PART 1hr av 0000UTC/09/02/2000
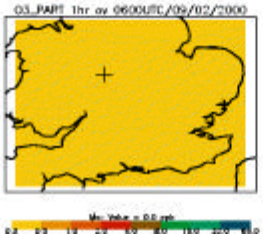
O3_PART 1hr av 0600UTC/09/02/2000
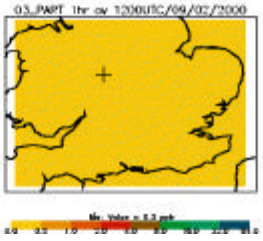
O3_PART 1hr av 1200UTC/09/02/2000
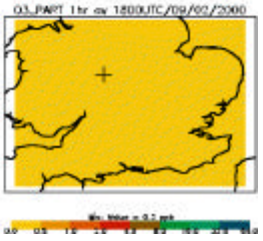
O3_PART 1hr av 1800UTC/09/02/2000

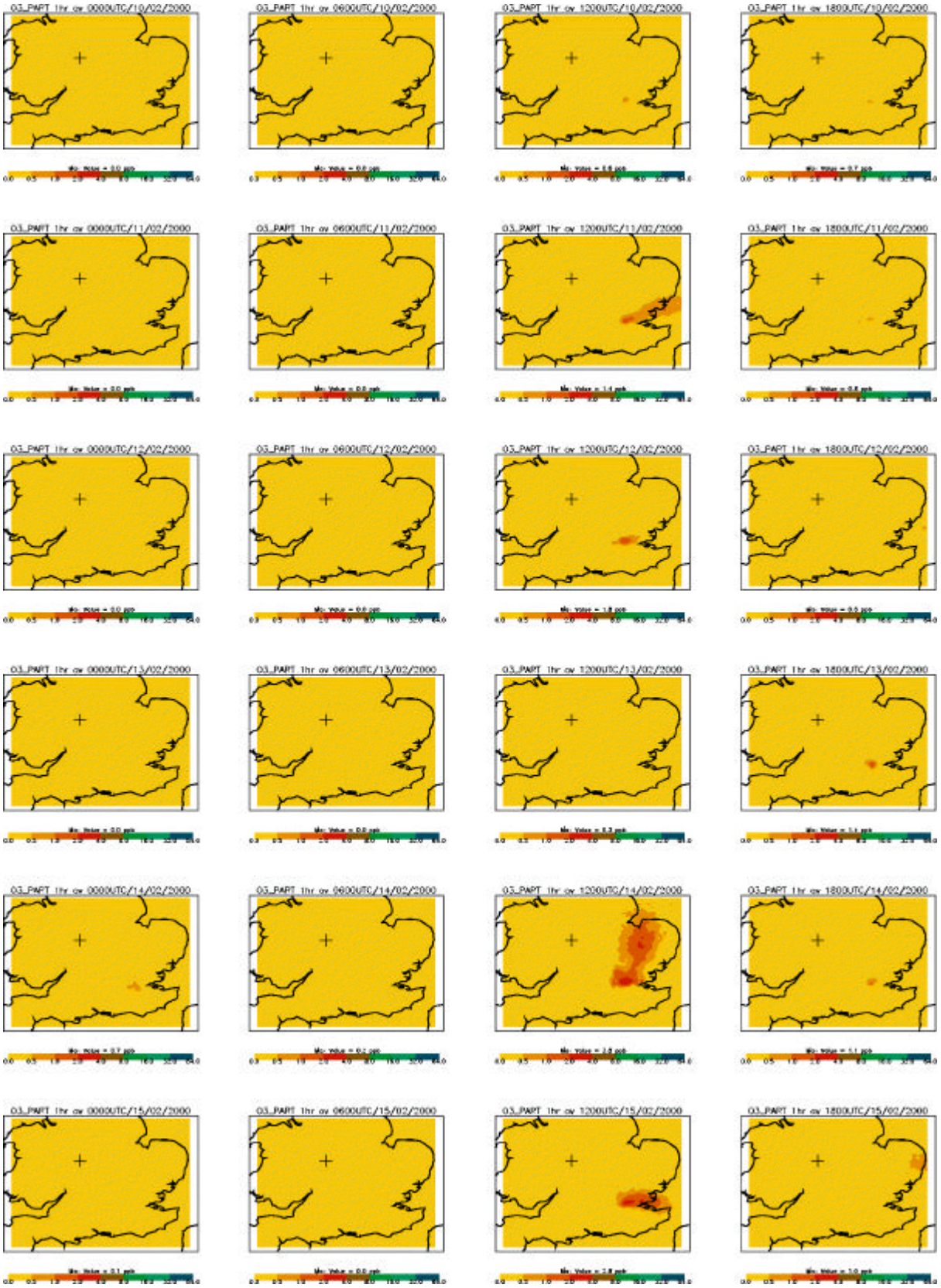
O3_PART 1hr av 0000UTC/10/02/2000
O3_PART 1hr av 0600UTC/10/02/2000
O3_PART 1hr av 1200UTC/10/02/2000
O3_PART 1hr av 1800UTC/10/02/2000
O3_PART 1hr av 0000UTC/11/02/2000
O3_PART 1hr av 0600UTC/11/02/2000
O3_PART 1hr av 1200UTC/11/02/2000
O3_PART 1hr av 1800UTC/11/02/2000
O3_PART 1hr av 0000UTC/12/02/2000
O3_PART 1hr av 0600UTC/12/02/2000
O3_PART 1hr av 1200UTC/12/02/2000
O3_PART 1hr av 1800UTC/12/02/2000
O3_PART 1hr av 0000UTC/13/02/2000
O3_PART 1hr av 0600UTC/13/02/2000
O3_PART 1hr av 1200UTC/13/02/2000
O3_PART 1hr av 1800UTC/13/02/2000
O3_PART 1hr av 0000UTC/14/02/2000
O3_PART 1hr av 0600UTC/14/02/2000
O3_PART 1hr av 1200UTC/14/02/2000
O3_PART 1hr av 1800UTC/14/02/2000
O3_PART 1hr av 0000UTC/15/02/2000
O3_PART 1hr av 0600UTC/15/02/2000
O3_PART 1hr av 1200UTC/15/02/2000
O3_PART 1hr av 1800UTC/15/02/2000

Modelled nitrogen dioxide production - summer campaign: One hour average concentrations (ppb) from 0-20 m, plotted every 6 hours. Birmingham is marked (+). Occasionally the concentration exceeds the top of the scale and is plotted in pink; the maximum value is indicated.

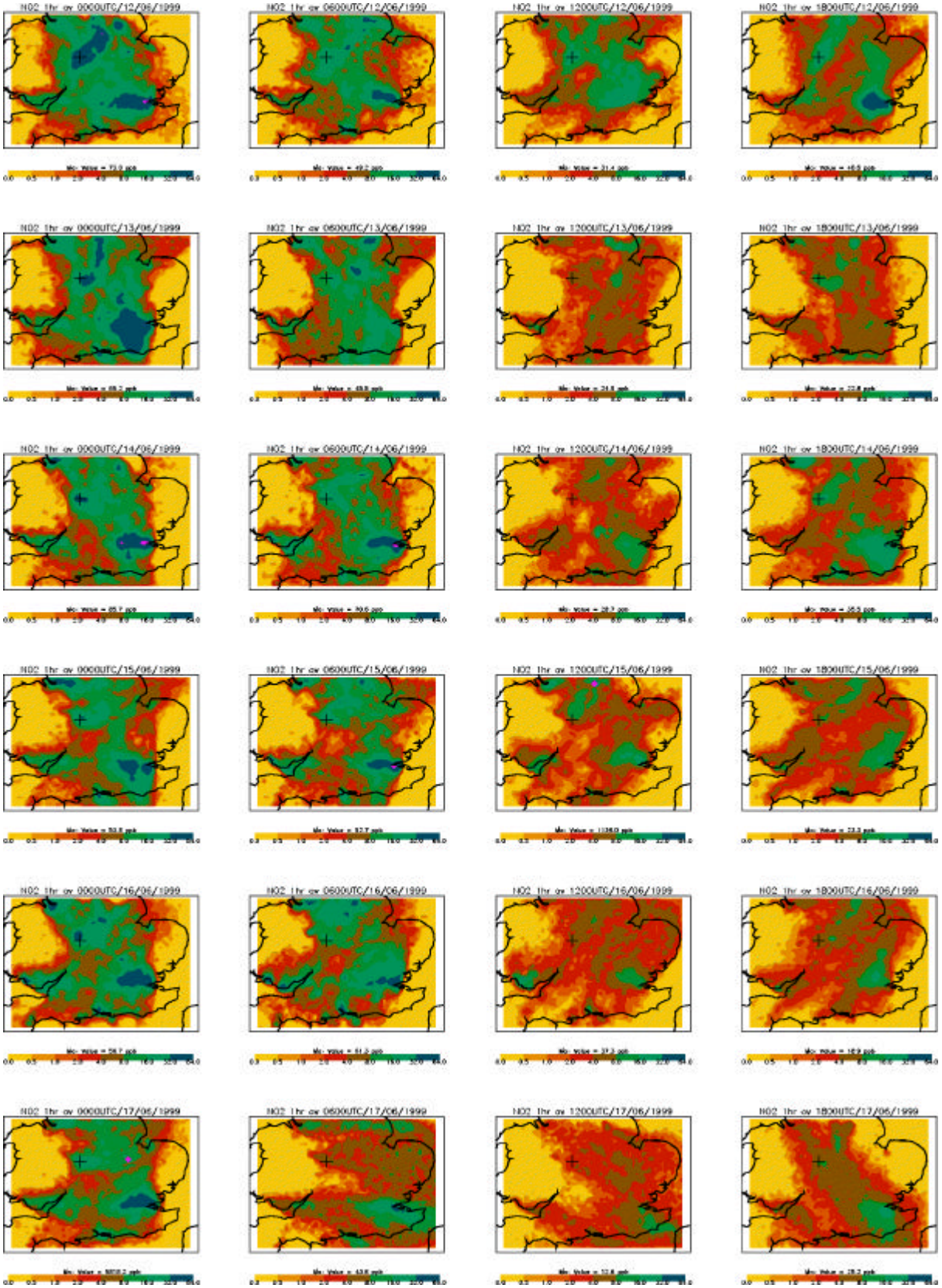

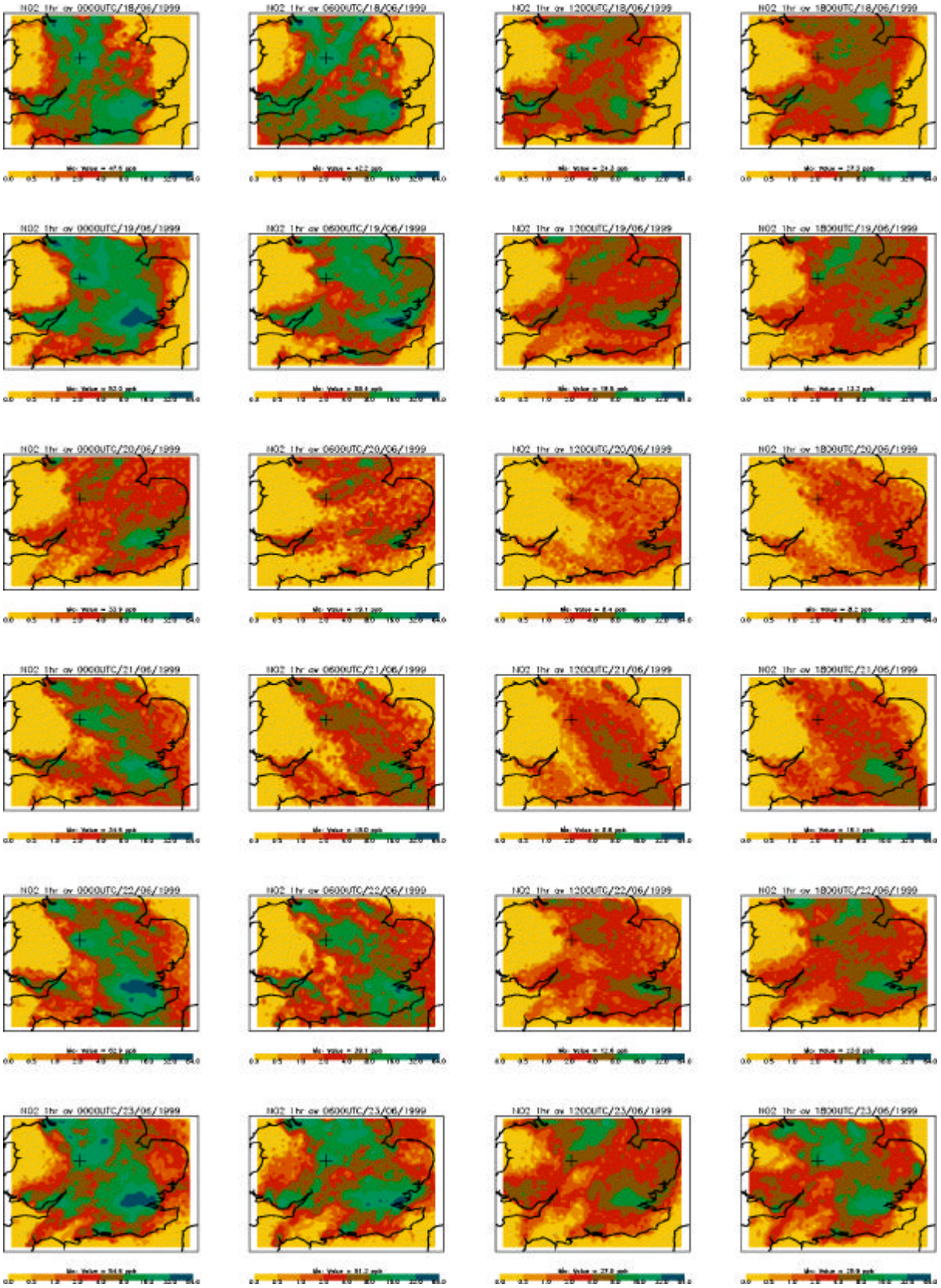
NO2 1hr av 0000UTC/18/06/1999
NO2 1hr av 0600UTC/18/06/1999
NO2 1hr av 1200UTC/18/06/1999
NO2 1hr av 1800UTC/18/06/1999
NO2 1hr av 0000UTC/19/06/1999
NO2 1hr av 0600UTC/19/06/1999
NO2 1hr av 1200UTC/19/06/1999
NO2 1hr av 1800UTC/19/06/1999
NO2 1hr av 0000UTC/20/06/1999
NO2 1hr av 0600UTC/20/06/1999
NO2 1hr av 1200UTC/20/06/1999
NO2 1hr av 1800UTC/20/06/1999
NO2 1hr av 0000UTC/21/06/1999
NO2 1hr av 0600UTC/21/06/1999
NO2 1hr av 1200UTC/21/06/1999
NO2 1hr av 1800UTC/21/06/1999
NO2 1hr av 0000UTC/22/06/1999
NO2 1hr av 0600UTC/22/06/1999
NO2 1hr av 1200UTC/22/06/1999
NO2 1hr av 1800UTC/22/06/1999
NO2 1hr av 0000UTC/23/06/1999
NO2 1hr av 0600UTC/23/06/1999
NO2 1hr av 1200UTC/23/06/1999
NO2 1hr av 1800UTC/23/06/1999

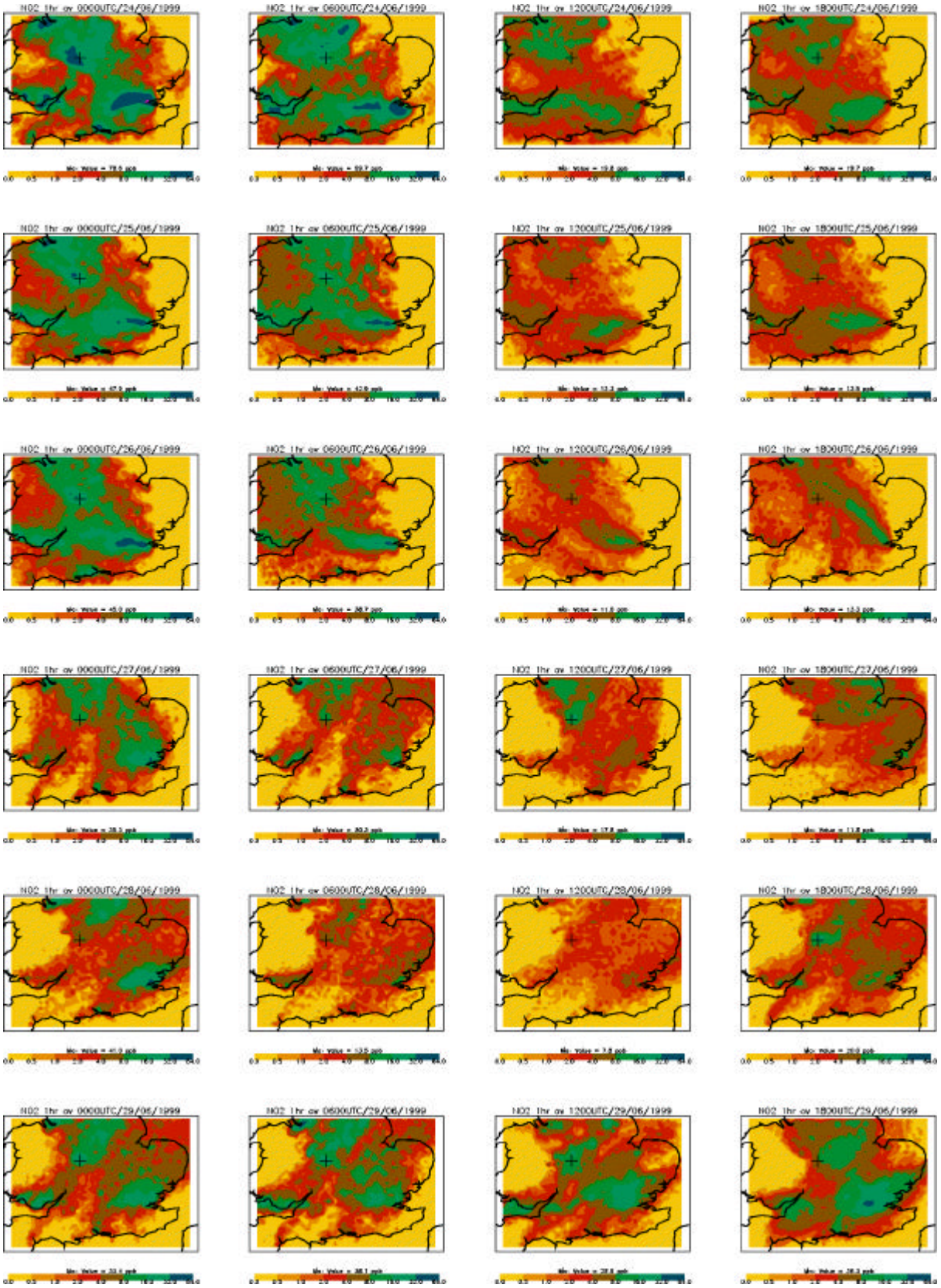
NO2 1hr av 0000UTC/24/06/1999
NO2 1hr av 0600UTC/24/06/1999
NO2 1hr av 1200UTC/24/06/1999
NO2 1hr av 1800UTC/24/06/1999
NO2 1hr av 0000UTC/25/06/1999
NO2 1hr av 0600UTC/25/06/1999
NO2 1hr av 1200UTC/25/06/1999
NO2 1hr av 1800UTC/25/06/1999
NO2 1hr av 0000UTC/26/06/1999
NO2 1hr av 0600UTC/26/06/1999
NO2 1hr av 1200UTC/26/06/1999
NO2 1hr av 1800UTC/26/06/1999
NO2 1hr av 0000UTC/27/06/1999
NO2 1hr av 0600UTC/27/06/1999
NO2 1hr av 1200UTC/27/06/1999
NO2 1hr av 1800UTC/27/06/1999
NO2 1hr av 0000UTC/28/06/1999
NO2 1hr av 0600UTC/28/06/1999
NO2 1hr av 1200UTC/28/06/1999
NO2 1hr av 1800UTC/28/06/1999
NO2 1hr av 0000UTC/29/06/1999
NO2 1hr av 0600UTC/29/06/1999
NO2 1hr av 1200UTC/29/06/1999
NO2 1hr av 1800UTC/29/06/1999

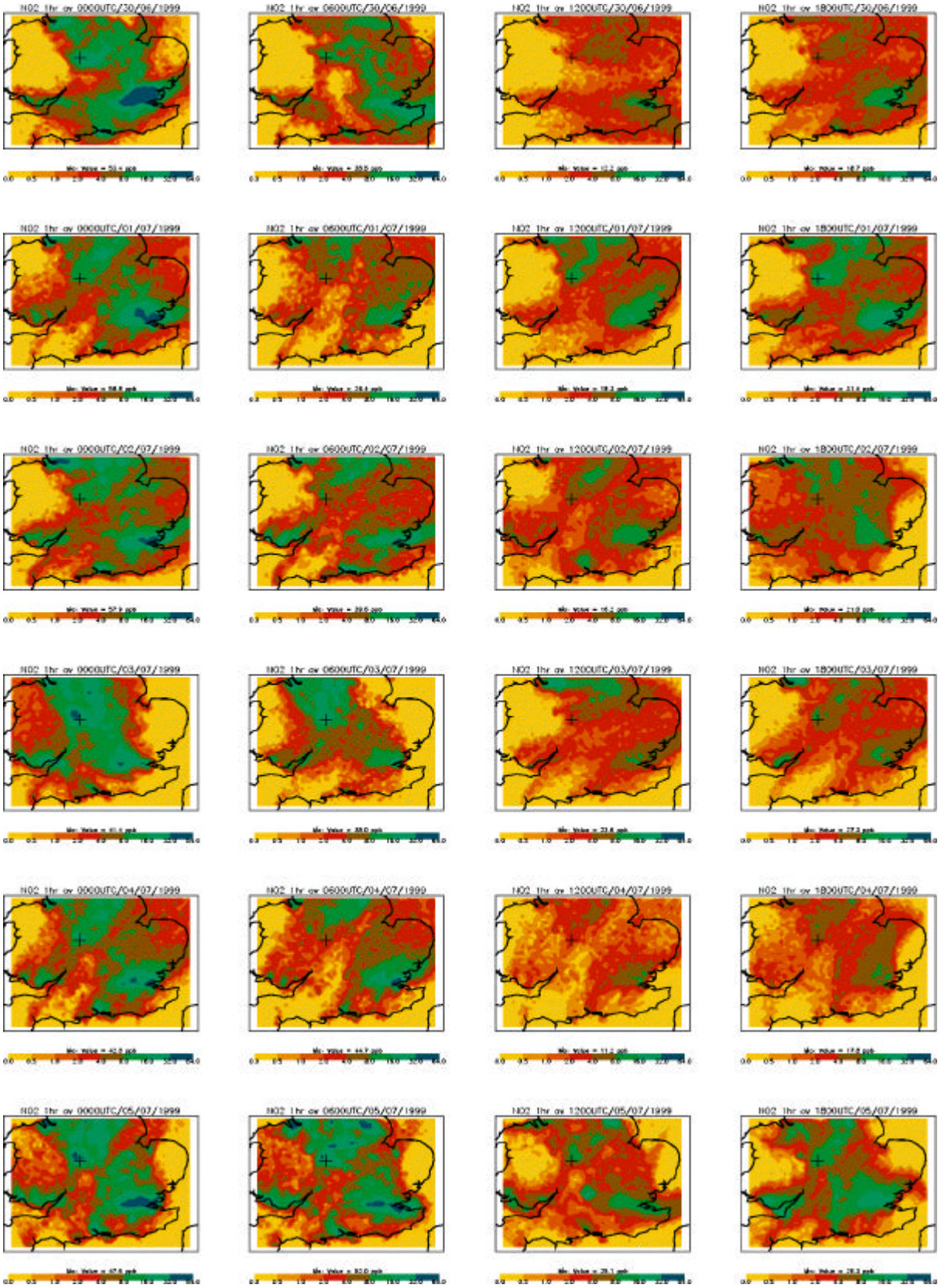
NO2 1hr av 0000UTC/30/06/1999
NO2 1hr av 0600UTC/30/06/1999
NO2 1hr av 1200UTC/30/06/1999
NO2 1hr av 1800UTC/30/06/1999
NO2 1hr av 0000UTC/01/07/1999
NO2 1hr av 0600UTC/01/07/1999
NO2 1hr av 1200UTC/01/07/1999
NO2 1hr av 1800UTC/01/07/1999
NO2 1hr av 0000UTC/02/07/1999
NO2 1hr av 0600UTC/02/07/1999
NO2 1hr av 1200UTC/02/07/1999
NO2 1hr av 1800UTC/02/07/1999
NO2 1hr av 0000UTC/03/07/1999
NO2 1hr av 0600UTC/03/07/1999
NO2 1hr av 1200UTC/03/07/1999
NO2 1hr av 1800UTC/03/07/1999
NO2 1hr av 0000UTC/04/07/1999
NO2 1hr av 0600UTC/04/07/1999
NO2 1hr av 1200UTC/04/07/1999
NO2 1hr av 1800UTC/04/07/1999
NO2 1hr av 0000UTC/05/07/1999
NO2 1hr av 0600UTC/05/07/1999
NO2 1hr av 1200UTC/05/07/1999
NO2 1hr av 1800UTC/05/07/1999

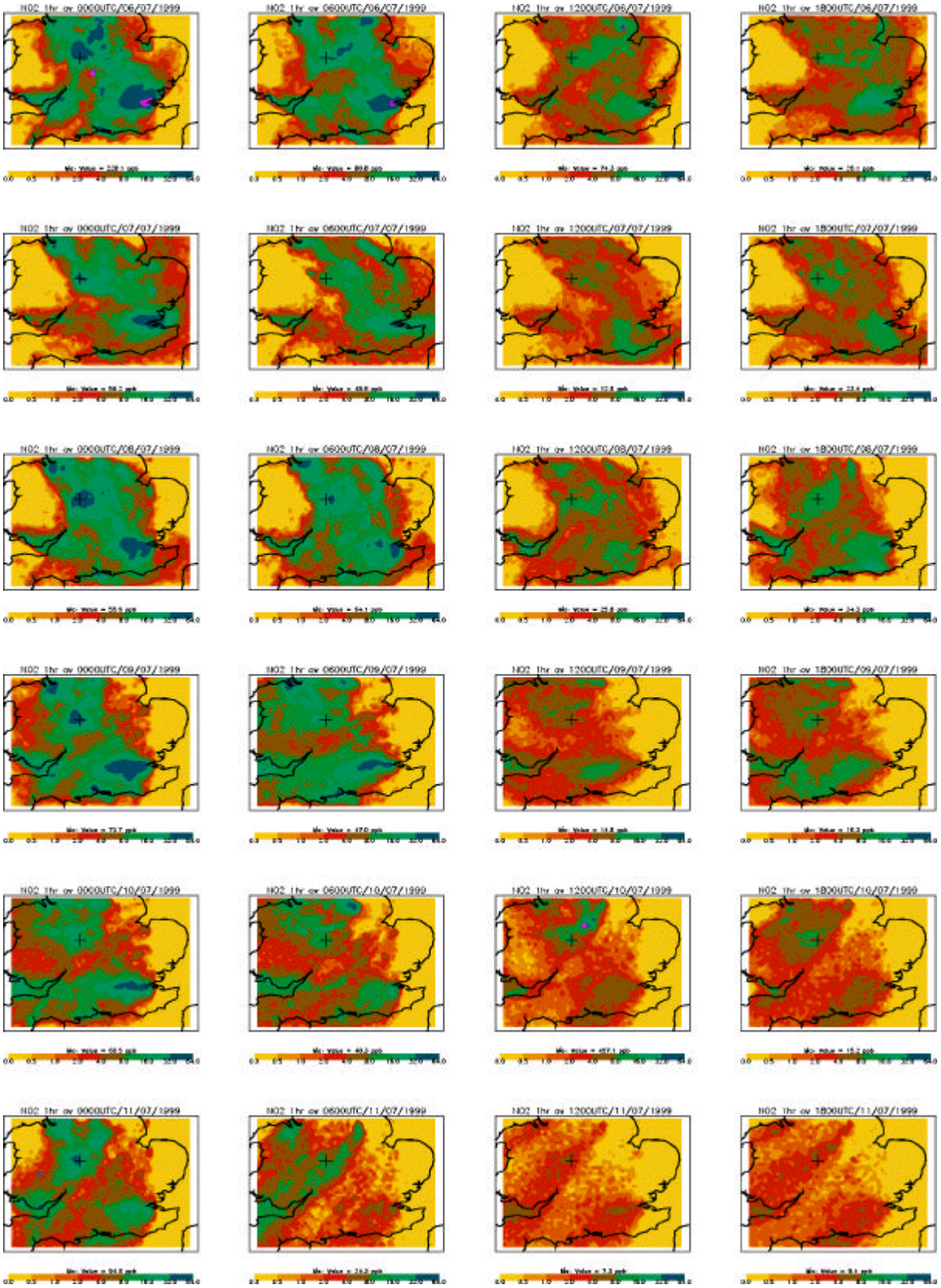
NO2 1hr av 0000UTC/06/07/1999
NO2 1hr av 0600UTC/06/07/1999
NO2 1hr av 1200UTC/06/07/1999
NO2 1hr av 1800UTC/06/07/1999
NO2 1hr av 0000UTC/07/07/1999
NO2 1hr av 0600UTC/07/07/1999
NO2 1hr av 1200UTC/07/07/1999
NO2 1hr av 1800UTC/07/07/1999
NO2 1hr av 0000UTC/08/07/1999
NO2 1hr av 0600UTC/08/07/1999
NO2 1hr av 1200UTC/08/07/1999
NO2 1hr av 1800UTC/08/07/1999
NO2 1hr av 0000UTC/09/07/1999
NO2 1hr av 0600UTC/09/07/1999
NO2 1hr av 1200UTC/09/07/1999
NO2 1hr av 1800UTC/09/07/1999
NO2 1hr av 0000UTC/10/07/1999
NO2 1hr av 0600UTC/10/07/1999
NO2 1hr av 1200UTC/10/07/1999
NO2 1hr av 1800UTC/10/07/1999
NO2 1hr av 0000UTC/11/07/1999
NO2 1hr av 0600UTC/11/07/1999
NO2 1hr av 1200UTC/11/07/1999
NO2 1hr av 1800UTC/11/07/1999

Modelled nitrogen dioxide production - winter campaign: One hour average concentrations (ppb) from 0-20 m, plotted every 6 hours. Birmingham is marked (+). Occasionally the concentration exceeds the top of the scale and is plotted in pink; the maximum value is indicated.

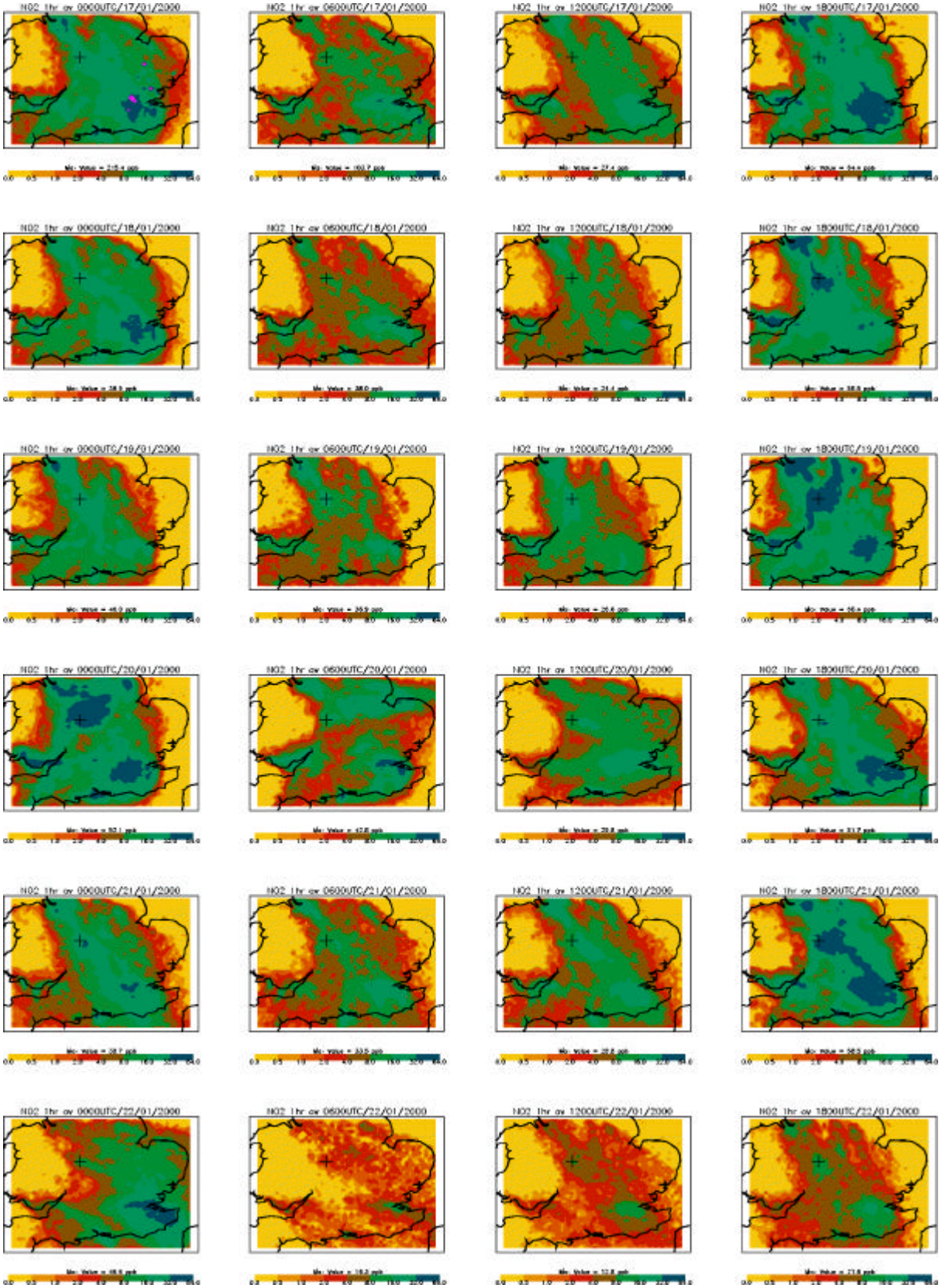

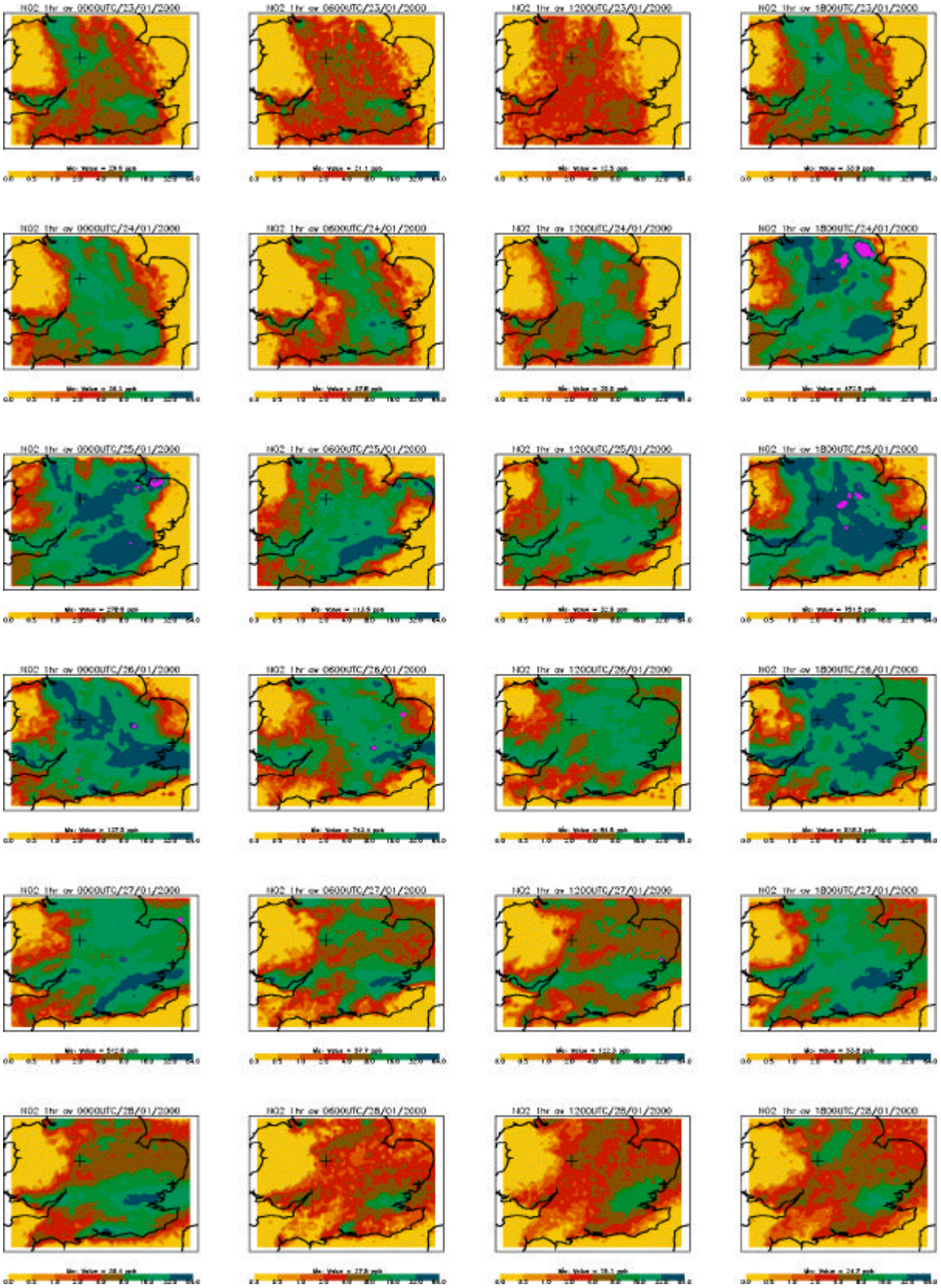
NO2 1hr av 0000UTC/23/01/2000
NO2 1hr av 0600UTC/23/01/2000
NO2 1hr av 1200UTC/23/01/2000
NO2 1hr av 1800UTC/23/01/2000
NO2 1hr av 0000UTC/24/01/2000
NO2 1hr av 0600UTC/24/01/2000
NO2 1hr av 1200UTC/24/01/2000
NO2 1hr av 1800UTC/24/01/2000
NO2 1hr av 0000UTC/25/01/2000
NO2 1hr av 0600UTC/25/01/2000
NO2 1hr av 1200UTC/25/01/2000
NO2 1hr av 1800UTC/25/01/2000
NO2 1hr av 0000UTC/26/01/2000
NO2 1hr av 0600UTC/26/01/2000
NO2 1hr av 1200UTC/26/01/2000
NO2 1hr av 1800UTC/26/01/2000
NO2 1hr av 0000UTC/27/01/2000
NO2 1hr av 0600UTC/27/01/2000
NO2 1hr av 1200UTC/27/01/2000
NO2 1hr av 1800UTC/27/01/2000
NO2 1hr av 0000UTC/28/01/2000
NO2 1hr av 0600UTC/28/01/2000
NO2 1hr av 1200UTC/28/01/2000
NO2 1hr av 1800UTC/28/01/2000

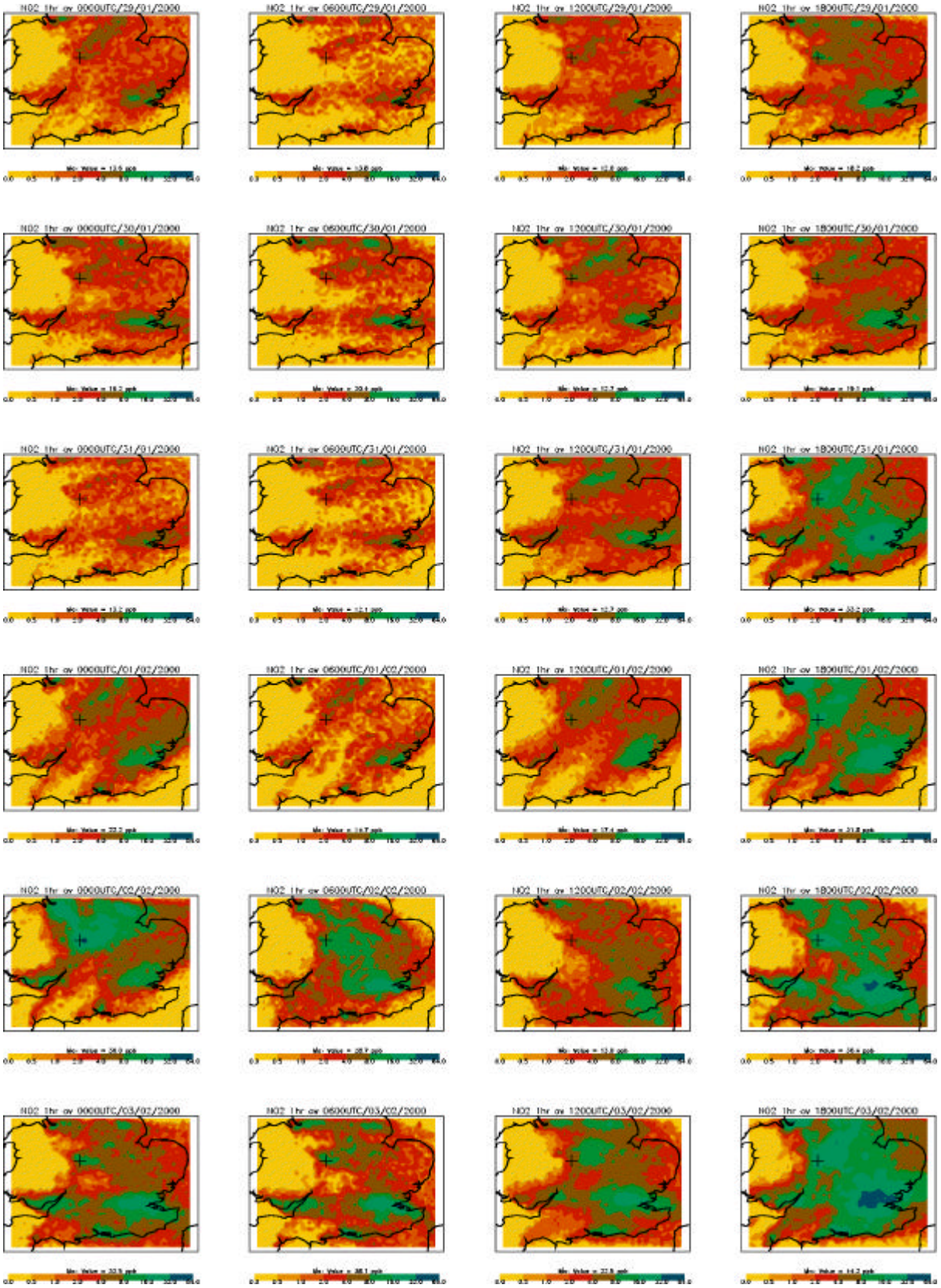
NO2 1hr av 0000UTC/29/01/2000
NO2 1hr av 0600UTC/29/01/2000
NO2 1hr av 1200UTC/29/01/2000
NO2 1hr av 1800UTC/29/01/2000
NO2 1hr av 0000UTC/30/01/2000
NO2 1hr av 0600UTC/30/01/2000
NO2 1hr av 1200UTC/30/01/2000
NO2 1hr av 1800UTC/30/01/2000
NO2 1hr av 0000UTC/31/01/2000
NO2 1hr av 0600UTC/31/01/2000
NO2 1hr av 1200UTC/31/01/2000
NO2 1hr av 1800UTC/31/01/2000
NO2 1hr av 0000UTC/01/02/2000
NO2 1hr av 0600UTC/01/02/2000
NO2 1hr av 1200UTC/01/02/2000
NO2 1hr av 1800UTC/01/02/2000
NO2 1hr av 0000UTC/02/02/2000
NO2 1hr av 0600UTC/02/02/2000
NO2 1hr av 1200UTC/02/02/2000
NO2 1hr av 1800UTC/02/02/2000
NO2 1hr av 0000UTC/03/02/2000
NO2 1hr av 0600UTC/03/02/2000
NO2 1hr av 1200UTC/03/02/2000
NO2 1hr av 1800UTC/03/02/2000

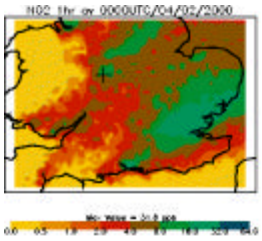
NO2 1hr av 0000UTC/04/02/2000
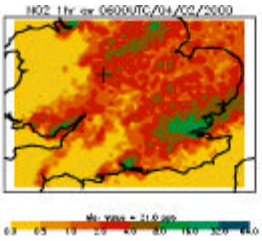
NO2 1hr av 0600UTC/04/02/2000
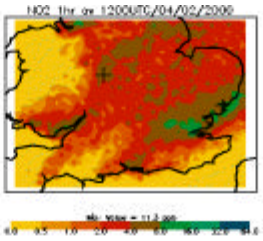
NO2 1hr av 1200UTC/04/02/2000
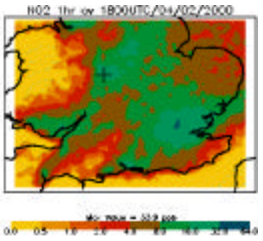
NO2 1hr av 1800UTC/04/02/2000
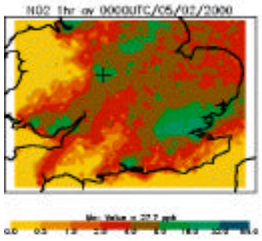
NO2 1hr av 0000UTC/05/02/2000
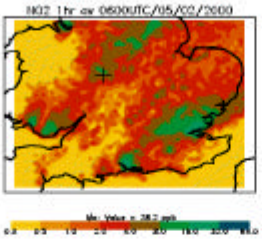
NO2 1hr av 0600UTC/05/02/2000
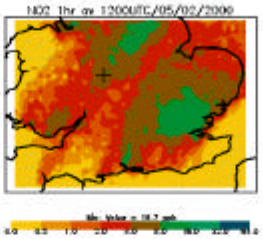
NO2 1hr av 1200UTC/05/02/2000
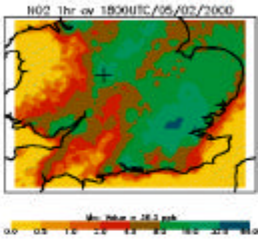
NO2 1hr av 1800UTC/05/02/2000
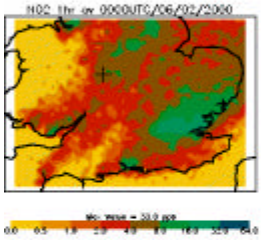
NO2 1hr av 0000UTC/06/02/2000
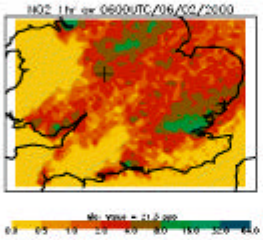
NO2 1hr av 0600UTC/06/02/2000
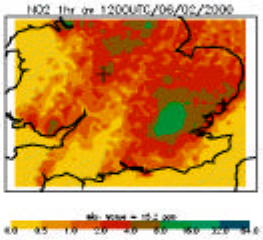
NO2 1hr av 1200UTC/06/02/2000
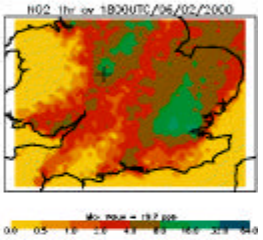
NO2 1hr av 1800UTC/06/02/2000
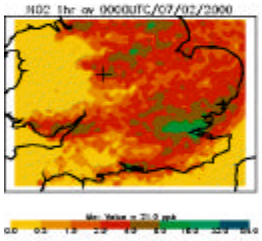
NO2 1hr av 0000UTC/07/02/2000
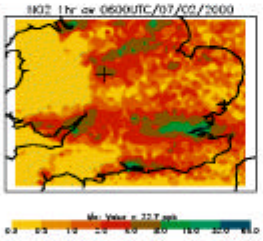
NO2 1hr av 0600UTC/07/02/2000
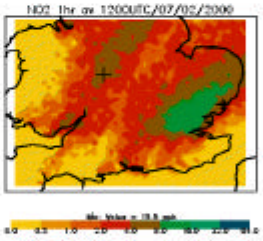
NO2 1hr av 1200UTC/07/02/2000
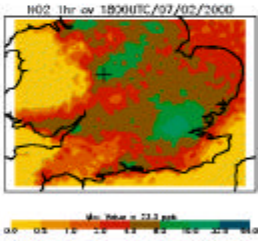
NO2 1hr av 1800UTC/07/02/2000
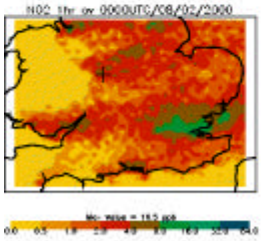
NO2 1hr av 0000UTC/08/02/2000
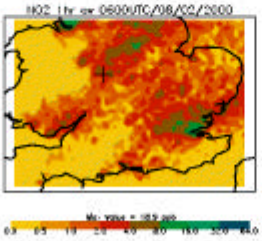
NO2 1hr av 0600UTC/08/02/2000
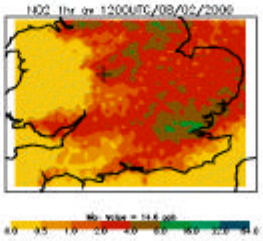
NO2 1hr av 1200UTC/08/02/2000
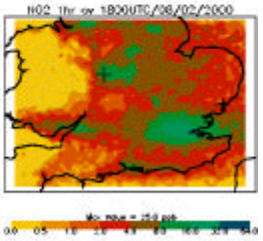
NO2 1hr av 1800UTC/08/02/2000
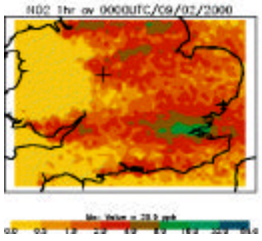
NO2 1hr av 0000UTC/09/02/2000
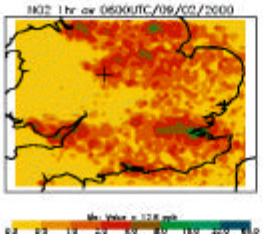
NO2 1hr av 0600UTC/09/02/2000
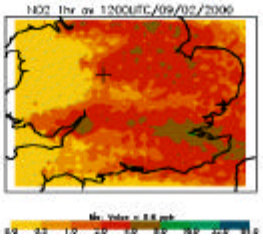
NO2 1hr av 1200UTC/09/02/2000
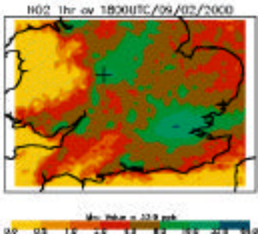
NO2 1hr av 1800UTC/09/02/2000

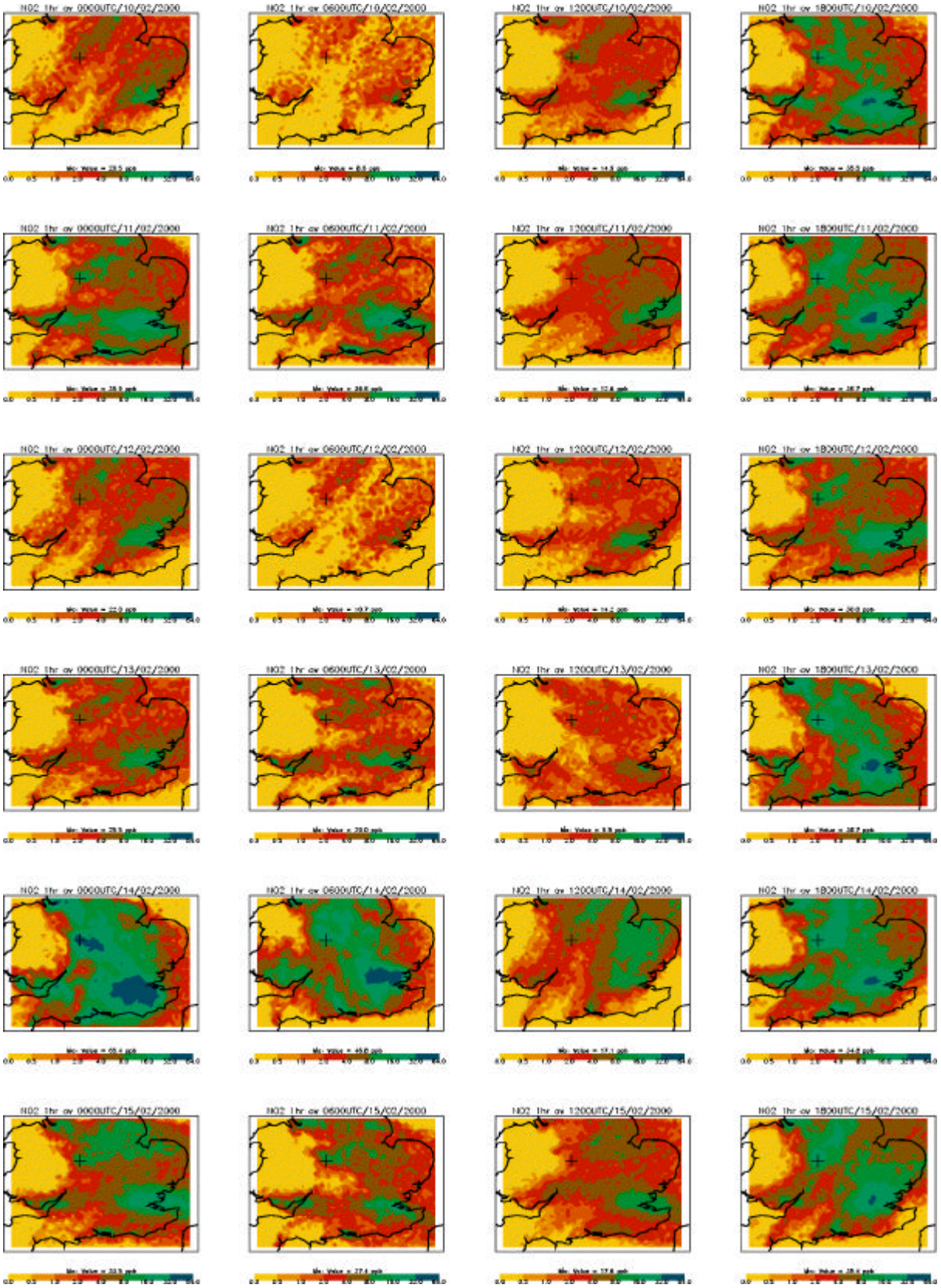
NO2 1hr av 0000UTC/10/02/2000
NO2 1hr av 0600UTC/10/02/2000
NO2 1hr av 1200UTC/10/02/2000
NO2 1hr av 1800UTC/10/02/2000
NO2 1hr av 0000UTC/11/02/2000
NO2 1hr av 0600UTC/11/02/2000
NO2 1hr av 1200UTC/11/02/2000
NO2 1hr av 1800UTC/11/02/2000
NO2 1hr av 0000UTC/12/02/2000
NO2 1hr av 0600UTC/12/02/2000
NO2 1hr av 1200UTC/12/02/2000
NO2 1hr av 1800UTC/12/02/2000
NO2 1hr av 0000UTC/13/02/2000
NO2 1hr av 0600UTC/13/02/2000
NO2 1hr av 1200UTC/13/02/2000
NO2 1hr av 1800UTC/13/02/2000
NO2 1hr av 0000UTC/14/02/2000
NO2 1hr av 0600UTC/14/02/2000
NO2 1hr av 1200UTC/14/02/2000
NO2 1hr av 1800UTC/14/02/2000
NO2 1hr av 0000UTC/15/02/2000
NO2 1hr av 0600UTC/15/02/2000
NO2 1hr av 1200UTC/15/02/2000
NO2 1hr av 1800UTC/15/02/2000